

# The hydrological flow path and options for sustainable water resources management in the overexploited Rio Bravo Basin

A preliminary analysis from remote sensing and hydrological modeling

A World Bank project

Final Report  
March 2006

This remote sensing study was sponsored by the Bank Netherlands Water Partnership Program (BNWPP) of the World Bank

The authors are Wim Bastiaanssen (Irrigation and Remote Sensing Specialist), Annemarie Klaasse (Land and Water Use and Remote Sensing Specialist) and Sander Zwart (Irrigation and Remote Sensing Specialist) from WaterWatch, together with Walter Immerzeel (GIS modeler) and Peter Droogers (Agro-Hydrologists) from FutureWater. These complementary and neighboring companies are both located in Wageningen, the Netherlands.

All rights reserved, March 2006

For more information, please contact [info@WaterWatch.nl](mailto:info@WaterWatch.nl)

---

## Executive summary

Forming a lifeline through the arid Chihuahuan Desert, the Rio Bravo is one of North America's most important river basins. The vulnerability of this river system has been on display for the last several years. With populations increasing all along the border and urban communities withdrawing more surface water resources, the irrigation sector in the Rio Bravo is increasingly challenged to produce more food from less water resources. Irrigation in the Rio Bravo comprises almost 1 million ha, and the withdrawal by this water use sector is one of causing factors for overexploitation.

It is a general conception by water policy makers that improving the irrigation sector water management will solve most other water related problems also. We doubt that this is the right vision and perspective, because the basin hosts many more water user groups that all could potentially contribute to a better balance between water demand and water supply. Moreover, it is envisaged that local sustainability is the most preferred way forward. The opportunity lays in tempering water depletion by reduced evaporation and taking care that return flows are properly utilized. Working out solutions that eliminate overexploitation requires a comprehensive description of all water flows in the Rio Bravo, in relation to the current land cover practices.

This project is an example of utilizing advanced computational tools in hydrology and integrated water resources management. Remote sensing based energy balance models for evapotranspiration and biomass production are linked with the distributed SWAT hydrological model that has been set up for this purpose.

In a nutshell, the major problems in the Rio Bravo basin are:

- Rapid population growth. Between 1990 and 2050, population is expected to increase by 228%, hence there will be more human and industrial water demands and a fierce competition with the agricultural sector
- Expanding irrigation. Irrigation is intensifying due to the introduction of modernized systems and this unprecedented growth reduces stream flow
- Depleted aquifers. Groundwater abstraction is increasingly used as a source of water to augment declining surface water resources; extraction exceeds recharge, essentially in areas with irrigation activities
- Environmental water stress. The water demands from aquatic ecosystems, wetlands, lakes, basin dilution and endangered fish species cannot be met
- Deforestation. Wood logging in the Sierra Madre in Chihuahua exacerbated droughts and caused peak flows with erosion and land degradation as a consequence

Our remote sensing-based vegetation cover change analysis of irrigated acreage between 1999 and 2004 reveals that the irrigated area becomes greener at a pace of 3.5% per year, which enhances the comprehensive evapotranspiration and can potentially deprive water beneficiaries in downstream areas. The scheme level irrigation efficiency is determined with the tools to be 64% on average and the irrigation efficiencies at basin scale are as high as 84 to 90%. Increasing local efficiencies is thus not necessarily improving the total irrigation performance in the Rio Bravo basin and instead merely a shift in the redistribution of water flows. There is also a great risk that the comprehensive evapotranspiration for the region increases due to higher irrigation efficiencies, which exacerbates the problem of water over-consumption. To achieve more radical thinking in integrated water resources management, the irrigation sector should undergo a paradigm shift from

(i) plot scale improvements to increasing effective irrigation efficiency at sub-basin and basin scale, (ii) focus on water productivity increases at basin level and (iii) tempering comprehensive evapotranspiration rather than expanding the irrigated areas with pressurized systems and more and more abstractions.

A considerable regional groundwater flow was detected by the SWAT model and water is laterally transferred from the higher dry desert plain areas to the lower moist flood plain in the southeast. This flow occurs only when sufficient recharge takes place. Continued groundwater irrigation in Chihuahua and groundwater withdrawals by other water use sectors, could adversely affect the water availability for the submontane scrubland and tamaupilan thornscrubland in Coahuila and Nuevo Leon. Less return flow can be explained positively (less non-beneficial ET losses in the downstream end of the basin) and negatively (less opportunities to recycle water downstream).

The integrated SEBAL-SWAT model suggests the average return flow from all water use sectors that divert water is 67%. It is key to think more about the meaning and impact of return flows when drafting basin-wide water resources plans because it implies that a large component of water is not consumed and is recaptured back in the hydrological cycle and is available for a second allocation. The legal framework should focus more on consumption and compulsory return flows in case these water resources are utilized productively, rather than on diversion. Because of lack of hydrological meaning, terminologies such as 'water use' should be avoided in IWRM plans.

The evaporative depletion by land cover revealed that the irrigation sector depletes 11.7 % of the basin wide water resources depletion ( $ET_{act}=20.5 \text{ km}^3$ ). The often quoted diversion of 80 to 90 % of stream flow to the irrigation sector is true by itself, but irrigated crops use not more than 10.4% of the basin-wide gross rainfall. The evaporative depletion from fragile desert ecosystems is 83 % of all basin-wide depletions. Irrigated crops extract more groundwater than being replenished locally (with falling heads as a consequence) and introduce local unsustainability. IWRM plans should touch base with options to reduce evapotranspiration in the natural ecosystems, and enhance stream flows and recharge aquifer systems to a level that reliance on groundwater resources can be eliminated.

Because of the high cost of irrigation, the Mexican Government has emphasized expanding production on existing farmland rather than expanding the area under irrigation. This policy is an appropriate point of departure for controlling the horizontal expansion of irrigated land. However, the net benefits of society in the Rio Bravo are increased by the conversion from non-beneficial and semi-beneficial water usage to beneficial water usage. Rainfall agriculture should be encouraged in the rainfall zone > 700 mm/yr (i.e. Nuevo Leon).

The Integrated Water Resources Management Plans (IWRMPs) should address:

- rights to deplete a maximum allowed ET per land cover type, rather than a right to extract water, thus from the right to divert to the right to consume
- promote land use changes such as the conversion of humid scrubland into rainfed crops
- increase water productivity of manageable agro-ecosystems
- control the horizontal expansion of irrigated areas
- stimulate cultivation of higher value crops (e.g. pecan and grapes)
- pursue local sustainability such that precipitation balances with evapotranspiration

This study demonstrates that a fleet of satellites is available to describe the water resources conditions in a spatially distributed manner. Landsat is suitable for crop

identification, crop ET, soil moisture, crop production and crop water productivity. MODIS is found useful for acquiring the basin wide picture of water depletion, soil moisture and biomass production of all agro-ecosystems including biomass water productivity. TRMM adds key information on the spatial distribution of rainfall. GOES has been explored for the retrieval of solar radiation, being the ultimate driving force behind ET processes. SPOT-Vegetation profiles have shown the capacity to acquire insights in changing irrigated acreages across a longer period of time.

This study assist IWPRM's with land cover, water use and other hydrological data such as catchment water yields, return flows etc. The hydrological flow path is not easily measurable with existing data (especially return flows are difficult to quantify) and the data – when put in place – has often inconsistencies. The SWAT model has been set up to assist the Comisión Nacional del Agua (CNA) with tools that can simulate the surface water – soil water - groundwater interactions.

Although the SWAT model and land cover and crop maps are all preliminary versions, it rolls out a new methodology that assist water policy makers in making firm decisions on water use, water diversion and water abstraction and where land cover changes could be considered. The analytical tools could after further refinement and calibration be utilized to explore (i) land cover changes (more chaparral, more rainfed crops, more high value irrigation crops), (ii) design ET quota on agricultural and ecological water users and (iii) more diversions to urban water users and study the impact on environmental and economical benefits.

These analytical tools are transferred to the Government of Mexico during a one-week workshop organized by CNA in Mexico City in February 2006. A web-based mapping tool is released via [www.waterwatch.nl/riobravo](http://www.waterwatch.nl/riobravo), which eases the accessibility to the hydrological data derived under this project for everybody who has interests in the Rio Bravo basin.



---

## Table of content

<b>1. Introduction</b> .....	<b>1</b>
<b>1.1 Background</b> .....	<b>1</b>
<b>1.2 Brief description Rio Bravo Basin</b> .....	<b>3</b>
<b>1.3 Scope and deliverables</b> .....	<b>4</b>
<b>2. The Rio Bravo Basin</b> .....	<b>7</b>
<b>2.1 Physical-geographical setting</b> .....	<b>7</b>
<b>2.2 Land cover</b> .....	<b>10</b>
<b>2.3 Agriculture and Irrigation synopsis</b> .....	<b>12</b>
<b>2.4 Climatology</b> .....	<b>17</b>
<b>3. Brief description of the analytical tools used</b> .....	<b>27</b>
<b>3.1 Images used</b> .....	<b>27</b>
<b>3.2 A brief introduction to SEBAL</b> .....	<b>28</b>
<b>4. Results from remote sensing</b> .....	<b>35</b>
<b>4.1 Rio Bravo basin</b> .....	<b>35</b>
4.1.1 Evaporative depletion .....	35
4.1.2 Precipitation and soil moisture .....	41
4.1.3 Biomass water productivity .....	44
<b>4.2 Water situation in Delicias District</b> .....	<b>47</b>
4.2.1 Crop water analysis MODIS.....	47
<b>5. Results from hydrological modeling</b> .....	<b>59</b>
<b>5.1 SWAT vs. SEBAL</b> .....	<b>59</b>
<b>5.2 The hydrology of Rio Bravo</b> .....	<b>61</b>
<b>6. Implications for water management</b> .....	<b>65</b>
<b>6.1 Irrigation efficiency</b> .....	<b>65</b>
<b>6.2 Rio Bravo water utilization</b> .....	<b>68</b>
<b>7. Training and dissemination</b> .....	<b>71</b>
<b>7.1 Website application</b> .....	<b>71</b>
<b>7.2 Workshop</b> .....	<b>72</b>
<b>8. Future outlook</b> .....	<b>77</b>
<b>9. Conclusions</b> .....	<b>81</b>
<b>References</b> .....	<b>83</b>
<b>Appendix A: SEBAL procedure description</b> .....	<b>A-1</b>

---

## List of tables

<b>Table 1: Land cover classification .....</b>	<b>12</b>
<b>Table 2: Distribution of irrigated area by sub-national unit .....</b>	<b>14</b>
<b>Table 3: Crop-wise breakdown of the irrigated areas in Delicias Irrigation District (Rio Conchos) according to the temporal variability of the 15-day intervals of biomass production .....</b>	<b>17</b>
<b>Table 4: Specification of meteorological stations used.....</b>	<b>20</b>
<b>Table 5: Specification of MODIS scenes used for SEBAL processing in 2003 .....</b>	<b>27</b>
<b>Table 6: Specification of the Landsat images used for SEBAL processing in 2003 .....</b>	<b>28</b>
<b>Table 7: Breakdown of layer-wise ET by land cover type in Rio Bravo.....</b>	<b>39</b>
<b>Table 8: Breakdown of agricultural water use among crop types in Chihuahua State .....</b>	<b>41</b>
<b>Table 9: Annual water balance Rio Bravo Basin according to SWAT by land cover type ....</b>	<b>43</b>
<b>Table 10: Generic streamflow patterns .....</b>	<b>43</b>
<b>Table 11: Biomass water productivity of all agro-ecosystems.....</b>	<b>46</b>
<b>Table 12: Bio-physical crop water productivity analysis on the basis of MODIS images in the Delicias Irrigation District .....</b>	<b>47</b>
<b>Table 13: Crop water productivity analysis on the basis of Landsat images.....</b>	<b>55</b>
<b>Table 14: Water productivity in the Rio Conchos Basin on the basis of conventional data collection procedures.....</b>	<b>56</b>
<b>Table 15: Annual SWAT water balance per land cover class.....</b>	<b>62</b>
<b>Table 16: Annual water balance terms of the 23 sub-watersheds .....</b>	<b>63</b>
<b>Table 17: SWAT-based water flows related to classical irrigation efficiencies .....</b>	<b>66</b>
<b>Table 18: Economical and ecological development of water use sectors in the Rio Bravo ..</b>	<b>69</b>
<b>Table 19: List of participants attending the one-week training course.....</b>	<b>73</b>

---

## List of figures

Figure 1: Political division of the Rio Grande/Bravo basin .....	3
Figure 2: False color MODIS image acquired on November 29 <sup>th</sup> (2003) .....	7
Figure 3: GTOPO30 digital elevation model of the Rio Grande basin .....	8
Figure 4: Soil map of the Rio Bravo Basin .....	9
Figure 5: Simplified aquifer map of Mexico .....	10
Figure 6: Land cover map based on 250 m MODIS time profiles of NDVI .....	11
Figure 7: Geographical distribution of irrigated areas in the Rio Bravo Basin .....	13
Figure 8: Change in fractional vegetation cover in the major irrigated areas.....	15
Figure 9: Temporal changes of green cover in (supplementally) irrigated land .....	16
Figure 10: Temporal profiles of the biomass production of discernable crop types in the Delicias scheme, Rio Conchos .....	17
Figure 11: Annual rainfall for 2003 deducted from the TRMM satellite.....	18
Figure 12: Monthly variation of the precipitation in 2003 averaged for the Rio Bravo Basin and interpreted by the TRMM satellite.....	19
Figure 13: Annual variation of near surface meteorological conditions (24-h air temperature) for 3 selected weather stations in 2003.....	21
Figure 14: Annual variation of near surface meteorological conditions (24-h air humidity) for 3 selected weather stations in 2003.....	21
Figure 15: Determination of air temperature lapse rates necessary for surface gridding...	22
Figure 16: Gridded values for 24-h average air temperature on MODIS overpass day August 18 (2003) .....	23
Figure 17: Example of solar radiation estimations from geostationary GOES visible satellite data.....	24
Figure 18: Remote sensing measurements procedures for the determination of spatially distributed ET fluxes.....	29
Figure 19: Major hydrological processes described within SWAT .....	31
Figure 20: Schematic diagram of the partitioning of infiltration into sub-surface water fluxes after water uptake by roots have taken place .....	32
Figure 21: Schematic representation of shallow and deep aquifers in SWAT .....	32
Figure 22: Parameterization of crop production processes for estimating crop yield .....	33
Figure 23: Watershed and 303 sub-basin boundaries for the SWAT model .....	34
Figure 24: Distribution of annual accumulated evapotranspiration (ETact) computed with the SEBAL model and MODIS images. ....	36
Figure 25: Variation of monthly actual and reference ET .....	37
Figure 26: Spatial variation of the annual ET in a river section .....	38
Figure 27: Volumetric evaporative depletion of water resources by land cover type .....	40
Figure 28: Accumulated monthly rainfall (TRMM) and ET (MODIS).....	41
Figure 29: Spatial variation of soil moisture in the upper 1 meter of soil.....	42
Figure 30: Streamflow stations.....	44
Figure 31: Annual total biomass production computed with the SEBAL model based on MODIS images .....	45

---

Figure 32: Crop classification in the Delicias Irrigation District in the Rio Conchos (Chihuahua) based on 250 m MODIS images .....	49
Figure 33: Landsat false color composite of the progression of crops.....	50
Figure 34: Landsat false color composite of the progression of crops.....	51
Figure 35: 24-h Actual evapotranspiration on July 15 (2003) based on SEBAL and Landsat images.....	52
Figure 36: Annual accumulated $ET_{act}$ for all agricultural fields in the Delicias Irrigation District.....	53
Figure 37: Frequency distribution of annual $ET_{act}$ of irrigated crops in the Delicias Irrigation District (2003) based on SEBAL and Landsat/MODIS images .....	54
Figure 38: Accumulated biomass production of irrigated crops in the Delicias Irrigation District.....	54
Figure 39: Frequency distribution of biomass production of irrigated crops in the Delicias Irrigation District based on SEBAL and Landsat/MODIS images.....	55
Figure 40: Analytical relationship between biomass production and ET for all plots located on the Landsat path 31 image .....	57
Figure 41: Scatterplot of reference ET values of both models (2003) .....	59
Figure 42: Spatial distribution of reference ET across the Rio Bravo Basin (2003) for both models.....	60
Figure 43: Spatial distribution of actual ET across the Rio Bravo Basin (2003) for both models.....	60
Figure 44: Scatterplot of actual ET values of SEBAL and SWAT. Annual values averaged for sub-basins are shown.....	61
Figure 45: Location of 23 sub-watersheds in the Rio Bravo Basin.....	62
Figure 46 Location of the major irrigation centers in the Rio Bravo Basin.....	66
Figure 47 Location of the major irrigation centers in the Rio Bravo Basin.....	67

---

# 1. Introduction

## 1.1 Background

Extensive irrigation projects carried out in the 1940s and 1950s greatly expanded Mexico's cropland, especially in the north. The Government created areas of intensive irrigated agriculture by constructing storage dams across the valleys of the Rio Grande, and by tapping subterranean aquifers. These water-control projects allowed Mexico to expand rapidly its total land area under cultivation. Between 1950 and 1965, the total area of irrigated land in Mexico more than doubled, from 1.5 million hectares to 3.5 million hectares. Despite a slowdown in the development of irrigated land after 1965, the total irrigated area had expanded to more than 6 million hectares now.

Due to the fast track development of irrigation schemes, Mexico has now critical and urgent water related problems including the overexploitation of surface water and groundwater resources in regions, where most of the population and most of the GDP is generated. The present situation is clearly not sustainable in the medium and long term. If not addressed soon, this situation will become an obstacle to continued economic development and will have serious social impacts including the possible abandonment of important parts of the country by significant parts of the population.

Mexico is trying to solve the water and environmental problems by improving irrigation efficiencies using the argument that efficient systems reduce the reliance on water resources. At all levels, including producers, consultants and high level policy makers, the notion is that doubling irrigation efficiency from the current 35 % to say 70% is the gateway for solving water scarcity. The risk is that this goes at the cost of more comprehensive ET, which physically implies that more water is pumped via crops into the atmosphere. It is time to introduce the concept of "real" water savings or ET reduction in Mexico, because water that is not evaporated remains physically present in the basin. Water resources planning in basins and aquifers needs to look at options of controlled EvapoTranspiration (ET), i.e. an ET rate that is not harmful for overdraft and other water user sectors. Any reduction in ET implies that more water resources remain available for downstream water user groups. This approach of planning evaporative depletion is known as ET management.

The National Water Law, amended in April 2004, mandates the development and implementation of Integrated Water Resources Management Programs (IWRMPs) in overexploited basins and aquifers, with the objective of achieving sustainable water resources management and use in these areas. Overexploitation of surface water occurs when environmental water demands (environmental flows, wetlands, lakes, coastal zones) can not be met. The Mexico Integrated Management of Basins and Aquifers, P082950, currently under preparation, will assist the Mexican Government to develop and implement IWRMPs in selected areas with critical overexploitation problems including the Rio Bravo basin.

Mexico has a number of policies and subsidies that incentivize overuse of water resources, particularly for growing low-value highly-consumptive irrigated agricultural crops (wheat, corn, sorghum, alfalfa) and the effect of these subsidies on downstream water availability was not properly realized when introducing these incentives. Now it is realized that vast amounts of scarce water are transported via crops into the atmosphere with very little economic benefits.

The World Bank is providing arguments on the environmental damage that these policies and subsidies are causing. Institutional changes are required along with sustainable availability of the water resources. The World Bank assists the Water Sector in Mexico with their formidable challenges to create sustainable conditions and keeping pace with rural economic development through various projects:

- Water Resources Management Project (PROMMA) 1996-2004
- Irrigated Agriculture Modernization Project (PMIR) 2004-2008
- Integrated Management of Basins and Aquifers Project (GICA) 2007-2010
- Water Rights Adjustment Project (PADUA) 2008-2011

The Rio Bravo is selected as an example to develop fresh ideas on achieving sustainable conditions. It is a case study with relevant outputs for all other basins in the semi-arid and arid zones of Mexico. The Rio Grande basin lies within North America's largest desert, the Chihuahuan Desert and holds one of the U.S.'s longest rivers, the Rio Grande (see Figure 1). The Rio Grande transverses across 5 states in Mexico (Chihuahua, Durango, Coahuila, Nuevo Leon and Tamaulipas) and 3 states in the US (Colorado, New Mexico, Texas).

Modern analytical tools such Remote Sensing, GIS and simulation models can help to swiftly obtain data to support the water management decision making process (e.g. Menenti et al., 1989; Bastiaanssen et al., 1992; Droogers and Bastiaanssen, 2002; Ines and Droogers, 2002; Droogers and Kite, 2002). A diagnosis of the Rio Grande has been made to demonstrate the current conditions of the resources for very vast areas with minimum data sets.

The objectives of this study are:

- Quantify differences between diversion, abstraction, depletion and return flow in the irrigation sector, and show that these flows have different management options, and that 'water use' is a misleading terminology
- Show that improvement of local irrigation efficiencies does not form a solution for sustainable water resources management in the basin context because the total efficiency at basin level will remain unaffected
- Introduce concepts of evapotranspiration management and real water savings, along with water productivity analysis
- Quantify agricultural and environmental water consumption and assess environmental water needs
- Investigate possibilities of introducing land cover changes and apply basin water resources planning methodologies
- Create awareness of technical possibilities to improve the water resources knowledge base from remote sensing data couple to simulation models



**Figure 1: Political division of the Rio Grande/Bravo basin**

## 1.2 Brief description Rio Bravo Basin

The Rio Bravo originates from the San Juan Mountains of Colorado at an elevation 4267 m, as a clear spring and snow-fed mountain stream. The river is referred to as Rio Grande in the US. The river cuts through the middle of New Mexico to the twin cities of El Paso and Ciudad Juárez, at the junction of Chihuahua (Mexico) and Texas (US). At that point, the Rio Grande becomes the international boundary between the United States and Mexico. The river empties into the Gulf of Mexico.

The Rio Bravo actually carries relatively little water compared to other rivers of its length. The 3,154 km long river is one of the longest rivers in the United States, and the 24<sup>th</sup> longest in the world. The Rio Grande/Rio Bravo and its tributaries drain a basin of some 656,100 km<sup>2</sup>, about 48% of which lies in Mexico. The average annual precipitation in the high mountain valleys of the Rio Grande’s headwaters can exceed 1250 mm. More downstream, as the river enters the Chihuahuan Desert, annual precipitation can drop as low as 200 mm. As water losses increase (through evaporation, plant transpiration and lateral seepage), and water yields from the contributing watershed decrease by increased water resources development and crop consumptive use, the river loses flow. While this is a natural process for rivers that traverse an arid region, the added human diversions of water

has actually caused the Rio Bravo to completely lose flow along certain reaches (from El Paso until the confluence with the Rio Conchos).

Water use and allocation has become a major political, social and economic issue in the entire basin. There is water demand from several categories such as (i) municipal (both residential and commercial water uses), (ii) irrigation, (iii) livestock, (iv) manufacturing, (v) hydropower, (vi) fish and (vii) mining. Water diversion accounts for 80 to 90 percent of the river's average annual flow.

Several international border disputes have been raised and were settled by various treaties. Under a 1944 treaty, Mexico must send an average of  $430 \cdot 10^6 \text{ m}^3$  (350,000 acre-feet) of water to the United States from its Rio Bravo tributaries annually. In return for the water, the United States gives Mexico  $1845 \cdot 10^6 \text{ m}^3$  (1.5 million acre-feet) of water from the Colorado River each year.

In a nutshell, the major problems in the Rio Bravo basin are:

- Rapid population growth. Between 1990 and 2050, population is expected to increase by 228%, hence there will be more human and industrial water demands and a fierce competition with the agricultural sector
- Expanding irrigation. Irrigation is intensifying due to the introduction of modernized systems and this unprecedented growth reduces stream flow
- Depleted aquifers. Groundwater abstraction is increasingly used as a source of water to augment declining surface water resources; extraction exceeds recharge, essentially in areas with irrigation activities
- Environmental water stress. The water demands from aquatic ecosystems, wetlands, lakes, basin dilution and endangered fish species cannot be met
- Deforestation. Wood logging in the Sierra Madre in Chihuahua exacerbated droughts and caused peak flows with erosion and land degradation as a consequence

### 1.3 Scope and deliverables

This study estimates evapotranspiration (ET), soil moisture and biomass growth values for the entire Rio Bravo basin in northern Mexico for January to December 2003 using the Surface Energy Balance Algorithm for Land (SEBAL) developed by WaterWatch. SEBAL is a remote sensing algorithm that estimates reference ET, potential ET and actual ET without *a priori* information on the hydrological, water management and land cover situation. A more detailed analysis will be conducted including crop specific analysis such as yield, ET and other related water flows for the Delicias District in the Rio Conchos (Chihuahua). The computations include:

- Creation of a time series with 15 day intervals of evapotranspiration, biomass growth and soil moisture with a resolution of 1-km (on the basis of bi-monthly MODerate resolution Imaging Spectrometer MODIS images)
- Production of a single high resolution Landsat path/row combination with evapotranspiration, biomass growth and soil moisture with a resolution of 30 m (on the basis of 5 Landsat images)
- Integration of MODIS and Landsat data resulting in crop yield and water productivity maps with a resolution of 30 meters for a single year in the Landsat track/frame combination chosen

This study includes also the preparation of a preliminary distributed hydrology Soil Water Assessment Tool (SWAT) model for the Rio Bravo. SWAT<sup>1</sup> was developed primarily by the United States Department of Agriculture (USDA) to predict the

---

<sup>1</sup> <http://www.brc.tamus.edu/swat/index.html>

---

impact of land management practices on water, sediment and agricultural chemical yields in large complex watersheds with varying soils, land use and management conditions over long periods of time (Neithsch et al., 2001). The SWAT model has been extensively used, is in the public domain and can be considered as becoming the de-facto standard in spatial decision support systems. SWAT will utilize the remotely sensed ET estimations in order to calibrate the soil and vegetation parameters of the model. FutureWater ([www.futurewater.nl](http://www.futurewater.nl)) has applied the SWAT model for the Rio Bravo Basin because they have developed procedures to calibrate this complex model for vast regions with scarce data sets (e.g. Hai Basin, China).

This study will be carried out in two phases. The first phase will be undertaken until March (2006) and will include the image analysis and SWAT modeling. The second phase deals with interpretation and scenario analysis by Mexican water managers.



## 2. The Rio Bravo Basin

### 2.1 Physical-geographical setting

This study focuses on the Rio Bravo elapsing from El Paso to the Gulf of Mexico. The tributaries of Rio Conchos (Mexico) that confluences the Rio Bravo on the Right Bank and the Rio Pecos (New Mexico) on the Left Bank, are included in this study. Figure 2 delineates the study area of 448,344 km<sup>2</sup>, which is 68% of the total basin (656,100 km<sup>2</sup>). The remaining 32% lays in Central and Northern New Mexico (US) and in Southern Colorado (US). The Mexican side of the Rio Bravo is completely encapsulated in the study area (see Figure 1). The US side is included for properly simulating watershed behaviour.

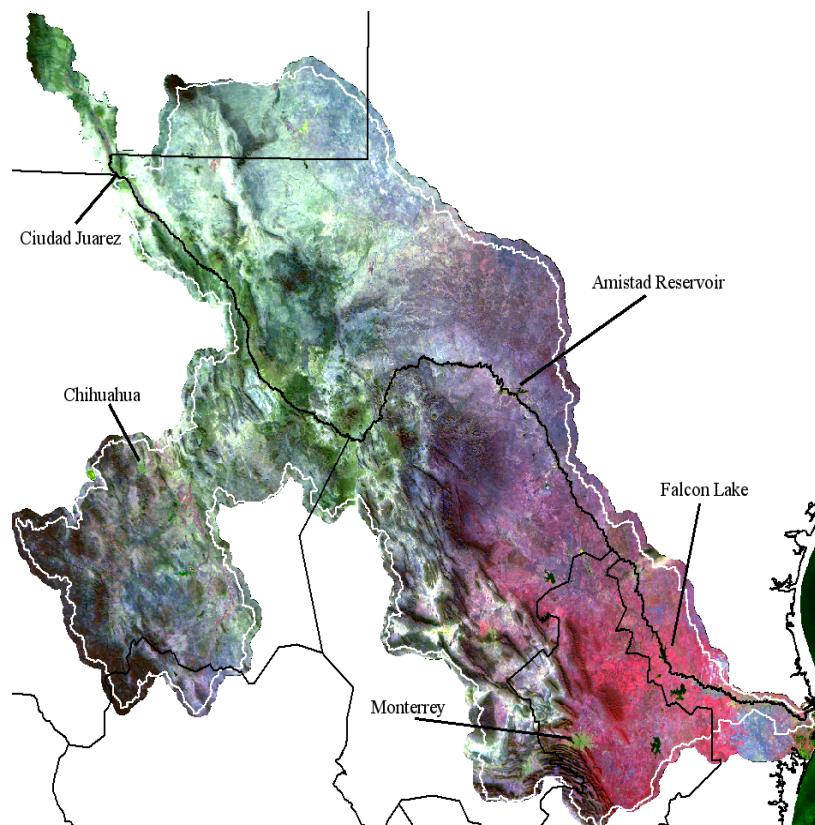


**Figure 2: False color MODIS image acquired on November 29<sup>th</sup> (2003) with basin states borders being superimposed. The corner coordinates are Upper Left XY: 529,000; 1,270,000 and Lower Right XY: 1,593,000; 295,000. The false color images consists of, red=band 2, green=band 1 and blue=band 6**

The Mexican Sierra's (3600 m elevation) form the continental water divide between the Eastern part draining into the Gulf of Mexico and the Western part draining to the Gulf of California. The eastern part of Chihuahua, most of Coahuila State and entire Nuevo Leon drains to the Rio Bravo, except some inland basins. A digital elevation model (DEM) is required to delineate the Rio Bravo into sub basins and to determine the direction of flow. The HYDRO1K Digital Elevation Model is used in this project (see Figure 3). The HYDRO1K dataset is a 1 km resolution pre-processed for

hydrological application DEM based on the GTOPO30<sup>2</sup> elevation dataset. For the Landsat analysis, the 90 m resolution SRTM DEM has been used (<http://srtm.usgs.gov>). The agreement between the DEM and raw MODIS images is striking: The reflectivity of the flood plain seems to change with elevation, and this draws the attention that the soil types and hydrological regime might be totally different. It is like having one basin but two hydrological systems. There are 22 MODIS images collected for this study, and Figure 2 is just one example. The stack of all MODIS images will be used to infer a land cover map that is fine tuned to the project.

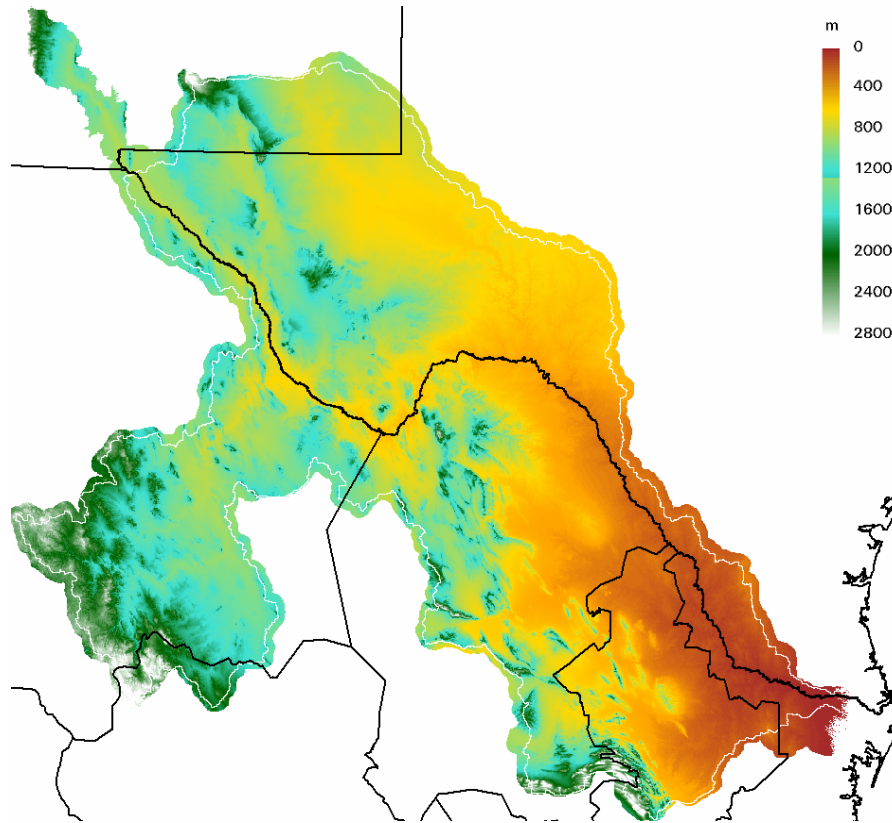


**Figure 3: GTOPO30 digital elevation model of the Rio Grande basin with the drainage network being superimposed (source: USGS)**

The occurrence of soil types is to a large degree associated with the presence of geological formations and mountains. Arable crops are cultivated on the alluvial soils with a good fertility and where water resources are present, and these conditions are met in the lower part of the basin and in the valleys of the Rio Grande and Rio Conchos. The soil map is used for the assignment of soil physical properties such as the soil water holding capacity and (unsaturated) soil hydraulic conductivity. The properties are used in SWAT for the computation of unsaturated soil water flow with the Darcy equation.

<sup>2</sup> <http://edcdaac.usgs.gov/gtopo30/gtopo30.asp>

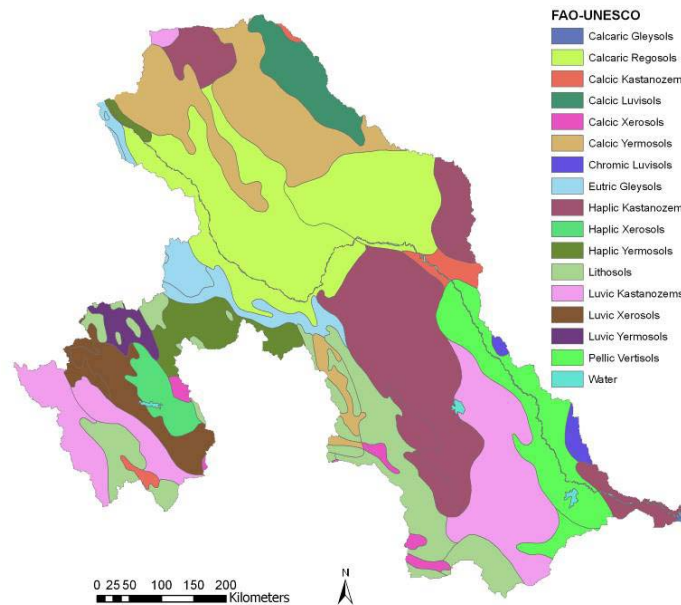


**Figure 4: Soil map of the Rio Bravo Basin (source: FAO)**

The Rio Grande aquifer system is a large system of aquifers in alluvial basins in the southwestern United States and Mexico. Although a large volume of water is stored in the basin deposits, pumpage easily exceeds natural recharge and leads to long-term depletion of the stored water. Ground water has been developed along the flood plain of the Rio Grande, where it is used mostly for irrigation; in other parts of the basin, groundwater is pumped only for livestock watering and domestic use. The Presidio Basin is in the western part of Presidio County and contains the southernmost aquifer of the Rio Grande aquifer system in Texas. Groundwater flows from the Presidio basin margins to the Rio Grande, where it is discharged either by ET or by seepage to the river. The extent of this international water transfer will be calculated later.

Figure 5 shows the location of the major aquifers in the entire State of Mexico. The aquifers in the Rio Bravo watershed include the Valle de Juarez along the river bank. This area is even visible in the false color composite depicted in Figure 2. Chihuahua State is further housing some small aquifers and the vast aquifer near Ciudad Delicias. The latter center is famous for its irrigated fruits and pecan nuts, among others. The most downstream aquifers lays East of Monterrey, where agriculture takes place. This area receives a substantial amount of rainfall (> 700 mm/yr), and has supplementary irrigation from groundwater resources during the dry season. There is considerable irrigated agriculture on the piedmont north and east of the city,. Local rivers provide hydroelectricity power.

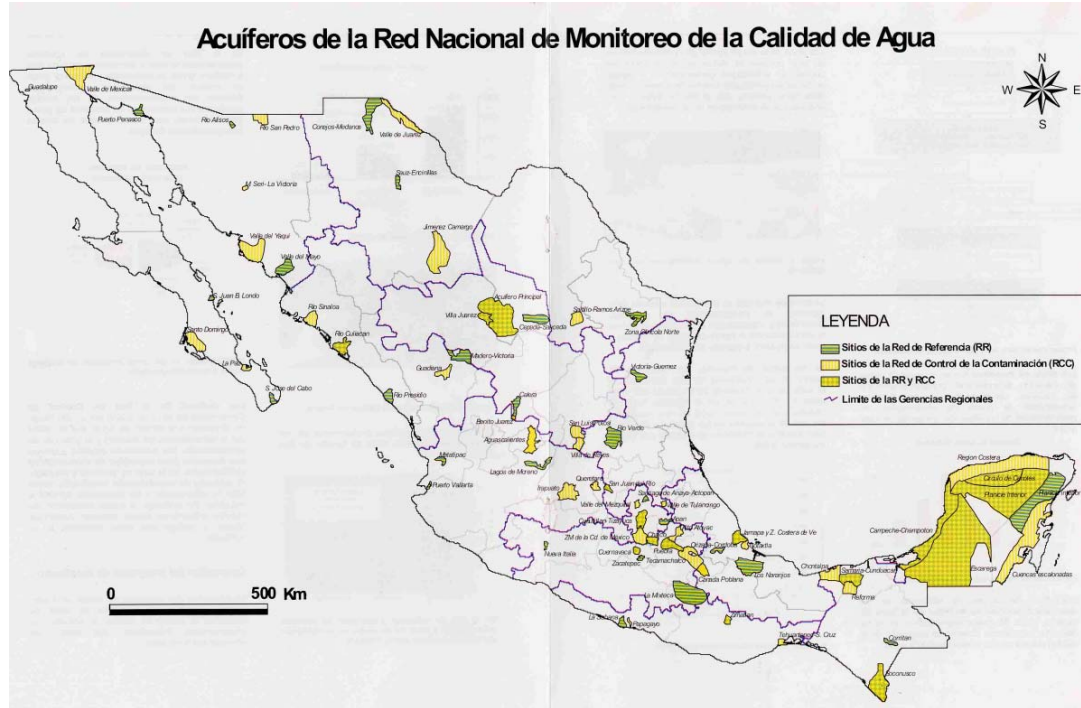
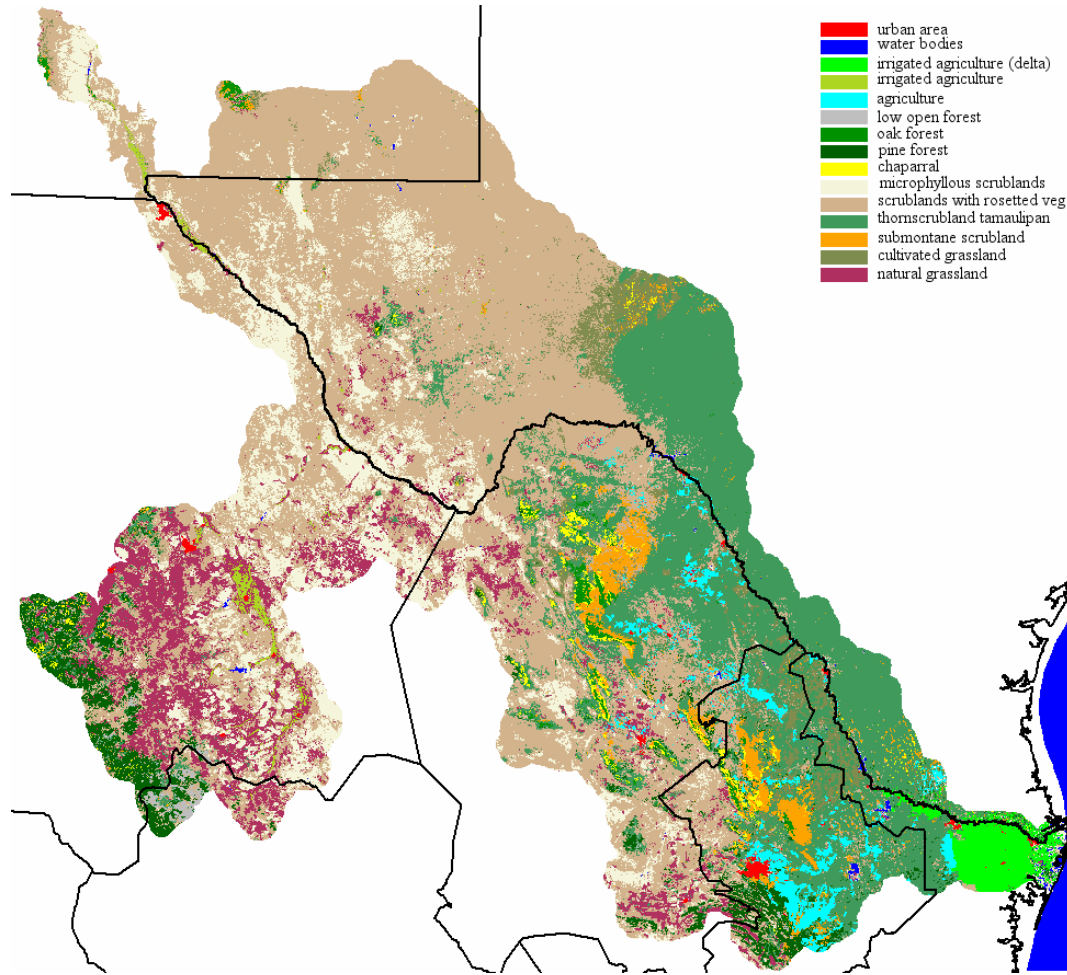


Figure 5: Simplified aquifer map of Mexico (source: CNA, 1999)

## 2.2 Land cover

Fractional vegetation cover is the percentage of soil that is covered by vegetation, and it is linearly related to Normalized Difference Vegetation Index (NDVI). MODIS bands 1 and 2 have a 250 m spatial resolution, and the NDVI values are based on these bands. The 22 NDVI images are well spread throughout the year, and this allows us to distinguish land cover classes on the basis of differences in NDVI during the annual cycle. In this way, a land cover map that is similar in definition, precision and methodological design at both sides of the international border can be compiled. A standardized land cover map for the basin is a pre-requisite for the SWAT hydrological study. An unsupervised classification procedure on the NDVI time profiles has been applied, resulted into 15 clusters that exhibit similar vegetation dynamics across the year within each class. Initially, a general distinction between water, vegetated and non-vegetated areas was prepared. Thereafter, the class of vegetated surfaces was further broken down into more land cover classes representing ecosystems.

Each land cover cluster has been named after the existing land cover classification of the Instituto Nacional de Estadística, Geografía e Informática (INEGI) and the Instituto Nacional de Ecología (Uso de Suelo y vegetacion, agrupado). The latter land cover map of 1996 (1:1,000,000) covers whole Mexico. The results are displayed in Table 1. The resulting land cover map with a 250 m resolution is presented in Figure 6.



**Figure 6: Land cover map based on 250 m MODIS time profiles of Normalized Difference Vegetation Index (NDVI) and an unsupervised land cover classification**

The land cover at higher elevation consists of timber and brush forest that capture sufficient rainfall to survive dry seasons. The dry gently sloping terrain of the Chihuahuan desert are mainly occupied by woodland canopies, mesquite (*Prosopis Slandulosa*), sage brush, senescent grasses and forage types of ecosystems. Mesquite shrubs grown on coppice dunes and can at places dominate the arid landscape. Grass communities dominated by black grama (*Bouteloua Eriopoda*) have been susceptible to shrubs. *Opuntia* forage is abundant and widely distributed for cattle, sheep and goats. Sixty percent of this forage is present in Chihuahua state in the land cover class scrubland with rosetted vegetation. The productivity of such ecosystem is relatively low and unstable, and strongly dependant upon climate, water, nutrients and management conditions. The largest parts are scrubland with rosetted vegetation (45.6 %) and microphyllous scrublands (12.1 %). Water bodies occupy 2.05% of the study area, and this relatively large number reveals that the Rio Bravo and its tributaries are highly regulated.

**Table 1: Land cover classification related to Figure 6**

Land cover (English)	Land cover (Spanish)	Area [ha]	Area [%]
urban area	zona urbana	149,744	0.4
water bodies	agua	52,150	0.1
irrigated agriculture (delta)	agricultura de riego	678,138	1.5
irrigated agriculture (valley)	agricultura de riego	261,775	0.6
supplemental irrigation	agricultura	796,975	1.8
low open forest	bosque bajo abierto	162,831	0.4
oak forest	bosque de Encino	259,738	0.6
pine forest	bosque de pino	1492,825	3.4
chaparral	chaparral	365,150	0.8
microphyllous scrublands	matorral desertico microfilo	5335,169	12.1
scrubland with rosetted vegetation	matorral desertico rosetofilo	20045,525	45.6
thornscrubland tamaulipan	matorral espinoso tamaulipeco	8600,625	19.6
submontane scrubland	matorral submontano	938,975	2.1
cultivated grassland	pastizal cultivado	1493,875	3.4
natural grassland	pastizal natural	3334,281	7.6
<b>total</b>		<b>44,834,481</b>	<b>100.0</b>

It is remarkable to note that more than half of the basin (57%) in the Northern part of the Rio Bravo is occupied by desert-type scrubland (matorral desertico). Another 19 % is occupied by thorn scrubland (matorral espinoso). Natural and cultivated grassland cover almost 11%, while less than 5% of the study area is occupied by forest.

Only 3.9 % of the basin is occupied by agricultural land. The 1,736,8888 ha of irrigated land (delta, valley, supplemental irrigation) consists partially of rainfed (especially in the downstream end of the basin) and it includes the irrigated lands South of Elephant Butte in New Mexico (US). Hence, our estimates of irrigated acreage exceed the census data because our data includes part of US. Corn and sorghum can be both irrigated and rainfed and this distinction is difficult to make from satellite spectral reflectances, especially when the crop received supplemental irrigation. It is likely that some of the rainfed agriculture receives supplemental irrigation to enhance the emergence of crops before the monsoon rains set on. Hence, the Rio Bravo hosts a fragile ecological system interchanged with scanty agricultural developments.

### 2.3 Agriculture and Irrigation synopsis

The Rio Grande first provided for crop irrigation by the Pueblo Indians, who settled along the main river and its tributaries. One explorer who entered New Mexico in 1583 reported finding "many irrigated corn fields with canals and dams, built as if by the Spaniards." The Pueblos of New Mexico currently use some of the same ancient irrigation ditches, or acequias, that their ancestors used centuries ago. A system of hydraulics as well as of customs and laws, acequias are the oldest living public works system in North America.

Mexico ranks number 5 on the list of international irrigation countries, and hosts according to the UN statistics a total of 6.2 million hectares with irrigation facilities. About half of these systems correspond to 80 bigger irrigation schemes ([www.icid.org/cp\\_mexico.html](http://www.icid.org/cp_mexico.html)). On a substantial percentage of this land, water supply occurs via groundwater wells (32 %). It is estimated that 18.4 km<sup>3</sup> of groundwater is extracted from the Mexican undergrounds for irrigation purposes.

The major Mexican irrigation systems can be found along the river courses of the Conchos, Pecos and the main course of the Rio Bravo. The main US agricultural areas can be found along the rivers Rincon and Mesilla Valleys in southern New

Mexico, the El Paso and Juarez Valleys in Texas, and the Rio Bravo Valley below Amistad Dam. A map of the irrigated areas is shown in Figure 7.

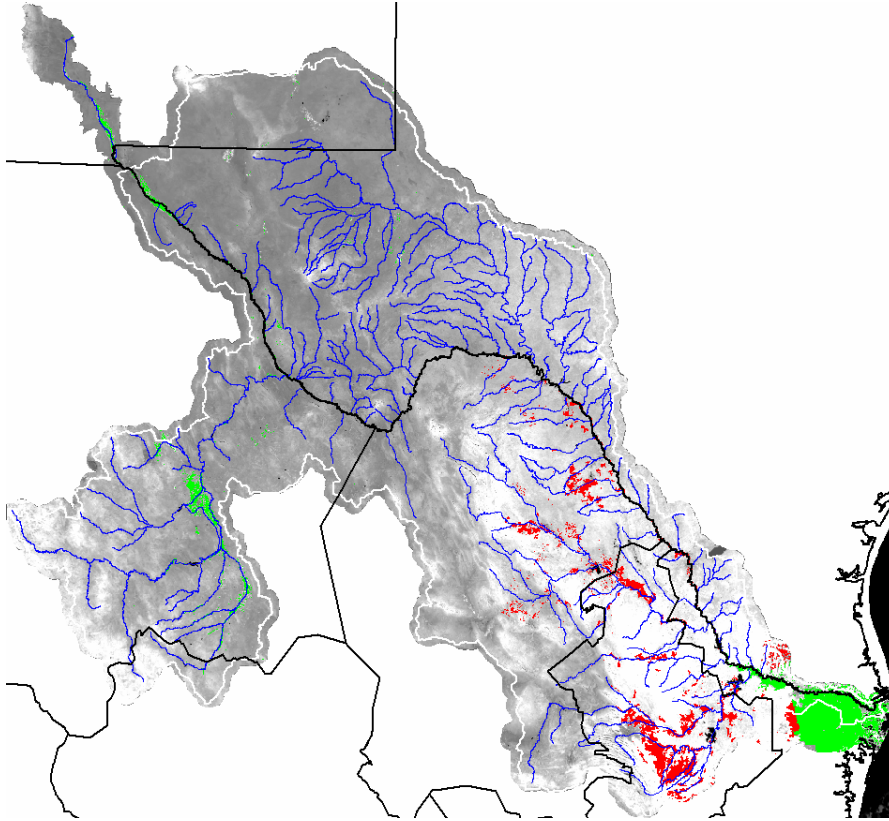


**Figure 7: Geographical distribution of irrigated areas in the Rio Bravo Basin based on the 3 land cover classes with irrigation. The red areas are supplemental irrigation and contain large portions of rainfed crops. The location of the irrigated areas often match with the presence of aquifers**

The breakdown of irrigation activities per State are specified in Table 2. The census data suggests 1.4 million ha to receive irrigation water in the 5 states that lay within the Rio Bravo. Our estimates of irrigated acreages stem from the irrigated area map, being superimposed with the administrative state boundaries and contains 1,735,850 ha. The Rio Bravo does not drain entire states, and part of the census data relates to irrigation schemes located in adjoining basins. New Mexico and Texas occupy together also 173,651 ha in the irrigated area map.

**Table 2: Distribution of irrigated area by sub-national unit for the Rio Bravo basin (source: ICID Mexico)**

<b>Administrative unit</b>	<b>Irrigated area census data (entire state 2000) (ha)</b>	<b>Irrigated area remote sensing data (Rio Bravo basin 2003) (ha)</b>	<b>Remarks</b>
Chihuahua	370,372	191,969	Comarca Lagunera lies outside Rio Bravo basin
Coahuila	249,652	231,669	Good agreement
Durango	147,750	2,119	Durango State encompasses 5% in Rio Bravo
Nuevo Leon	163,202	461,350	65% rainfed crops
Tamaulipas	478,155	675,094	30% rainfed crops
New Mexico		29,138	In US
Texas		144,513	In US
<b>TOTAL</b>	<b>1,409,131</b>	<b>1,735,850</b>	

The irrigated harvested area increased 35% between 1980 and 1999. Despite the great pressure on the Rio Bravo water system, crop irrigation and production have continued to grow in the Rio Conchos Basin. Advanced methods of irrigation are upcoming, the most popular being sprinklers, low pressure systems using multi-gated pipelines, buried drip pipes and drip irrigation. An aggressive program is being implemented to mechanize farm irrigation systems. This program boosts 20 to 30% of total irrigated area to be pressurized. It is expected to increase the irrigation efficiency from the current 35% to 47% in the future.

According to certain sources, Chihuahua has a net gain in irrigated area by vegetables, melons, fruits and nuts. It is estimated that irrigated alfalfa acreage increased 11% from 1999 to 2001 (Parr Rosson et al., 2002). The same authors claim that use of wells for irrigation has – accordingly – increased because producers have switched from crops that use less water to crops that use more water, causing total water use to rise by more than the increase in total irrigated acreage.

A closer inspection was made to better appraise the recent changes in the irrigated areas. The difference of annually averaged fractional vegetation cover (ranging from 0 to 100 %) between 1999 and 2004 was investigated by means of 10 day interval SPOT-Vegetation NDVI values. Figure 8 demonstrates that the Juarez Valley has clumps that contain less irrigated land in 2004 as compared to 1999, besides areas that do not exhibit any change. El Paso is converting irrigation water to municipal use and this transfer of expected to grow. This also happens in the Mesilla Valley between Las Cruces and El Paso in New Mexico (US). The irrigated acreages in the Juarez Valley are thus dwindling.

Delicias Valley exhibits a different picture with degrading areas (in red) and newly irrigated areas (in green). In the vicinity of Santa Rosalia de Camargo and North of Ciudad Delicias, new schemes can be spotted, because they could not be located during 1999. There is a shift towards growing alfalfa and sorghum to supply dairy farms and cattle feedlots in this area. More irrigation is underway in the central and northern areas of the Delicias District, and the required water resource are delivered from the Boquilla and Madero dams. The Delta of the Rio Bravo in Tamaulipas displays that irrigated cropland in the central part is shrinking and that simultaneously new land at the outskirts of the Delta are reclaimed and equipped for irrigation.

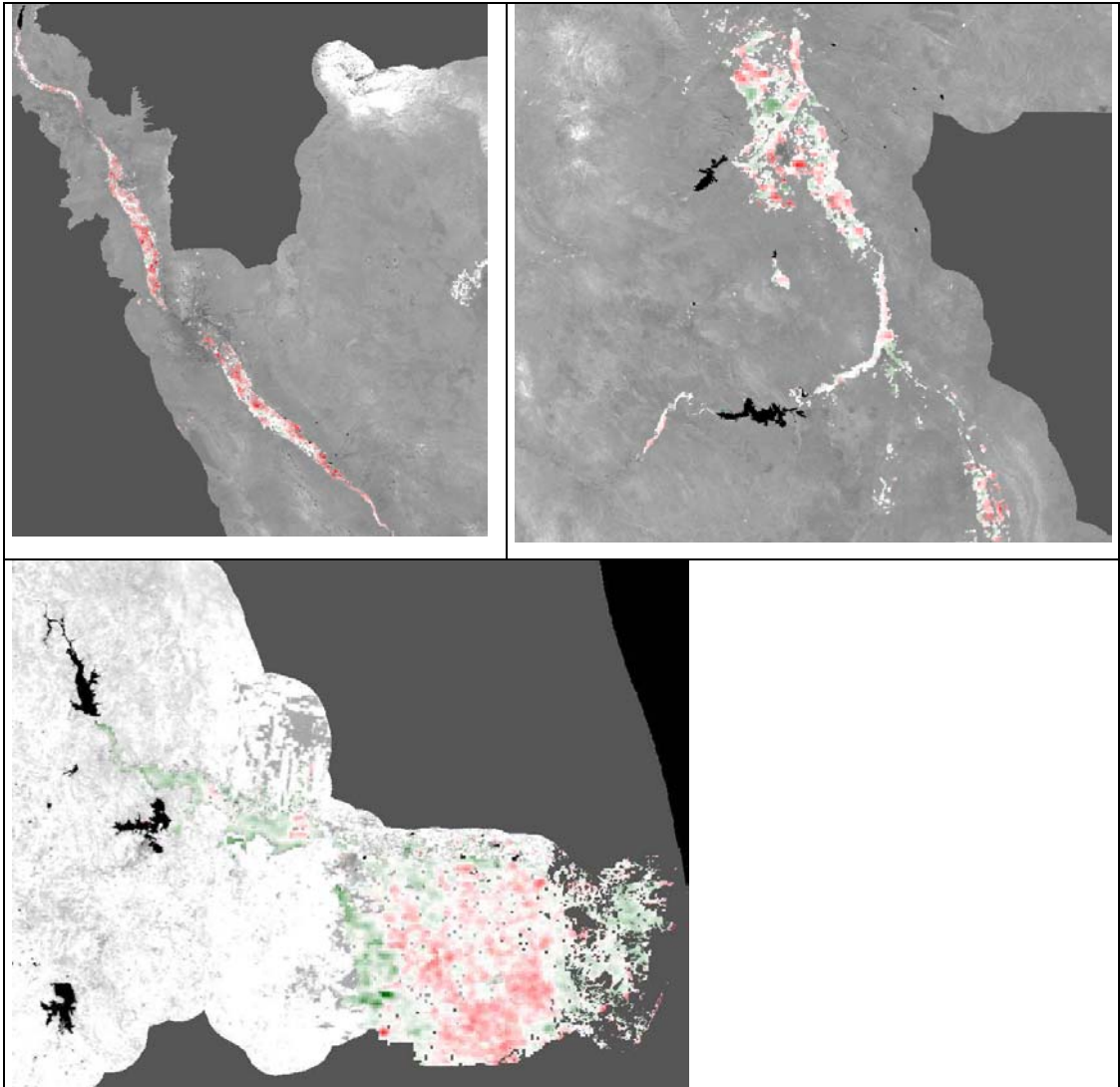


**Figure 8: Change in fractional vegetation cover in the major irrigated areas in the Rio Bravo. Green areas have become 30% greener and red areas 40 % more bare. White did not undergo noticeable changes. The SPOT-Vegetation satellite data with a 1 km spatial resolution and 10 day intervals**

To more systematically detect how much changes in irrigated land has occurred, the entire 1,735,850 ha area is exposed to a change detection. This time series is chosen because SPOT-Vegetation data was available for this period. The period 2000 to 2002 shows a dip in total irrigated acreage. The recent 2004 season show higher vegetation cover and it is 30% more green than in 2001. Certain policies to invest in modern irrigation systems seem to work! The average increment of fractional vegetatio cover for the 6 year period is 3.5% per year, and this number can be considered as a surrogate for irrigated acreage. Hence, the basin-wide irrigated area is still expanding.

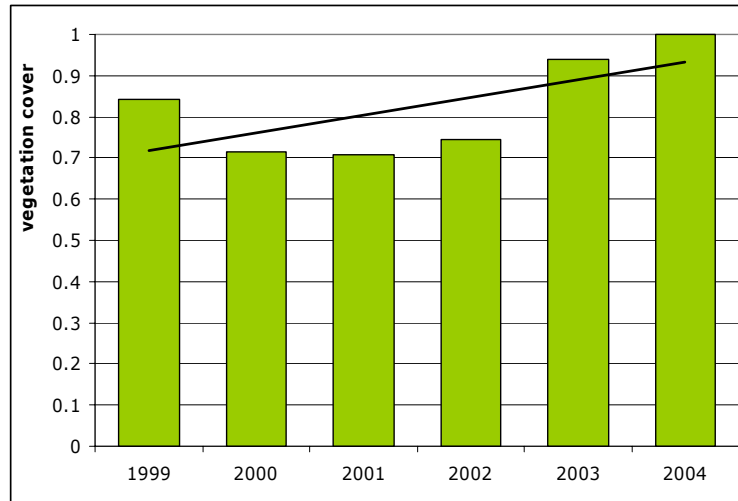


**Figure 9: Temporal changes of green cover in (supplementally) irrigated land (1,735,800 ha)**

The typical crops are cotton, corn, sorghum, alfalfa, citrus, sugarcane and vegetables. Most of the corn, the dominant crop in Mexico, goes into domestic livestock and poultry feed, with a little moving into export. Rio Conchos and West Texas specialize in cotton, peppers, onions, and pecans (a hard-shelled nut). Information of the growing season of corn is varying. USGS states that most corn is planted during a period referred to locally as the "first season", which stretches from October to June. This crop requires 210 days from seeding to maturity, and normal harvest time is May. Irrigation of corn is common, especially in the Northern part of Mexico.

(<http://www.fas.usda.gov/pecad2/highlights/2001/06/mex/mxtrep501b.htm>). Corn is also cultivated as a rainfed crop and in Spring-Summer and harvested in January and February.

For a better understanding of the complex Mexican cropping calendars, temporal profiles of biomass production for 10 crop classes in Rio Conchos around the town of Delicias are displayed in Figure 10. The biomass data is included only for the sake of discerning different crop types from MODIS images (not for productivity analysis). The classification into 10 classes was done by means of an unsupervised cluster analysis. The crops were labeled according to their biomass rhythm only, and no field inspection has taken place. The census data suggest 94,553 ha under irrigation, and Table 3 shows that our estimate of 101,006 ha is good.

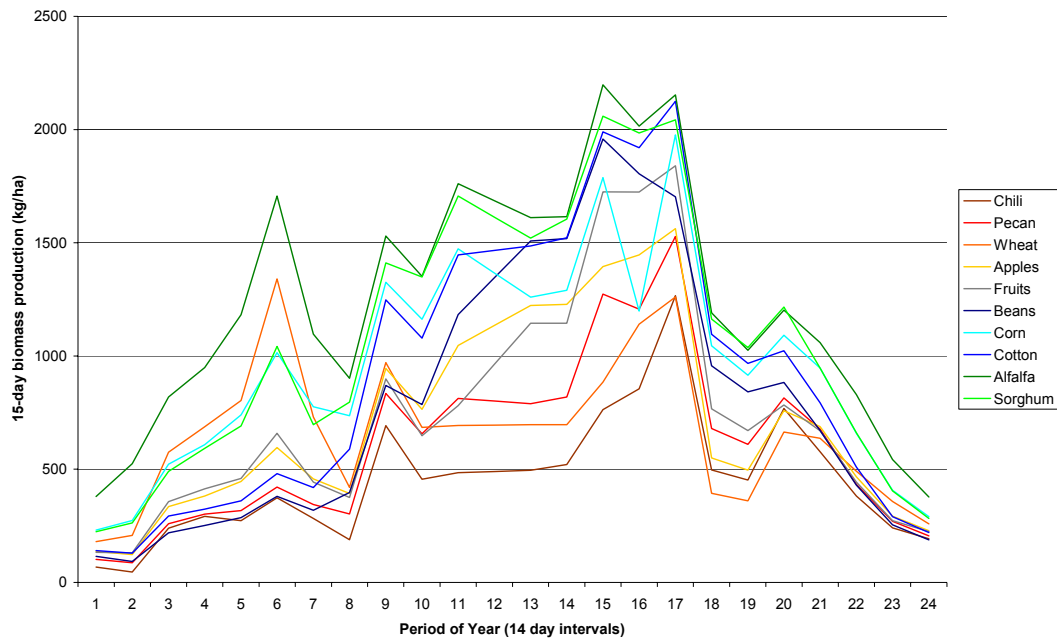


**Figure 10: Temporal profiles of the biomass production of discernable crop types in the Delicias scheme, Rio Conchos**

**Table 3: Crop-wise breakdown of the irrigated areas in Delicias Irrigation District (Rio Conchos) according to the temporal variability of the 15-day intervals of biomass production**

<b>Crop type</b>	<b>Acreage (ha)</b>	<b>Acreage (%)</b>
Chili	8,300	8.2
Pecan	11,737	11.6
Wheat	3,437	3.4
Apple	12,462	12.3
Other fruits	7,569	7.5
Beans	8,262	8.1
Corn	13,718	13.6
Cotton	10,381	10.3
Alfalfa	12,593	12.5
Sorghum	12,543	12.4
	<b>101,006</b>	<b>100</b>

The conclusion is that alfalfa, wheat, corn and sorghum are irrigated in the Winter and that the harvest takes place at the end of April. This agrees with the 'first season' that is essentially a dry winter season. An example of a Landsat false color composite acquired on 25 March (2003) is inserted in Figure 33 for showing the distribution of the Winter crops. The Summer crops are cultivated from May to September and the peak in crop biomass production occurs in August/September when crops benefit from rainfall. Perennial crops such as alfalfa, grapes and pecan nuts are green throughout the entire year.

## 2.4 Climatology

Monthly precipitation values have been retrieved from the Tropical Rainfall Measurement Mission satellite (TRMM) that is equipped with a C-band passive microwave imager dedicated for precipitation measurements at a spatial resolution

of 25 km. An advantage of TRMM measurements is the availability of a regular measurement grid throughout the basin, including reasonable estimates of rainfall in mountains. The global rainfall algorithm (3B-43) combines the estimates generated by combined instrument rain calibration (3B-42) and global gridded rain gauge data from CAMS, produced by NOAA's Climate Prediction Center and/or global rain gauge product, produced by the Global Precipitation Climatology Center (GPCC). The output is rainfall for 0.25x0.25 degree grid boxes for each month. For more details of the algorithm, go to <http://trmm.gsfc.nasa.gov/3b43.html> The average basin wide precipitation in the Rio Bravo for 2003 was 450 mm, being slightly more than the average value between 1997 to 2004 according to TRMM ( $\pm$  400 mm). It is essential to recognize that 2003 is an above average rainfall year. Most precipitation in the basin falls at either end of the river, as snow near its headwaters or as rain near its mouth. The annual rainfall in 2003 at the mouth near Matamoros was 920 mm. The highest precipitation ( $>1200$  mm) was received northeast of Monterrey in Nuevo Leon. These amounts of rainfall create a humid climate suitable to host crops.

The mountain ranges are a physical barrier for atmospheric air moving in from the Gulf of Mexico and the lower plain area receive windward rainfall regimes. In between origin and mouth, the Rio Bravo flows through a dry landscape. Figure 11 shows a clear northwest to southeast precipitation variation across the Rio Bravo basin. An exception to this regional trend are the Chihuahua mountains (3500 m) - that form the origin of the Conchos river - with an annual precipitation of 415 mm. The northern part of the study area near the twin cities of El Paso and Ciudad Juarez did not receive more than 100 mm in 2003.

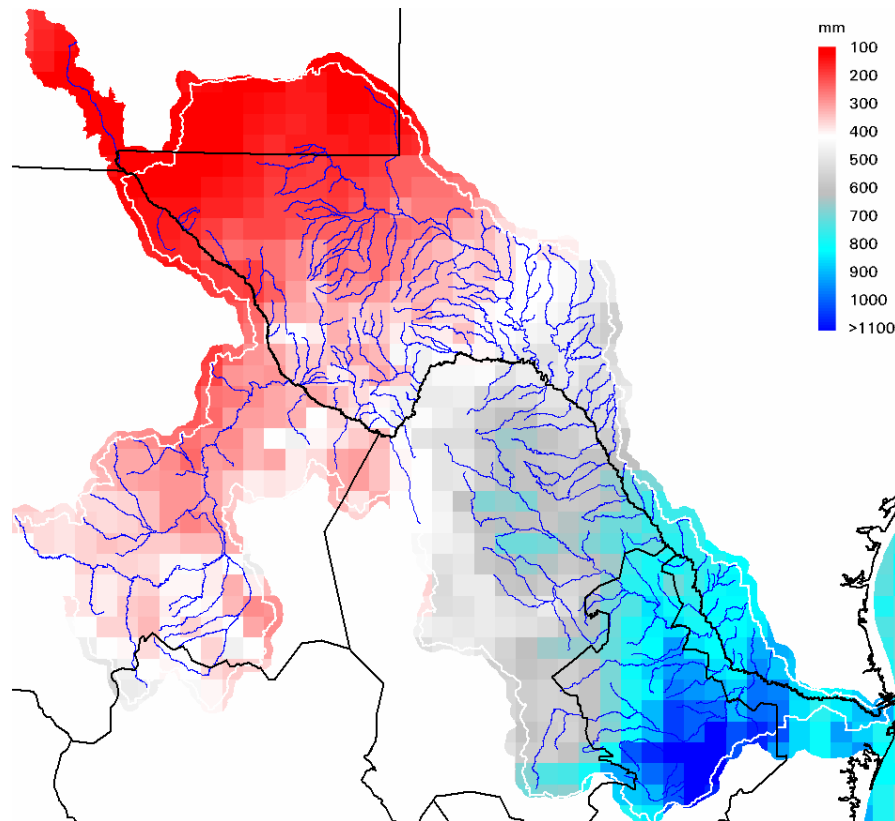


**Figure 11: Annual rainfall for 2003 deduced from the TRMM satellite**

The monthly variation of rainfall is demonstrated in Figure 12. The basin as a total behaves as a monsoonal system with scant rainfall during the Winter and well

developed rainfall during the Summer. The regional variations can be significant as shown in Figure 11.

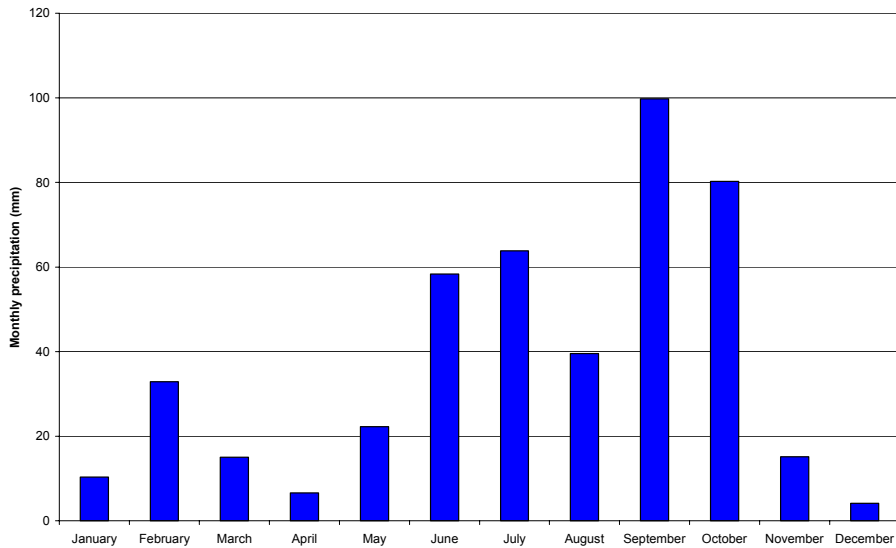


**Figure 12: Monthly variation of the precipitation in 2003 averaged for the Rio Bravo Basin and interpreted by the TRMM satellite**

Besides precipitation, the climatic system over the basin exhibits a significant spatial variation of air temperature and air humidity. Meteorological station measurements have been downloaded from [www.wunderground.com](http://www.wunderground.com). This site provided comprehensive data sets for 34 meteorological stations including mean air temperature  $T_{mean}$ ,  $T_{max}$ , and Relative Humidity  $RH_{min}$ ,  $RH_{max}$ . Whereas  $T_{mean}$ ,  $RH_{min}$  and  $RH_{max}$  (for computation of  $RH_{mean}$ ) are all used for the 24 hour computation of actual ET with the SEBAL model,  $T_{max}$  and  $RH_{min}$  are explored for instantaneous SEBAL calculations during the Aqua satellite overpass in the early afternoon.

**Table 4: Specification of meteorological stations used to infer the physical conditions of the near-surface atmospheric boundary layer on MODIS image acquisition days**

<b>Mexico Name</b>	<b>Latitude</b>	<b>longitude</b>	<b>United States Name</b>	<b>latitude</b>	<b>longitude</b>
Chihuahua University	28.7	-106	Artesia (NM)	32.8	-104.4
Matamoras	25.8	-97.5	Carlsbad (NM)	32.4	-104.2
Monterrey Airport	25.9	-100.2	Hobbs (NM)	32.7	-103.2
Nuevo Laredo	27.4	-99.6	Alamogordo (NM)	32.9	-105.9
Ciudad Juarez	31.6	-106.4	Truth of consequences (NM)	33.1	-107.2
Reynosa	26.0	-98.2	Ruidoso (NM)	33.3	-105.7
Culiacan	24.8	-107.4	Clovis (Cannon Air Force base)	34.4	-103.2
Mazatlan Airport	23.2	-106.3	Deming (NM)	32.2	-107.8
Zacatecas Airport	22.9	-102.7	Moriarty (NM)	35.0	-106.1
Tampico Airport	22.3	-97.9	Roswell (NM)	33.4	-104.5
			Las Cruces (NM)	32.3	-106.7
			Alice (TX)	27.7	-98.1
			El Paso (TX)	32.0	-106.6
			Brownsville (TX)	26.0	-97.5
			Corpus Christi (TX)	27.8	-97.4
			Marfa (TX)	30.3	-104.0
			San Angelo (TX)	31.5	-100.5
			Wink (TX)	31.8	-103.2
			Fort Stockton (TX)	30.9	-102.9
			McAllen (TX)	26.2	-98.2
			Laredo (TX)	27.5	-99.5
			Cotulla (TX)	28.3	-99.3
			Harlingen (TX)	26.2	-97.7
			Guadalupe Mountains National Park (TX)	31.8	-104.8

The annual variation of air temperature and air humidity is displayed in Figure 13 and Figure 14 for 3 different stations. Station Chihuahua (elevation: 1346 m) represent the mountain conditions. Station El Paso (elevation: 1162 m) represent the hot and high plateau deserts, and the Reynosa station (elevation: 36 m) is located on the coastal belt of the Gulf of Mexico. The coastal belt is warmer and more humid in both Summer and Winter (see Figure 13 and Figure 14). Chihuahua has due to the higher elevation the lowest temperature. Because of the large distance from the sea, and the low desert evaporation, the air humidity is low in Chihuahua. The lowest air humidity of 10% occurs during May before the Summer monsoons starts on. The climatology of El Paso is an average of these two extremes.

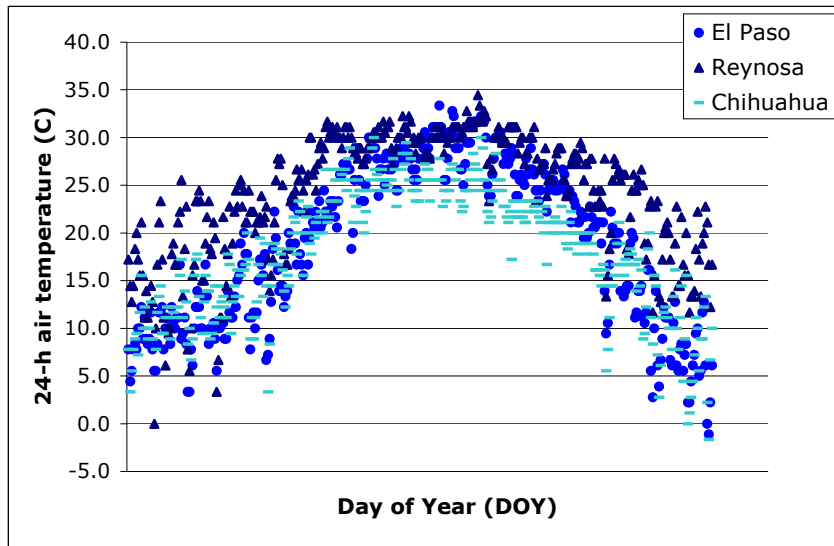


Figure 13: Annual variation of near surface meteorological conditions (24-h air temperature) for 3 selected weather stations in 2003

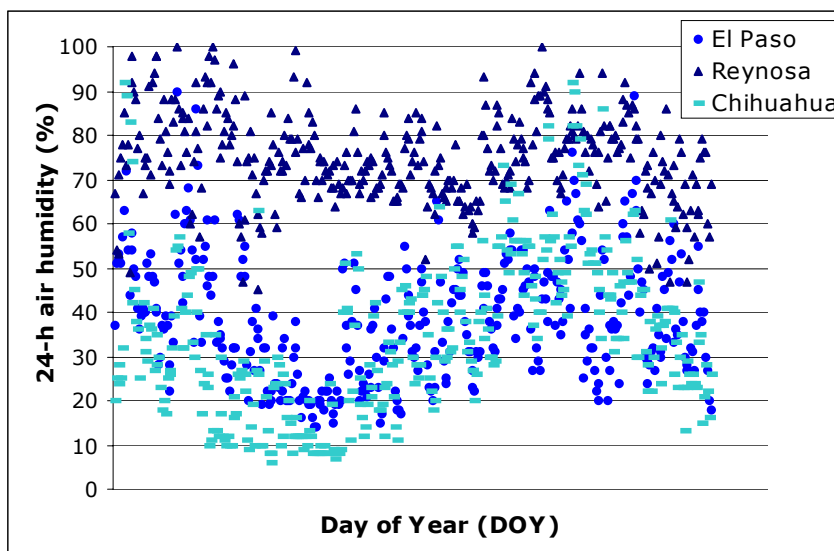
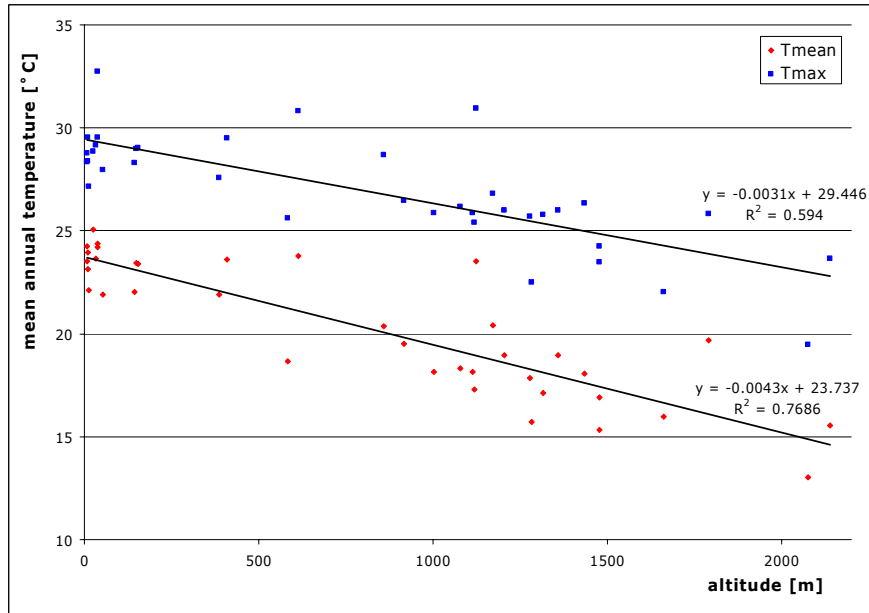


Figure 14: Annual variation of near surface meteorological conditions (24-h air humidity) for 3 selected weather stations in 2003

The SEBAL computation of pixel-specific values of ET requires air temperature and air humidity to be uniquely identified for every pixel. Climatic zones are not realistic because changes in climatology are gradual across a basin. The dry and cold mountains in the Sierra and the hot and humid parts near the Gulf of Mexico require a more sophisticated interpolation technology, especially when considering the orographical complexities (see Figure 3 and Figure 6). The 34 points with routine weather data have been gridded. First the point measurements of air temperature are transferred to sea level. An air temperature lapse rate for  $T_{\text{mean}}$  (4.3 °C/km) and  $T_{\text{max}}$  (5.6 °C/km) has been found by plotting the annual mean values of  $T_{\text{mean}}$  and  $T_{\text{max}}$  against the altitude of the meteorological stations (see Figure 15).



**Figure 15: Determination of air temperature lapse rates necessary for surface gridding**

The at-sea level point values of air temperature were, subsequently, gridded using a standard spline algorithm, and 'brought back' to their true elevations using the same lapse rates in an inverse manner. Through this procedure, it is feasible to generate realistic grids and unique values for every pixel. An example of 24 hour averaged air temperature on MODIS day August 18 (2003) is presented in Figure 16. The effects of mountain and valleys, as well as deserts and coastal lowlands on near-surface air temperature are clearly visible. The locally measured air humidity values were extrapolated in a similar way

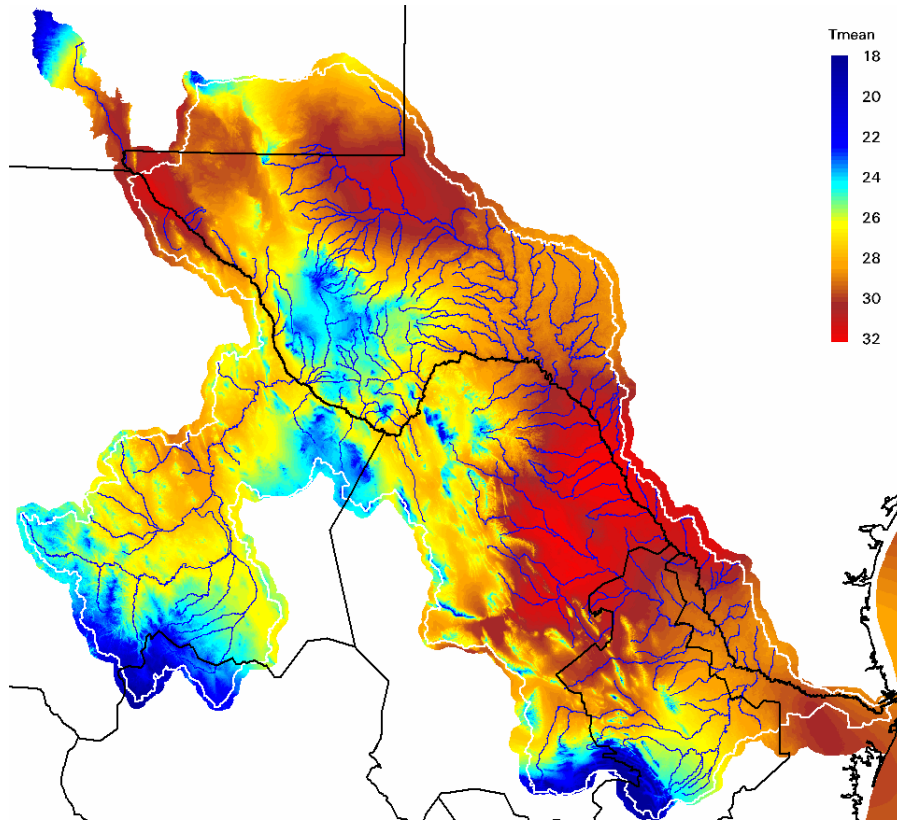


**Figure 16: Gridded values for 24-h average air temperature on MODIS overpass day August 18 (2003)**

The University of Sonora (UNISON) and the Instituto Tecnológico de Sonora (ITSON) have jointly developed a technology to determine cloud cover from geostationary satellites (Stewart et al., 1999; Garatuza and Watts, 2005). Using 4 km resolution Geostationary Operational Environmental Satellite (GOES) visible channel measurements, shortwave atmospheric transmittance and solar radiation were estimated on MODIS overpass days. Using the same methodological approach, 15-day averaged atmospheric transmittance and solar radiation ( $W/m^2$ ) were processed as well. These solar radiation grids assume a flat surface. Extra-terrestrial radiances in mountainous terrain were separately computed using the Digital Elevation Model (DEM) and a radiation model adapted to mountains in Idaho as developed by the University of Idaho (unpublished). The shortwave atmospheric transmittance from GOES was thereafter integrated with the extra-terrestrial solar radiation in mountain areas, to obtain the at-surface solar radiation for all topographical variations. An example is provided in Figure 17.

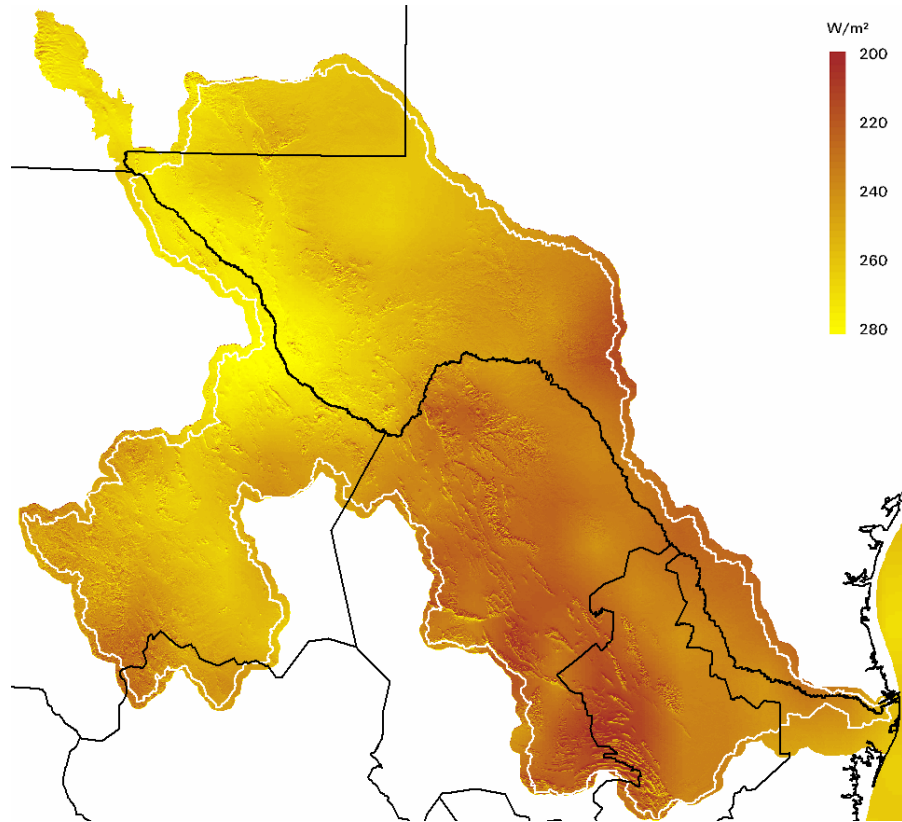


**Figure 17:** Example of solar radiation estimations from geostationary GOES visible satellite data (average value for period 1 – 15 September 2003.)

The pixel-based values of air temperature, air humidity and solar radiation are used to determine reference and actual ET by both SEBAL and SWAT models. By applying the same meteorological grids to both models (and also the same land cover map, see Figure 6), it is ensured that the ET differences are caused by differences in hydrology, plant properties and soil properties. Through the adaption of soil properties in SWAT, the SEBAL-based ET spatial patterns can be reproduced in SWAT.

## 2.5 Rio Bravo drainage network

The Rio Bravo is a vast drainage system, which besides the Rio Conchos, contains 6 other tributaries (El Cuchillo, Marte Gomez, La Fragua, V. Carranza, San Miguel and Centenario). The Elephant Butte Dam located North of Las Cruces in New Mexico, opened in 1916 and was meant to provide a steady supply of irrigation water on demand. This was one of the first regulating efforts to tame the Rio Grande flow. Over the years, water resources developments in the Rio Bravo water intensified, and a fragmentation of the river corridor has occurred: The Rio Bravo is no longer one river. Of the river water that reaches El Paso/Ciudad Juarez in a typical year, Mexican users are assured of 14 percent, U.S. users take 79 percent, and only 6 percent flows downstream--an arrangement rooted in a 1906 compromise between the neighboring countries.

The river does not resume significant flows until the confluence with the Rio Conchos at Presidio ([www.rioweb.org/basinfact.htm](http://www.rioweb.org/basinfact.htm)). The Rio Bravo gains strength as the Rio Conchos rushes down from the Sierra Madre mountains in Chihuahua to join the main river course. There are 6 storage facilities on the Rio Conchos. The

biggest storage is Presa de la Boquilla reservoir near Ciudad Camargo in the upstream part of the basin. Madero, West of Ciudad Delicias, Luis L Leon (east of Chihuahua city), San Gabriel, Aguila, Chihuahua and El Rejon are smaller reservoirs

In the transect between Presidio and Ojinaga, the Rio Bravo flows through the canyons of the Cañon de Santa Elena and Maderas del Carmen Protected Areas and the Boquillas del Carmen National Park, and on the US side, the Big Bend National Park. This region includes breathtaking mountains, vast deserts, and the canyons at Santa Elena, Mariscal, and the scenic Boquillas.

The headwaters of the Pecos river originate as snowmelt east of Santa Fe in the Sangre de Cristo mountains, 50 km east of Sante Fe. The Pecos River flows southerly through New Mexico and Texas, and discharges into the Rio Grande near Langtry (Texas) just before the Rio Bravo touches with the Devils Lake behind the Amistad dam. Flows of the Pecos River are controlled by releases from the Alamogordo reservoir in New Mexico and the Red Bluff Reservoir at border between New Mexico and Texas. Storage in these reservoirs is affected by the snowpack on the Sangre de Cristo mountains.

The Mexican-United States Treaty of 1944, committed both countries to the construction of two international dams: Amistad and Falcon. The reservoirs were designed for storage capacities. The Amistad (friendship) Dam was finished in 1969 and is located near Ciudad Acunas (Mexico) and Del Rio (US). The section of the Rio Bravo that goes from Presidio/Ojinaga to La Amistad dam is 450 km long. The Amistad Dam diverts water for both countries. Some 56 percent of the facility's total water storage capacity belongs to the U.S. while Mexico owns nearly 44 percent, based on the reservoir design.

The twin cities of Del Rio-Ciudad Acuña and Eagle Pass-Piedras Negras nestle along the river between the wilderness of Big Bend and Laredo-Nuevo Laredo. Laredo is the major metropolitan area along the river's middle section, and the busiest inland port on the U.S.-Mexico border, draws 98 percent of its water, supplying homes, businesses, industry, farms, and ranches, from the river. It is expected that the river has considerable recharge losses between the confluence of the Conchos river up to La Amistad dam and again between Amistad and the Falcon dam.

Built in 1953, the Falcon dam fills a reservoir providing also water to both countries. The river reaches one of the most fertile agricultural regions in either country here, with farms as far as one can see growing fruits and vegetables. Water released from Falcon Dam is restricted to meet the needs of farmers, border communities and metropolitan areas with nearly 1.5 million people, including the city of Monterrey.

Increasing demands for extracting Rio Grande River water are straining the basin ecosystem. Water supply can now fall far short of consumption, especially following a low-snowpack winter, such as the winter of 1995-1996. Right now, the water in the Rio Grande is fully appropriated, which means that every drop is claimed by somebody.



---

# 3. Brief description of the analytical tools used

## 3.1 Images used

This study relies substantially on freely available images of the Moderate Resolution Imaging Spectroradiometer (MODIS) sensor on board of the Terra (mid-morning overpass) and Aqua (mid-afternoon overpass) satellites. Images can be downloaded from the Earth Observing System Data Gateway of the NASA (<http://edcimswww.cr.usgs.gov/pub/imswelcome/>).

MODIS has been selected because of its thermal band for measuring land surface temperature. Another advantage for using MODIS is its very short return period (daily images of both Aqua and Terra) that allows proper temporal monitoring of rapid changes in crop development and water use. Furthermore, MODIS has a swath width of 2,500 km wide, thus enabling to cover the whole study area by one single image.

Our MODIS analysis is based on the Aqua satellite. Only individual dates have been used; the MODIS standard 16 day products have been omitted because it was feasible to acquire sufficient daily images for which the quality of the product due to proper weather conditions is superior and for these images it is ensured that they are not blended with other lower quality images. Aqua's overpass time is between 1 and 3 pm local time, the moment of the day that the temperature is highest and relative humidity is lowest. MODIS' spectral bands have 250 (NDVI), 500 and 1000 meter (surface temperature) resolution. All 22 individual images are geo-referenced using the following projection: Albert Conical Equal Area, WGS 84, WGS 84, latitude of 1st parallel: 27.42, latitude of 2nd parallel: 34.92, longitude of the central meridian: -103, latitude of origin: 31.17, false eastening: 1,000,000, false northing: 1,000,000. Except for July and September (when moist rainfall took place, see Figure 12), two good images for every month could be located and downloaded. Table 5 shows the acquisition dates of the MODIS images that were downloaded and processed with the SEBAL model to obtain  $ET_{act}$  and biomass production.

**Table 5: Specification of MODIS scenes used for SEBAL processing in 2003**

Day of year	Date	Day of year	Date
2	2 January 2003	173	22 June 2003
18	18 January 2003	194	13 July 2003
47	16 February 2003	219	7 August 2003
54	23 February 2003	230	18 August 2003
82	23 March 2003	255	12 September 2003
89	30 March 2003	274	1 October 2003
91	1 April 2003	292	19 October 2003
116	26 April 2003	308	4 November 2003
127	7 May 2003	333	29 November 2003
139	19 May 2003	347	13 December 2003
162	11 June 2003	351	17 December 2003

To demonstrate the additional value of high resolution imagery for crop irrigation analysis, a more detailed study has been carried out for the Delicias Irrigation District in Chihuahua. Landsat images are used with a spatial resolution of 30 m to describe the agricultural water management practices with more precision such as crop-wise ET, crop yield, water productivity and irrigation efficiencies. The majority of the fields are irrigated with groundwater from the Jimenez Camargo aquifer (see Fig. 5). Table 6 specifies the Landsat-5 images that were purchased. The location of

Delicias scheme is unfortunately at the crossing of 4 individual Landsat path/row combinations so that the total irrigated area is not encompassed on one image. Although a shift in rows along the same path can be accommodated, shifts in paths are not technically feasible because individual paths are acquired on different satellite overpass dates. The images from path/row 31/40 are shifted for enhancing the coverage, but it is not ideal.

**Table 6: Specification of the Landsat images purchased and used for SEBAL processing in 2003 (path/row 31/40)**

March 25 (2003)  
April 26 (2003)  
June 13 (2003)  
July 15 (2003)  
October 3 (2003)

### **3.2** A brief introduction to SEBAL

SEBAL provides a way to estimate and monitor ET spatially, independent from moisture and vegetation conditions. The latter facilitates the insight in the hydrological processes, water consumption and ET management. SEBAL solves the surface energy balance for heterogeneous terrain on the basis of reflected radiation and emitted thermal radiation (surface temperature). The energy consumed by EvapoTranspiration (ET) is estimated from radiances. This is an alternative to the traditional ET estimation methods based on soil type, crop type and irrigation practices culminated into a certain standardized crop coefficient. Problems in crop statistics are thus not propagated into the ET estimates. The actual ET fluxes from SEBAL reflect the real world field conditions, and deviate from the standard equations that compute the potential ET, assuming all management factors are optimal and pristine (this assumption is imbedded in the concept of crop coefficient  $K_c$ ).

The SEBAL model has been deployed to assess the 'comprehensive' ET of every individual MODIS pixel. This ET can be related to desert soil, open water evaporation, evaporation from sparse natural vegetation, rainfed crops, irrigated crops etc. Each satellite image needs to be cloud-free to be processed for energy balance purposes. SEBAL is one of the first mathematical procedures that can operationally estimate spatially distributed actual ET from field to river basin scale. SEBAL has been used in more than 30 countries (Bastiaanssen et al., 2005) and since 2002 in World Bank projects in Mexico (Sonora State; Chihuahua State), China, Uzbekistan, Pakistan, Egypt, Saudi Arabia, Sudan and Ethiopia. The inputs to SEBAL consist of (i) satellite data and (ii) routine weather data only.

The MODIS and Landsat data will be used to infer (i) surface temperature, (ii) surface albedo and (iii) Normalized Difference Vegetation Index (NDVI). These three parameters form the primary input data into SEBAL (see Figure 18).

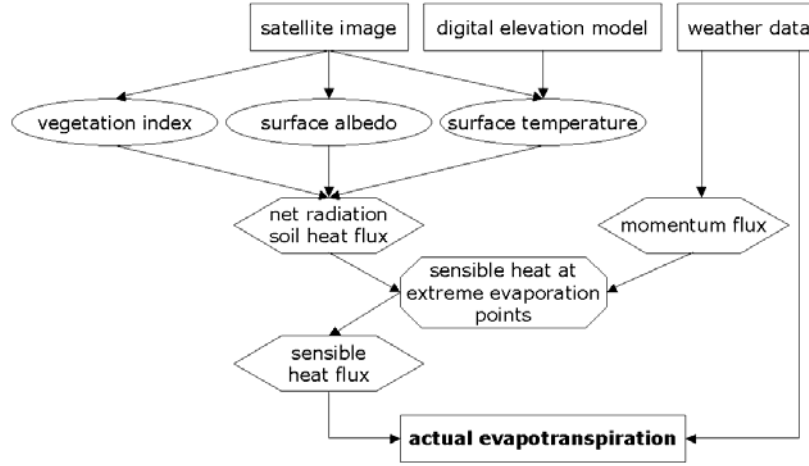


**Figure 18: Remote sensing measurements procedures for the determination of spatially distributed ET fluxes**

Evapotranspiration is related to the surface energy balance, which reads as:

$$R_n = G_0 + H + \lambda E \quad (\text{W m}^{-2}) \quad (1)$$

where  $R_n$  ( $\text{W m}^{-2}$ ) is the net radiation,  $G_0$  ( $\text{W m}^{-2}$ ) is the soil heat flux,  $H$  ( $\text{W m}^{-2}$ ) is the sensible heat flux and  $\lambda E$  ( $\text{W m}^{-2}$ ) is the latent heat flux associated with evapotranspiration. Equation (1) can be re-written and expressed as evaporative fraction  $\Lambda$  and net available energy ( $R_n - G_0$ ):

$$\lambda E = \Lambda (R_n - G_0) \quad (\text{W m}^{-2}) \quad (2)$$

where

$$\Lambda = \frac{\lambda E}{R_n - G_0} = \frac{\lambda E}{\lambda E + H} \quad (-) \quad (3)$$

The net available energy ( $R_n - G_0$ ) in Equation (2) may have different time scales, from instantaneous (for example, during a satellite overpass) to daily-integrated values, or to periods elapsing between consecutive satellite measurements. Depending on the time scale chosen, different time integrations of ( $R_n - G_0$ ) need to be obtained. For the daily time scale,  $ET_{24}$  is formulated as:

$$ET_{24} = \frac{86400 \cdot 10^3}{\lambda \rho_w} \Lambda \zeta (Rn24 - G24) \quad (\text{mm d}^{-1}) \quad (4)$$

where  $R_{n24}$  ( $\text{W m}^{-2}$ ) is the 24-h averaged net radiation,  $\lambda$  ( $\text{J kg}^{-1}$ ) is the latent heat of vaporization,  $\rho_w$  ( $\text{kg m}^{-3}$ ) is the density of water and  $\zeta$  (-) is an advection enhancement parameter. The chief assumption in SEBAL is that the evaporative fraction  $\Lambda$  specified in Eq. (3) remains constant during daytime hours. Experimental work has demonstrated that this holds true for environmental conditions where soil

moisture does not significantly change and advection can be ruled out (e.g. Shuttleworth et al., 1989; Brutsaert and Sugita, 1992; Nicols and Cuenca, 1993; Kustas et al., 1994; Crago, 1996; Farah, 2001).

Advection occurs when desert air is heated up during the morning by the sensible heat ( $H$ ) of the surface energy balance, and will be blown over the cold irrigated areas in the afternoon. These regional scale breezes arise from differences in air densities. The regional scale atmospheric circulation adds extra energy to the irrigated crops, known as the oasis effect. This extra energy enhances ET such that it can surpass the net available energy ( $R_n - G_0$ ), which from an energy balance point of view implies that the sensible heat flux is directed towards the surface for bringing this extra energy available for ET processes ( $H$  is negative). This advection is incorporated into the  $\zeta$  parameter that varies with the weather conditions and the moisture of the underlying soils. The impact of weather conditions on advection is expressed by the changes of the evaporative fraction of the reference crop  $\Lambda_{grass}$  between satellite overpass and the 24-h counterpart governed by day and night weather conditions. The influence of advection decreases non-linearly with soil moisture content.

The evaporative fraction is a determinant of soil moisture. Wet land surfaces will use a large fraction of the net available energy ( $R_n - G_0$ ) for latent heat flux. So, a high  $\Lambda$  can be associated with wet soils. Above dry land surfaces, most net available energy is consumed by sensible heat flux to heat up the atmospheric boundary layer. Scott et al. (2003) have developed an empirical relationship that fits data sets collected from US, Mexico, Spain and Pakistan:

$$\theta/\theta_{sat} = \exp \{ (\Lambda - 1) / 0.421 \} \quad (-) \quad (5)$$

where  $\theta/\theta_{sat}$  is the degree of soil moisture saturation as a fraction between 0 and 1.0.

The standard 1 km Digital Elevation Model (DEM) has been used for the correction of air pressure and related air density and psychrometric constant at high elevation. The DEM is also used to correct the absorbed solar radiation values, both for slope and aspect. Southern facing terrain due to the angle of incidence absorb, namely, more solar radiation per unit land than the Northern facing slope (see Figure 17). More background information on SEBAL is provided in Appendix A and in Bastiaanssen et al. (1992; 1998; 2002; 2005).

### **3.3** A brief introduction to SWAT

SWAT represents all the components of the hydrological cycle including: rainfall, snow, snow-cover and snow-melt, interception storage, surface runoff, up to 10 soil storages, infiltration, evaporation, evapotranspiration, lateral flow, percolation, pond and reservoir water balances, shallow and deep aquifers, channel routing. It also includes irrigation from rivers, shallow and deep groundwater stores, ponds/reservoirs and rivers, transmission losses and irrigation onto the soil surface. Sediment production based on a modified version of the Universal Loss Equation and routing of sediments in river channels is computed. SWAT tracks the movement and transformation of several forms of nitrogen and phosphorus in the watershed. It also tracks the movement and decay of pesticides. All include channel routing components and carrying of pollutants by sediments. SWAT has a modular set-up and it goes beyond the scope of this report to get into detail on each of these modules, but reference is made to the theoretical documentation (Neitsch et al, 2001).

As a distributed rainfall-runoff model, SWAT divides a catchment into smaller discrete calculation units for which the spatial variation of the major physical

properties are limited, and hydrological processes can be treated as being rather homogeneous. The total catchment behaviour is a net result of manifold small sub-basins. Sub-basins are delineated from the total basin using the DEM. The basin-wide soil map and land cover map within sub-basin boundaries are used to generate unique combinations, and each combination will be considered as a homogeneous physical property, i.e. Hydrological Response Unit (HRU). The water balance for HRU's is computed on a daily time step.

Irrigation on particular HRU's in SWAT can be scheduled by the user or automatically determined by the model depending on a set of criteria. In addition to specifying the timing and application amount, the source of irrigation water must be specified, which can be: canal water, reservoir, shallow aquifer, deep aquifer, or a source outside the basin. Irrigation may be scheduled manually or applied automatically by the model as response to a water deficit in the soil. Irrigation water applied to a sub basin is obtained from one of five types of water sources: a reach, a reservoir, a shallow aquifer, a deep aquifer, or a source outside the watershed. For this study it is assumed that all water originated from the shallow aquifer. If automatic irrigation is applied all soil layers are filled up to field capacity. If manually scheduling is used all scheduled water is applied and potential excess water percolates to the shallow aquifer. In this study irrigation water is applied automatically based on a predefined water stress criterion per sub basin. Water stress is 0.0 under optimal water conditions and approaches 1.0 as the soil water conditions vary from the optimal. Water stress is simulated by comparing actual and potential plant transpiration:

$$wstrs = 1 - \frac{E_{t,act}}{E_t} = 1 - \frac{W_{actualup}}{E_t}$$

where  $wstrs$  is the water stress for a given day,  $E_t$  is the maximum plant transpiration on a given day (mm H<sub>2</sub>O),  $E_{t,act}$  is the actual amount of transpiration on a given day (mm H<sub>2</sub>O) and  $w_{actualup}$  is the total plant water uptake for the day (mm H<sub>2</sub>O). The water stress criterion is used in calibrating simulated  $E_{t,act}$  with the measured SEBAL  $E_{t,act}$ .

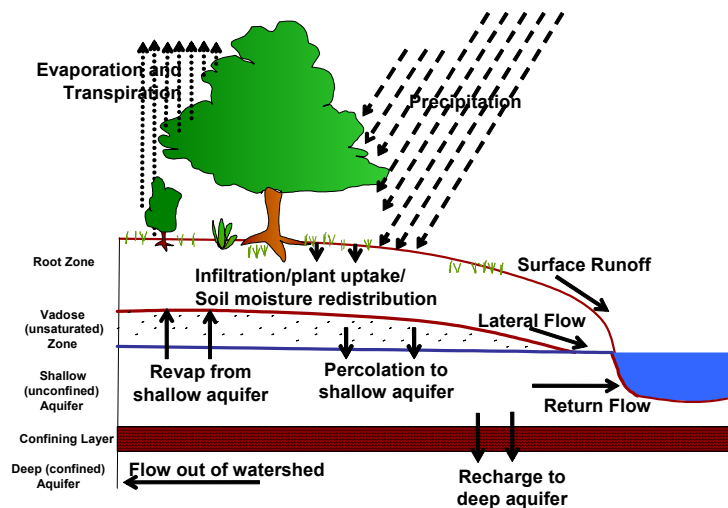


Figure 19: Major hydrological processes described within SWAT

Recharge to unconfined aquifers occurs via percolation of excessively wet root zones. Recharge to confined aquifers by percolation from the surface occurs only at the upstream end of the confined aquifer, where the geologic formation containing the aquifer is exposed at the earth's surface, flow is not confined, and a water table is present. River courses and irrigation canals are connected to the groundwater system, and surface water – groundwater interactions are taken care for.

After water is infiltrated into the soil, it can basically leave again the ground as lateral flow from the upper soil layer – which mimics a 2D flow domain in the unsaturated zone – or from return flow that leaves the shallow aquifer and drains into a nearby river. The remaining part of the soil moisture can feed into the deep aquifer, from where it can be pumped back by means of artificial extraction. The total return flow thus consists of surface runoff, lateral outflow from root zone and aquifer drainage to river.

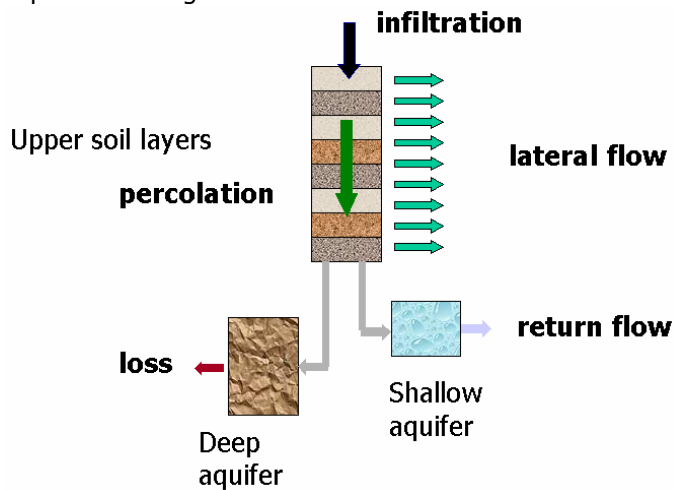


Figure 20: Schematic diagram of the partitioning of infiltration into sub-surface water fluxes after water uptake by roots have taken place

SWAT simulates two aquifers in each subbasin. The shallow aquifer is an unconfined aquifer that contributes to flow in the main channel or reach of the subbasin. The deep aquifer is a confined aquifer. Water that enters the deep aquifer is assumed to contribute to streamflow somewhere outside of the watershed. The effects of groundwater extractions on baseflow ( $Q_{gw}$ ), defined as the contribution of the shallow aquifer to stream flow, is of specific relevance in this study.

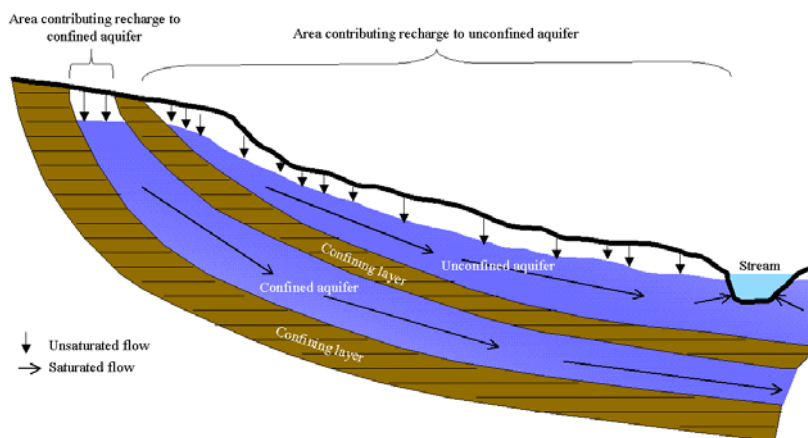


Figure 21: Schematic representation of shallow and deep aquifers in SWAT (Neitsch et al, 2001)

Base flow calculations are based on a combination of Hooghoudt (1940) and Smedema and Rycroft (1983) according to

$$Q_{gw,i} = Q_{gw,i-1} \cdot \exp[-\alpha_{gw} \cdot \Delta t] + w_{rchrg,sh} \cdot (1 - \exp[-\alpha_{gw} \cdot \Delta t])$$

where  $Q_{gw,i}$  is the groundwater flow into the main channel on day  $i$  (mm H<sub>2</sub>O),  $Q_{gw,i-1}$  is the groundwater flow into the main channel on day  $i-1$  (mm H<sub>2</sub>O),  $\alpha_{gw}$  is the baseflow recession constant,  $\Delta t$  is the time step (1 day),  $w_{rchrg,sh}$  is the amount of recharge entering the shallow aquifer on day  $i$  (mm H<sub>2</sub>O). To enable the simulation of the effect of groundwater extractions a component was added to the model which assumes a minimal baseflow defined as a percentage of the actual amount of water stored in the aquifer. For calculations of water table fluctuations a specific yield is assumed of 0.15 m<sup>3</sup>/m<sup>3</sup> is assumed.

For each day of simulation, potential plant growth, i.e. plant growth under ideal growing conditions is calculated. Ideal growing conditions consist of adequate water and nutrient supply and a favorable climate. The biomass production functions are to a large extent similar to SEBAL; First the Absorbed Photosynthetical Radiation (APAR) is computed from intercepted solar radiation as a function of LAI, followed by a Light Use Efficiency (LUE) that is in SWAT essentially a function of carbon dioxide concentrations and vapor pressure deficits. Whilst LAI is simulated in SWAT, the fractional Photosynthetical Active Radiation (fPAR) is measured in SEBAL. The crop yield is computed as the harvestable fraction of the accumulated biomass production across the growing season.

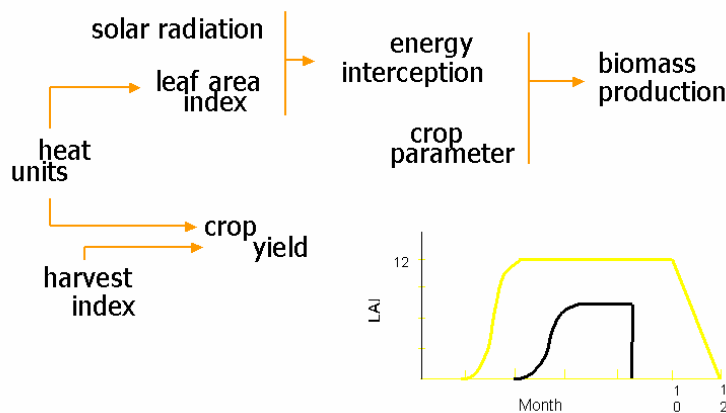


**Figure 22: Parameterization of crop production processes for estimating crop yield**

The project main interest is in the Mexican side of the border. To prevent the need to simulate water flows from New Mexico and Colorado – which will be complex due to all the regulated river flows, inflow at the boundary of the SWAT domain is defined. Stream flow in the Rio Grande at El Paso, and in the Rio Pecos at Red Bluff Lake are defined as boundary condition for SWAT. All other water resources are assumed to originate from the catchment inside the Rio Bravo basin itself.

The basin and sub basins were delineated using the AVSWAT GIS extension of the SWAT model and the DEM. The following steps were taken:

The existing river network was superimposed on the DEM. The software “burns” the river network into the DEM automatically. A threshold area of 75000 hectares was used for stream and sub-basin delineation (see Figure 23). An inlet is defined at El Paso. The total basin area modelled by SWAT is with 382,541 km<sup>2</sup> little smaller

than for SEBAL because the flow domain upstream of El Paso is not incorporated. There is also a small difference at the mouth of the basin where different boundaries of the Rio Bravo in the coastal lowlands exist. A total of 303 sub-basins were delineated using this approach (see Figure 20 and Figure 23).

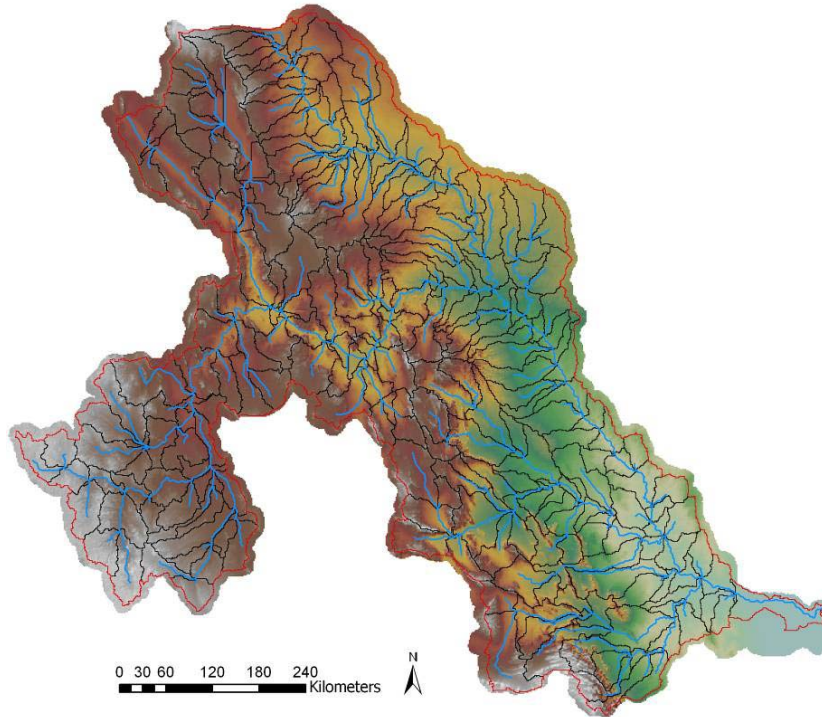


**Figure 23: Watershed and 303 sub-basin boundaries for the SWAT model in the Rio Bravo basin**

## 4. Results from remote sensing

### 4.1 Rio Bravo basin

#### 4.1.1 Evaporative depletion

The annual reference ET for the standard clipped grass supported by FAO (Allen et al., 1998) and the American Association of Civil Engineers ASCE (Allen et al., 2005) has been computed for all pixels in the basin. Mean weather parameters for the 15 day (twice monthly) intervals are used in the Penman-Monteith equation for  $ET_{ref}$ . Most  $ET_{ref}$  values for the basin lays between 1800 to 2100 mm/yr (average is 1891 mm), and values can be as low as 1200 mm/yr and as high as 2400 mm/yr. This implies that the atmospheric water demand of the Rio Bravo is highly variable due to climatology and orography. This unavoidably affects the value of actual ET.

The actual ET from MODIS-based SEBAL is presented in Figure 24. The annual average actual ET for the whole basin is 397 mm/yr. The potential ET is 832 mm/yr and both  $ET_{act}$  and  $ET_{pot}$  are thus considerably less than the reference ET (1891 mm), because the arid landscape with sparse plant canopies has neither a developed LAI ( $ET_{pot}$  is governed by  $ET_{ref}$  and LAI) nor a sufficient soil moisture value to maintain the ET process going (hence  $ET_{act} < ET_{pot}$ ). By absence of water to evaporate - and leaves to evaporate from -  $ET_{act}$  values are systematically lower than  $ET_{ref}$ . Also in the relatively wet September month, rains in the Chihuahua desert are not strong enough for turning the desert into a contiguously green landscape.

The highest layer wise  $ET_{act}$  values occur from water bodies and irrigated areas. The water evaporation from reservoirs varies between 1500 to 2000 mm/yr. Devils Lake evaporates with 1800 to 2000 mm/yr more than Falcon Lake (1400 to 1800 mm/yr), which is related to the higher level of aridity of the overlying atmospheric boundary layer in the middle part of the basin, as compared to the more humid downstream part. The average lake evaporation from all reservoirs is 1578 mm. The evaporation exhibits substantial variation within certain lakes, and this is related to the water depth, water quality and the effects of water constituents on light extinction.

Outside the irrigated and agricultural areas, the largest ET occurs in the transition zone from high to low mountains. This coincides with the location of the submontane scrubland areas that have a high atmospheric demand, but are according to the MODIS surface temperature maps relatively cold, i.e. indicating good evaporative conditions. The high atmospheric demand ( $ET_{pot}$ ) and possible underground moisture seeping in make their  $ET_{act}$  with 300 to 1200 mm/yr substantially higher than one would expect on the basis of rainfall. Submontane scrubland taps thus lateral groundwater flow that originates from the higher located desert scrubland vegetation types. This confirms that:

- the river basin should be considered as one hydrological continuum
- return flows make sense and need to be quantified and monitored

Upon further inspection of the NDVI and precipitation, it appears that permanently green scrubland is present with a NDVI higher than 0.3 on low flood plains with  $ET > 600$  mm/yr during the dry period elapsing from January to June. For the

Edwards Plateau at the Left Bank of the Rio Bravo, NDVI fluctuates around 0.35 the whole year round for an area of interest of 118 km x 90 km. This is thus perennial vegetation that must have access to water resources outside the rainy season. Groundwater seems to be the only plausible source. Another area of interest lies in the vicinity of South of Devils Lake shows the same effect, although Fall is with NDVI~0.38 little greener than Spring (NDVI~0.33). A 3<sup>rd</sup> area of a reasonable dimension (120 km x 50 km) is selected North of Falcon Lake, and the latter area exhibits a distinct response to precipitation of 400 mm in September and October. The 2003 precipitation events in Falcon are concentrated in a smaller time frame, and are influenced by the Gulf of Mexico rain storms. The fact that the average NDVI in all three areas during Spring is 0.3, vegetation must tap groundwater resources. They are either phreatophytes or have a deep rooted vadoze zone. This subject of groundwater abstraction by natural vegetation needs to be further investigated and discussed in the SWAT chapter.

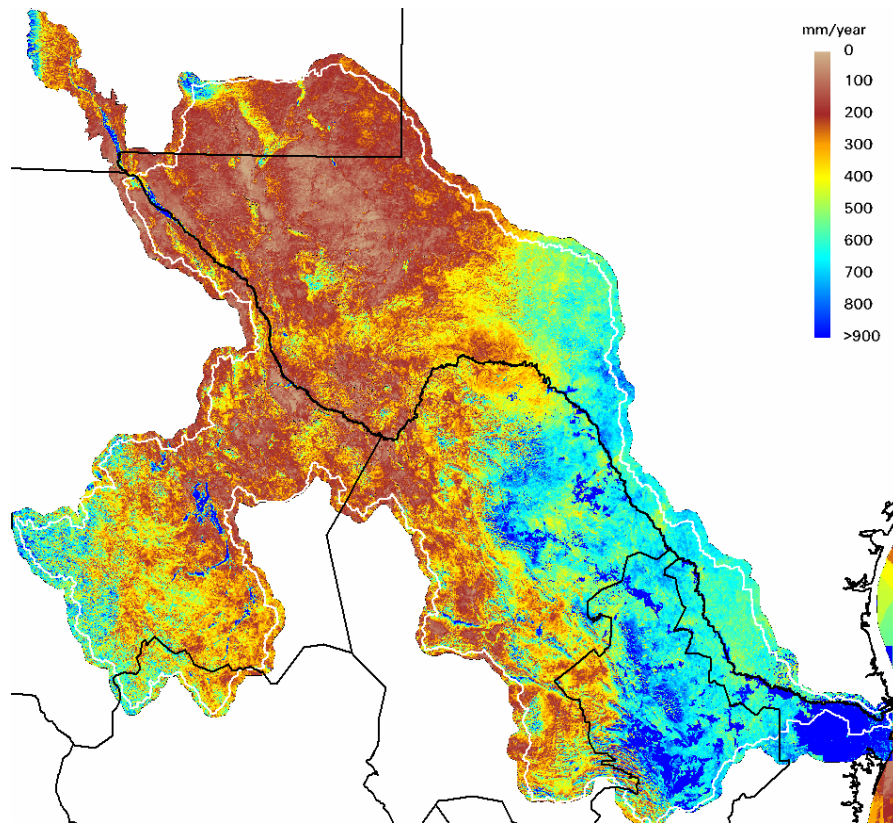


**Figure 24: Distribution of annual accumulated evapotranspiration (ETact) across the Rio Bravo basin (2003) computed with the SEBAL model and MODIS images. The average value for ETact is 397 mm/yr.**

The distribution of actual ET throughout the year is worked out in Figure 25. The period January to April has an ET of approximately 20 mm/month, hence less than 1 mm/d. The largest ET (48 mm/month) occurs during September when the solar radiation is still strong and the soils are moist due to antecedent rainfall from July and August. Overall, the values are much lower than the reference ET, for good reasons explained before. Whereas  $ET_{ref}$  has its peak value in May (sun is powerful, not much clouds, dry atmosphere), the peak value in  $ET_{act}$  occurs in September, being a delay of 4 months.

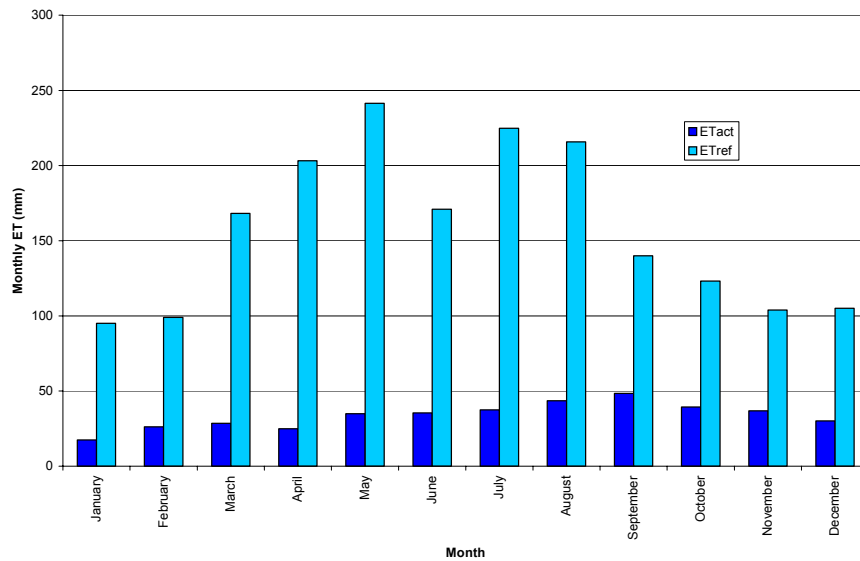


**Figure 25: Variation of monthly actual and reference ET averaged for the 44 million ha large Rio Bravo during 2003**

The breakdown of  $ET_{act}$  into land cover classes is presented in Table 7. The lowest ET occurs from the microphyllous scrublands (237 mm) and scrubland with rosetted vegetation (263 mm), because these CAM plants (Crassulacean Acid Metabolism) have an extra thick cuticula and their own metabolism. The urban areas have an unexpectedly high ET, which can be attributed to the presence of many traditional lane trees in Mexican cities for providing the necessary shadow and social life. Due to artificial water supply to city trees and turf, city ET is 803 mm, and is higher than from the oak and pine forests. Forest ET consumes typically 480 to 540 mm.

The irrigated crops southeast of Monterrey have an  $ET_{act}$  of 1700 mm/yr. The MODIS pixel ET results relate to a 1 km x 1 km cell and the results should be regarded as an equivalent ET layer. Within a given pixel, ET values can be lower and higher. It is thus very likely that certain fields have an ET that exceeds 1700 mm/yr. The average ET value for the irrigated crops near Monterrey and other areas in Coahuila is 1242 mm, and it is the highest ET for all irrigation classes. It can be explained by the higher water availability from rain and groundwater resources in this area. Crops in Monterrey evaporate more than the ET of the arid valleys of Chihuahua (898 mm on average). Local variations due to crop duration, LAI and crop height (taller crops evaporate more) are expected to be significant. The latter will be investigated separately with Landsat images in Section 4.2.2. Wang et al. (2005) investigated the ET from a pecan orchard and an alfalfa field South of Las Cruces. They had an eddy covariance tower of 16 m height to measure the ET fluxes over the crown of Pecan trees. In their paper they report ET fluxes from 7 different days ranging from April to October. The average ET on these 7 days for pecan was 5.2 mm/day, and these days coincided with Landsat overpass days for the application of a local SEBAL study. Considering that the periodically averaged weather conditions are less favorable than for the 7 individual good weather Landsat days, and there is no real Winter day included in the reported data series, the longer term average ET for pecans must be approximately 4 to 4.5 mm/d, hence  $\pm 1500$  mm/yr. The MODIS result shows annual values in this Las Cruces area ranging between 1450 to 1570 mm/yr (see Figure 26). Wang et al. (2005) concluded in their own SEBAL study that the absolute error between the

eddy co-variance tower and ASTER-based SEBAL results was 11% for single day events.

Another SEBAL study was executed by the University of Idaho in the Middle Rio Grande on the transect between Santa Fe and San Acacia, the latter being approximately 50 km North of Elephant Butte. Their ET estimates of a mixture of perennial vegetation (salt cedar, cottonwood) and alfalfa crops lays between 600 to 1800 mm/yr with the average approximately 1500 mm/yr (Allen, Forth Collins Workshop). The USDA facility on the Southern High Plains in Bushland (Texas) is internationally reputed for their ET research. In a summary paper, it is reported that winter wheat in Texas consumes 877 mm, corn 771 mm and cotton 578 mm of water (Howell et al., 1997). Sorghum and wheat can be produced under full irrigation, limited irrigation and dryland regimes. Wheat ET has usually lower values and is in arid zones often around 600 mm (Colorado: El Kaysi et al., 1997). A crop combination of wheat - corn will thus consume about 1650 mm/yr. The experimental ET values confirm that the MODIS-based ET of irrigated crops in the arid zones of the basin is plausible.

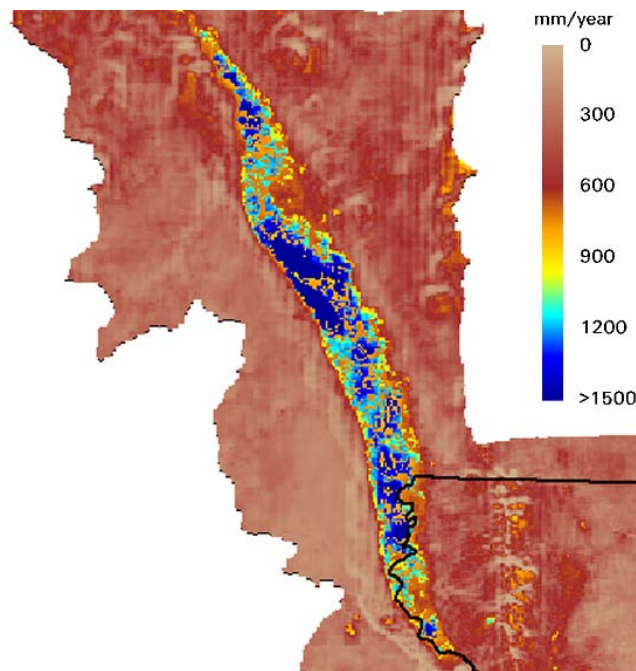


**Figure 26: Spatial variation of the annual ET in the river section between Las Cruces and El Paso that drains into the Rio Grande. The areas with higher evaporation coincides with the field sites of the University of New Mexico (Wang et al., 2005)**

**Table 7: Breakdown of layer-wise ET by land cover type in Rio Bravo (2003). The total evaporative depletion from 44 million ha is 175 km<sup>3</sup>**

Area ha	Area Beneficial %	Land cover	ET <sub>act</sub> (mm)	ET <sub>pot</sub> (mm)	ET <sub>deficit</sub> (mm)	ET <sub>act</sub> (km <sup>3</sup> )	ET <sub>act</sub> (%)
149,744	0.4	Beneficial urban area	803	1048	245	1.2	0.7
52,150	0.1	Non-beneficial water bodies	1578	1578	0	0.8	0.5
678,138	1.5	Beneficial irrigated agriculture (delta)	1202	1346	144	8.2	4.7
261,775	0.6	Beneficial irrigated agriculture (valley)	898	1040	142	2.4	1.3
796,975	1.8	Beneficial supplemental irrigation	1242	1298	58	9.9	5.6
162,831	0.4	Semi-beneficial low open forest	483	1272	789	0.8	0.4
259,738	0.6	Semi-beneficial oak forest	538	1747	1209	1.4	0.8
1,492,825	3.4	Semi-beneficial pine forest	487	1272	785	7.3	4.2
365,150	0.8	Low-beneficial Chaparral	481	1424	943	1.8	1.0
5,335,169	12.1	Low-beneficial microphyllous scrublands	237	501	264	12.7	7.2
20,045,525	45.6	Low-beneficial scrubland with rosetted vegetation	263	616	353	52.9	30.2
8,600,625	19.6	Low-beneficial thornscrubland tamaulipan	583	1254	671	50.2	28.6
938,975	2.1	Low-beneficial submontane scrubland	711	1605	894	6.7	3.8
1,493,875	3.4	Beneficial cultivated grassland	516	1129	1078	7.7	4.4
3,334,281	7.6	Semi-beneficial natural grassland	342	642	300	11.4	6.5
<b>43,967,775</b>	<b>100</b>					<b>175</b>	<b>100</b>

Water deficit felt by vegetation can be expressed as the difference in actual and potential ET. The difference can be ascribed to soil moisture in the root zone among others. The lowest ET deficits values ( $ET_{pot} - ET_{act}$ ) are noted in water bodies (0 mm), supplemental irrigation (58 mm), irrigated agriculture in the delta ( $ET_{def}=144$  mm/yr) and valley ( $ET_{def}=142$  mm/yr). A deficit of 50 to 150 mm/yr is very acceptable in arid regions and normal practice. ET deficit improves the irrigation efficiency, because there will be less surface runoff and percolation losses to the underground because these processes are a function of soil moisture. The relatively low value of ET deficit for supplementary irrigation in Table 7 is probably related to the high rainfall in this area, causing the alluvial soils to be moist and aquifers in replenishment conditions for a long duration of the year.

Irrigated agriculture and supplementary irrigation all together will deplete an amount of 20.5 km<sup>3</sup>/yr, which is 11.6% of all depletions in the Rio Bravo. Note that a part of this 20.5 km<sup>3</sup> consists of rainfed agriculture, and that the depletion of the irrigation sector must be lower ( $\pm 15$  km<sup>3</sup>/yr). We will use the 20.5 km<sup>3</sup> in the subsequent analysis for the sake of having a derived quantity. Scrubland with rosetted vegetation is with 30.2% the largest water consumer ( $ET_{act}=52.9$  km<sup>3</sup>/yr). The thorn scrubland tamaulipan has a high ET layer (583 mm/yr) that is comparable with rainfed crops, and it has a vast extension as well. Its volumetric depletion occupies 28.6 % of the basin wide evaporative depletion ( $ET_{act}=50.2$  km<sup>3</sup>/yr). From the viewpoint of ET management, it is interesting to study the biophysical behavior of these scrublands. A 10% ET reduction in these 2 ecosystems will yield a water saving of 10.8 km<sup>3</sup>/yr, which is 50% of the entire agricultural sector. It should be well understood that the current overexploitation can be arrested by either:

- reducing ET depletion worth 20.5 km<sup>3</sup>/yr in the irrigation sector
- reducing ET depletion worth 103 km<sup>3</sup>/yr in natural and maintain the current irrigated acreage

ET reduction in scrubland is feasible by means of a lower shrub density, and by more intensive cattle grazing. This study is not meant for providing IWRM solutions,

but instead shows examples how IWRM planning can benefit from an adequate knowledge base.

The water depletion in the Rio Bravo is characterized by high proportions of non-beneficial water depletion (70.8 %). Scrubland ET is important for the environment. The beneficial water depletion for intended processes in cities such as lane trees, ponds and turf as well as irrigated agriculture and cultivated grassland is 16.7 % only. The remaining 12.5 % is an example of semi-beneficial use because forest are good for wood production and environmental conservation (reduce soil erosion and sequestration of carbon). Other water use groups divert water for cleaning, cooling, power generation etc, but this resource is not depleted and returns back. Without any further complex analysis, it is obvious that water depletion by environmental systems is manifold the water depletion by intended processes. More emphasis need to go to water consumption of natural vegetation.

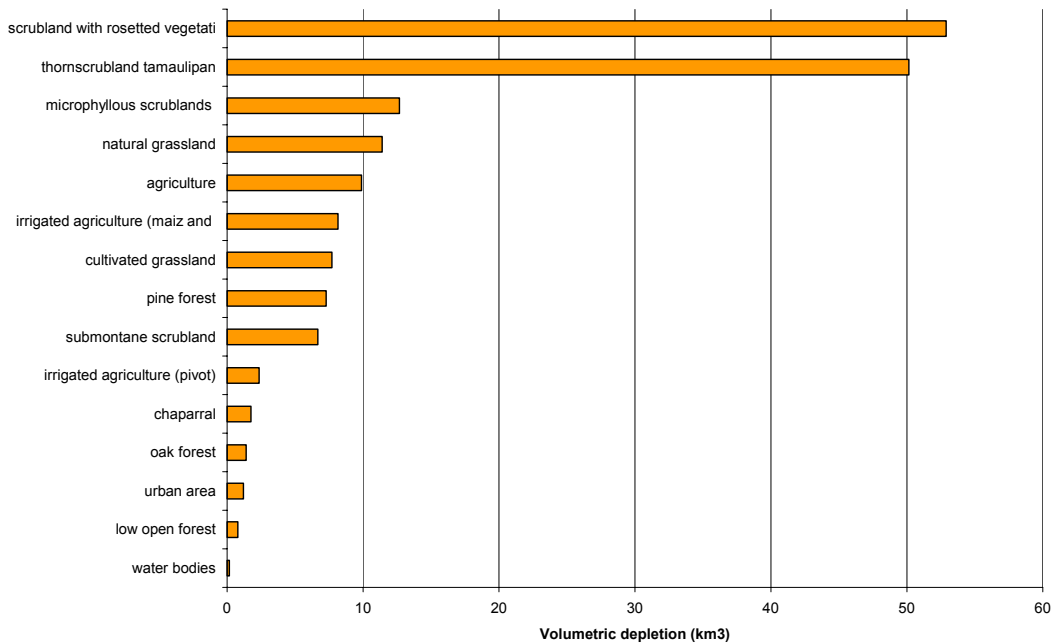


**Figure 27: Volumetric evaporative depletion of water resources by land cover type in the Rio Bravo (2003)**

A further breakdown of the evaporative depletion of the irrigated crops is outlined in Table 8. According to Parr Rosson et al. (2000), who used the CROPWAT model for the computation of potential ET, the total estimated irrigation water use in Chihuahua State during 1999 was 1.95 km<sup>3</sup> (1.58 MAF). Our estimate for the entire Rio Bravo basin (including parts of New Mexico and Texas) is 20.5 km<sup>3</sup>. The value of Table 8 is the percentage wise breakdown within the agricultural sector. Hence corn and alfalfa are the leading water consumers in the irrigation sector, and they consume significantly more water resources than vegetables and nuts.

For comparison, alfalfa uses about 20 to 27 percent of California's water (thus even more dominant than Chihuahua) and research is under way to increase the irrigation efficiency through better irrigation scheduling and improved irrigation systems (thus technical solutions in California and Mexico are identical). Regulated deficit irrigation of alfalfa might improve profit during those times when yield per unit of applied water is low compared to continuous irrigation (Hanson and Putnam, 2000).

The other side of the flip coin is that efficient irrigation systems encompass a larger area under service with the same extraction  $Q$ . This causes more water to be evaporated and has adverse impacts on the water availability of downstream water consumers. They will 'feel' reduced stream flows and lower lateral groundwater movements. When water policy makers are drawing plans for water rights, they should thus distinguish between water *diverted* and water *depleted*.

**Table 8: Breakdown of agricultural water use among crop types in Chihuahua State (after Parr Rosson et al. 2002)**

Crop type	Volumetric water depletion (km <sup>3</sup> )	Evaporative depletion (%)
Corn	0.361	18.5
Alfalfa	0.321	16.5
Cotton	0.276	14.1
Sorghum and wheat	0.243	12.4
Apples	0.239	12.2
Pecans	0.215	11.0
Vegetables	0.196	10.0
Other crops	0.099	5.1
<b>TOTAL</b>	<b>1.950</b>	<b>100</b>

#### 4.1.2 Precipitation and soil moisture

The TRMM analysis discussed before (and calibrated against a network of unknown ground stations) shows a total rainfall of 197 km<sup>3</sup> (equivalent layer 450 mm). The annual ET is 174 km<sup>3</sup> (equivalent layer 397 mm). The difference is caused by storage changes in reservoirs, aquifers and in the vadose zone and the outflow to the Gulf of Mexico. The accumulated values of rainfall and ET are plotted in Figure 28. During January and February, rainfall and ET are in good balance, and the surplus is negligible small. The period elapsing from March to June is the depletion period in which ET exceeds rainfall and water is withdrawn from storage reservoirs and aquifers to complement the gap between rainfall and ET. From July to December, accumulated rainfall is in excess of ET, and the river drainage network is flowing, and reservoirs and aquifers recharged.

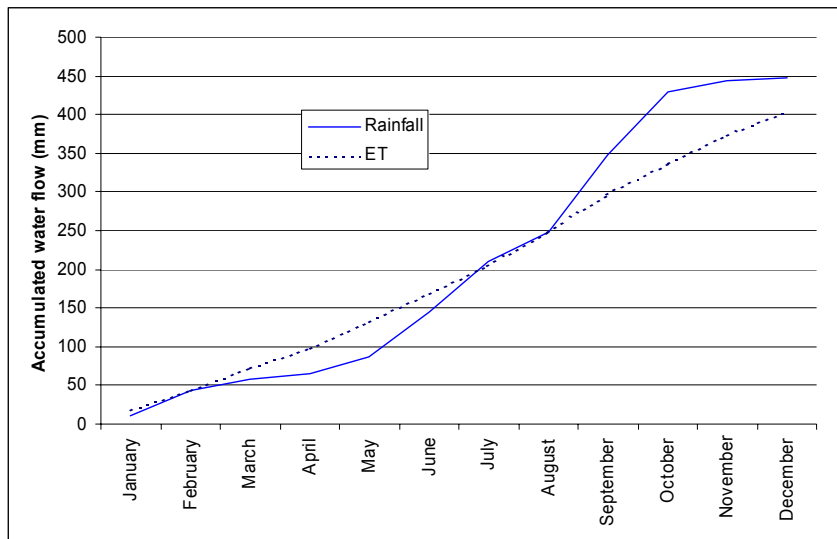


**Figure 28: Accumulated monthly rainfall (from microwave TRMM satellite data) and ET (from thermal MODIS satellite data) in the Rio Bravo basin (2003)**

The soil wetness in the irrigated agricultural areas are with 0.58 to 0.59 similar to tamaupilan thornscrubland (0.55) and submontane scrubland (0.59). These moisture values express the degree of moisture saturation between 0 and 1. A value of 0.5 to 0.6 is little lower than field capacity. The months April and September have the most contrasting wetness conditions. Because of some cloud contaminations, Figure 29 displays the spatial patterns of soil moisture in May and November instead. The Left Bank of the Lower Rio Bravo seems to be wetter than the Right Bank, also in May. While forests and agriculture are quasi-constant, the deserts are very dry in April and little dry in September. The difference in moisture status of the Delta area is striking, which is related to the cropping calendars and shift from Summer to Winter crop in November.

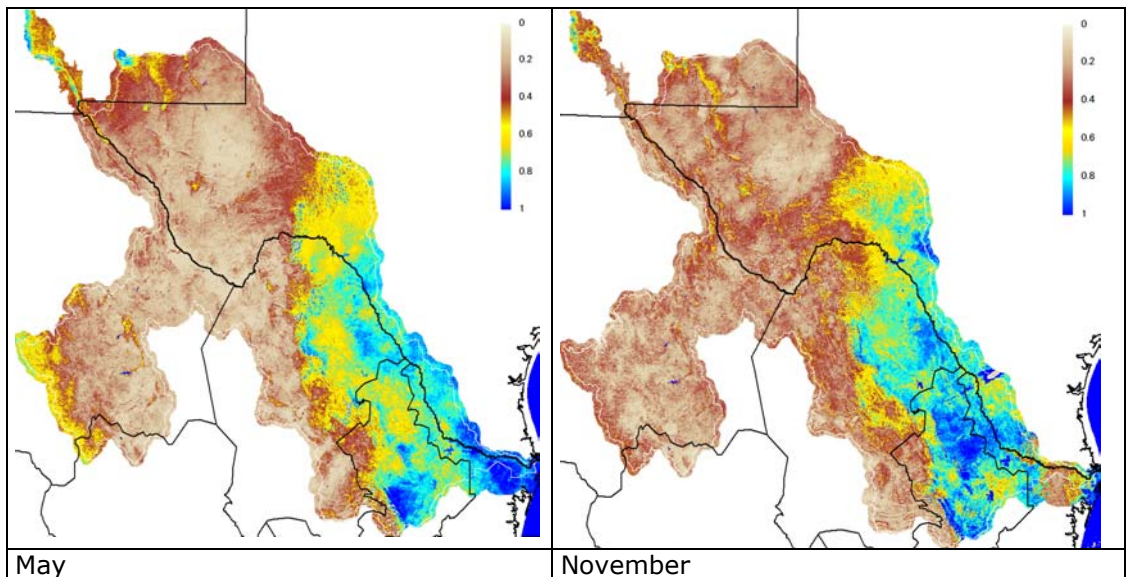


**Figure 29: Spatial variation of soil moisture in the upper 1 meter of soil during May and November 2003. The values represent the degree of soil moisture saturation**

The layer-wise largest net supplier of water is chaparral ( $P-ET_{act}=115$  mm; see Table 9). This ecosystem receives above average rainfall (596 mm) - because chaparral is grown in mountains - and has an ET close to the average basin value (481 mm). As a result, water excess from chaparral is recharging streams and aquifers. Because of its 1% occurrence on the land cover map, volumetric water production of chaparral is limited ( $0.4$  km<sup>3</sup>/yr), and more water can be harvested if more ecosystems are turned into chaparral. This is an issue of eco-hydrologists to think about. The volumetric best water harvest is performed on scrubland with rosetted vegetation ( $14.3$  km<sup>3</sup>). This higher located ecosystem recharges aquifers that crop out in the sub-montane scrubland. The groundwater flow at the Texas side of the border is generally in the direction of the Rio Bravo. This implies that underground basin transfer could take place, and that the lower floodplain receives water from two contradictory directions (Texas and Chihuahua/Coahuila).

The storage change in the upper soil layer of 1000 mm (1 m) at a porosity of a sandy desert soil of 35% is computed from the changes in soil moisture during the first 15 day period of the year (January 1 to 15) and the last 15 days period (December 16 to 31). Because of the above average precipitation, soil storage change is positive ( $+15$  km<sup>3</sup>).

**Table 9: Annual water balance Rio Bravo Basin according to SWAT by land cover type**

Area Ha	Area Land cover %	ET (mm)	Act Rain (mm)	Surplus (mm)	Surplus		Average	Storage	Storage
					(mm <sup>3</sup> )	(-)	Moisture change (mm)	change (km <sup>3</sup> )	
149744	0.4	urban area	803	593	-211	-0.3	0.39	+44	+0.07
52150	0.1	water bodies	1578	758	-820	-0.4	1.00	0	0
678138	1.5	irrigated agriculture (delta)	1202	856	-346	-2.3	0.59	-39	-0.26
261775	0.6	irrigated agriculture (valley)	898	261	-637	-1.7	0.39	+46	+0.12
796975	1.8	supplementary irrigation	1240	852	-388	-3.0	0.58	+77	+0.61
162831	0.4	low open forest	483	468	-16	-0.0	0.33	+17	+0.03
259738	0.6	oak forest	538	552	14	+0.0	0.46	+44	+0.11
1492825	3.4	pine forest	487	576	89	+1.3	0.36	+29	+0.43
365150	0.8	Chaparral	481	596	115	+0.4	0.46	+44	+0.02
5335169	12.1	microphyllous scrublands	237	323	85	+4.6	0.21	+34	+1.81
20045525	45.6	scrubland vegetation	263	336	72	+14.3	0.27	+26	+5.21
8600625	19.6	tamaulipan thornscrubland	583	670	86	+7.4	0.55	+53	+4.56
938975	2.1	submontane scrubland	711	709	-3	-0.0	0.59	+84	+0.79
1493875	3.4	cultivated grassland	515	567	51	+0.8	0.51	+38	+0.57
3334281	7.6	natural grassland	342	398	55	+1.8	0.26	+32	+1.07
<b>43,967,775 100</b>					<b>+22.8</b>			<b>+15.14</b>	

The international character of the basin has prompted the adjoining countries to design and operate an adequate flow monitoring network. For a number of key stations, the longer term average stream flow data is specified in Table 10. The change in incremental increase and decrease in stream flow are significant due to regulation and diversions. The discharge in Rio Bravo is reaching the maximum value at Laredo before the flow enters Falcon reservoir. The average flow into the Gulf of Mexico at Brownsville is 63 m/s, which is equivalent to 2.0 km<sup>3</sup>/yr.

**Table 10: Generic streamflow patterns (Source: <http://water.usgs.gov/nasqan/progdocs/factsheets/riogfact/engl.html>)**

No. <sup>1</sup>	Flow Gauge	Drainage	Incremental	Mean	Incremental
		Area	Increase in	streamflow	increase/decrease
		km <sup>2</sup>	area	m <sup>3</sup> /s	in streamflow
			km <sup>2</sup>		
1	Rio Grande at El Paso, TX	75,769	75,769	18	18
2	Rio Grande at Foster Ranch near Langtry, TX	209,031	133,263	55	37
3	Pecos River near Langtry, TX	91,074	91,074	7	7
4	Rio Grande below Amistad Dam near Del Rio, TX	318,803	109,771	71	9
5	Rio Grande below Laredo, TX	343,229	24,426	97	26
6	Rio Grande below Falcon Dam, TX	412,331	69,102	91	-6
7	Arroyo Colorado at Harlingen, TX	471	N/A	7	N/A
8	Rio Grande near Brownsville, TX	456,505	44,174	63	-28

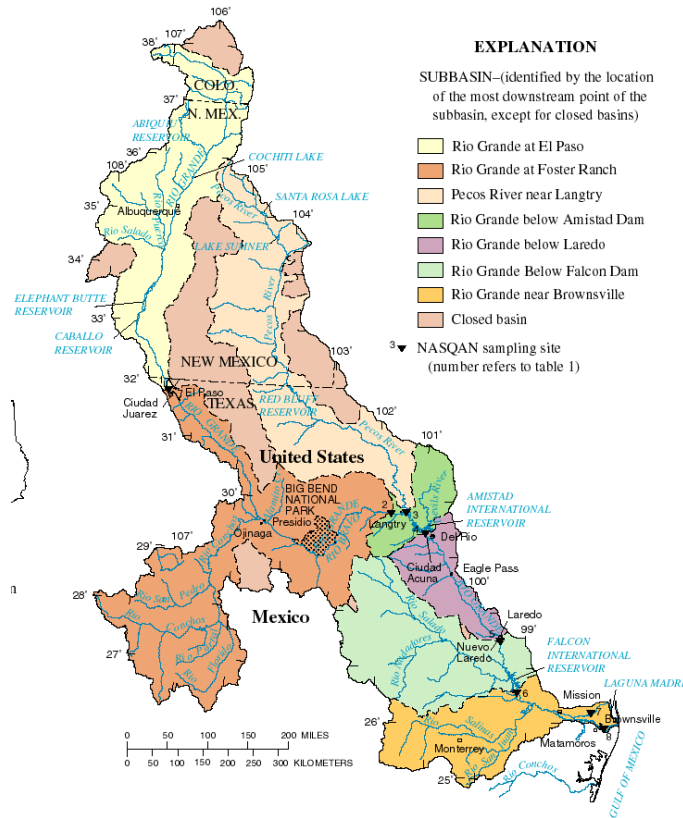


Figure 30: Stream flow stations (<http://water.usgs.gov/nasqan/progdocs/factsheets/riogfact/engl.html>)

The major water accounts can now be summarized. The storage change in the upper soil layer is positive ( $15.1 \text{ km}^3$ ). There is however also deep groundwater recharge, capillary rise and base flow. The SWAT-based water balance shows a total storage of saturated and unsaturated zone of  $51 \text{ mm}$ , which is equivalent to  $22.3 \text{ km}^3$ . The interbasin water transfer is unknown and a first order approximation can be established for the 2003 hydrological conditions. Fixing outflow as  $2.0 \text{ km}^3$ , interbasin water transfer can be estimated as being  $2.7 \text{ km}^3$ .

<b>Rio Bravo Basin Water Accounts 44 million ha (2003)</b>		
	<b>INFLOW</b>	<b>OUTFLOW</b>
Rainfall	: $197 \text{ km}^3$	
Beneficial ET	:	$29.4 \text{ km}^3$
Semi-beneficial ET	:	$20.9 \text{ km}^3$
Non-beneficial ET	:	$125.1 \text{ km}^3$
Storage change	:	$+22.3 \text{ km}^3$
Interbasin water transfer	: $2.7 \text{ km}^3$	
Outflow to Gulf of Mexico	:	$2.0 \text{ km}^3$
<b>TOTAL</b>	<b>: <math>199.7 \text{ km}^3</math></b>	<b><math>199.7 \text{ km}^3</math></b>

#### 4.1.3 Biomass water productivity

Productivity reflects the ability of plants to capture energy in the form of solar radiation and convert it into biomass. Because plants require energy to liver

(respiration), carbon dioxide is inhaled while water vapor is exhaled. The result is a net primary production. This biomass consists largely of organic compounds made up of carbon, hydrogen and oxygen. It contains food, feed, forest and fuel produced from ET consumptive use.

Submontane scrubland has with 25,788 kg/ha the highest biomass production – it exceeds even supplemental irrigation (22,383 kg/ha). The values for scrubland (2717 to 6006 kg/ha) are substantially lower. Due to algae and floating water plants, the biomass production of water bodies is little more than zero (73/kg/ha/yr).

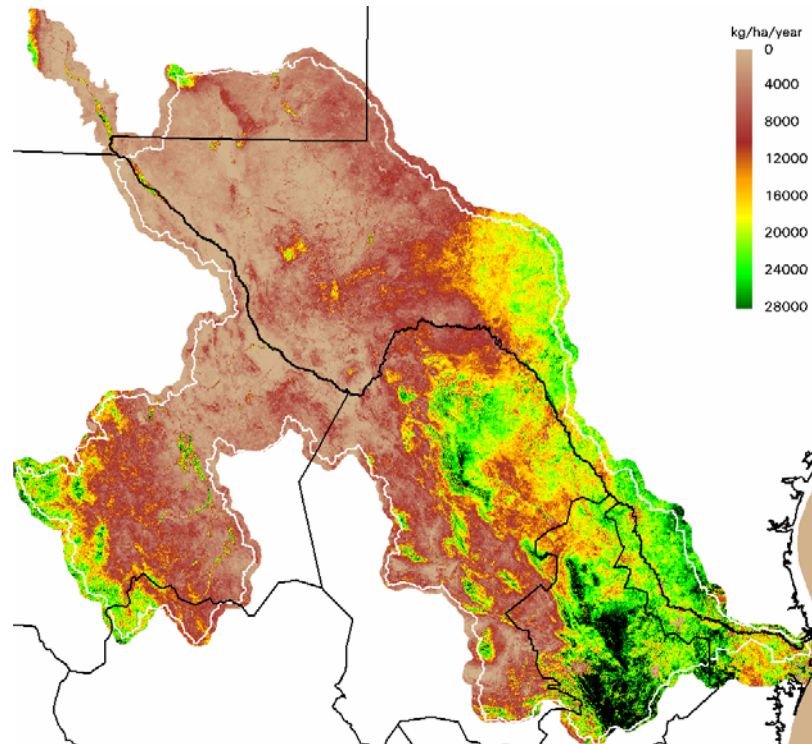


**Figure 31: Annual total biomass production in Rio Grande (2003) computed with the SEBAL model based on MODIS images**

**Table 11: Biomass water productivity of all agro-ecosystems present in the Rio Bravo (2003)**

<b>Land cover</b>	<b>ET<sub>act</sub> (mm)</b>	<b>Biomass production (kg/ha)</b>	<b>Biomass water productivity (kg/m<sup>3</sup>)</b>
urban area	969	6,642	0.83
water bodies	1578	73	0.0
irrigated agriculture (delta)	1202	17,752	1.48
irrigated agriculture (valley)	898	17,035	1.90
supplementary irrigation	1240	22,383	1.81
low open forest	483	20,204	4.17
oak forest	538	22,883	4.25
pine forest	487	21,589	4.43
Chaparral	481	21,715	4.51
microphyllous scrublands	237	2,717	1.14
scrubland with rosetted vegetation	263	6,006	2.28
thornscrubland tamaulipan	583	19,577	3.36
submontane scrubland	711	25,788	3.63
cultivated grassland	515	16,817	3.26
natural grassland	342	7,871	2.30

Since water is the binding constraint to biomass production (there are enough land resources, solar radiation and an adequate ambient temperature), it is useful to express biomass production per unit of water consumed (see Table 11). The most effective producer of dry matter is chaparral (4.51 kg/m<sup>3</sup>), followed by pine (4.43 kg/m<sup>3</sup>) and oak forests (4.25 kg/m<sup>3</sup>). These forests have a healthy production and need relatively little water due to high air humidity in mountains. It is interesting to note that the dry scrubland vegetation is quite effective in turning water into dry matter (2.28 to 3.63 kg/m<sup>3</sup>). It reflects a natural adaptive mechanism of arid zone vegetation to survive in harsh desert climates.

#### **Interim conclusions Rio Bravo**

- Majority of water is consumed for ecological purposes (70.8%). Agriculture depletes only 11.7 % of the precious water resources. Although agriculture is a minor consumer, it has management options to conserve water
- Considerable underground lateral water transfer occurs, both within the basin as well as (international) interbasin transfer
- Chaparral vegetation has the highest water harvest per unit of land
- There is a substantial usage of groundwater, also by the natural vegetation due to seepage from higher elevated deserts. It is likely that natural vegetation has adapted to this hydrological systems by adapted rooting systems
- Rainfall in the downstream end of the basin is sufficient for the cultivation of rainfed corn and sorghum in areas with P>700 mm/yr. Other semi-arid crops could be introduced (e.g. almonds, pulses) in areas with P>500 mm/yr
- MODIS is suitable for assessing land cover, ET, biomass production and biomass water productivity

## 4.2 Water situation in Delicias District

### 4.2.1 Crop water analysis MODIS

The distribution of the crop types discriminated from monthly biomass production profiles is presented in Figure 32. An unsupervised classification was applied as mentioned before and there are thus uncertainties associated with this map because no field verification took place. This is acceptable as long as these maps are used to illustrate the power of satellite imagery to discern agricultural water management practices by crop type. The acreages are summarized in Table 12. Corn, alfalfa, sorghum, apples, pecan nuts and cotton occupy together 72.7 % of the agricultural area. From public documents it is known that Delicias hosts alfalfa, grains (sorghum, corn, wheat, barley, rye), cotton, fruits (apple, peach), vegetables (potato, cantaloupe, water melon, onion, tomato, chili), nuts (pecans, peanuts) and beans (dry beans, soybeans). It is said that irrigated corn, alfalfa, cotton, pecans, apples, dry beans and chili represent 73% of the total irrigated crop acreage in Chihuahua during 1999. This is in a good agreement with our simple MODIS crop class map. The 30 m resolution Landsat images are more suitable to determine the ET and biomass production from specific fields, and for this reason a Landsat component has been inserted in this study as well.

**Table 12: Bio-physical crop water productivity analysis on the basis of MODIS images in the Delicias Irrigation District. Water productivity per unit of depletion is considered. The results relate to annual values**

<b>Crop type</b>	<b>Acreage (ha)</b>	<b>Acreage (%)</b>	<b>ET<sub>act</sub> (mm)</b>	<b>ET<sub>act</sub> (km<sup>3</sup>)</b>	<b>Biomass Production (kg/ha)</b>	<b>Harvest index (-)</b>	<b>Crop yield (kg/ha)</b>	<b>Crop water productivity (kg/m<sup>3</sup>)</b>	<b>ET<sub>deficit</sub> (mm)</b>
Chili	8300	8.2	502	0.06	10,897	2.0	21,794	4.34	216
Pecan	11738	11.6	679	0.10	14,541	0.1	1,454	0.21	166
Wheat	3437	3.4	676	0.03	15,829	0.4	6,332	0.94	281
Apple	12463	12.3	753	0.12	17,091	2.0	34,182	4.54	178
Other fruits	7569	7.5	800	0.07	17,671				164
Beans	8263	8.2	876	0.08	18,960	0.3	5,688	0.65	137
Corn	13718	13.6	988	0.16	41,575	1.5 (sillage)	62,361	6.31	184
Cotton	10381	10.3	967	0.11	21,915	0.15 (lint)	3,288	0.34	126
Alfalfa	129593	12.5	1169	0.18	29,707	0.6 (dry forage)	17,824	1.52	270
Sorghum	12543	12.4	1057	0.16	46,435	0.35	16,252	1.53	217
<b>TOTAL</b>	<b>101,006</b>	<b>100</b>		<b>1.08</b>					

This section is prepared with the intention to show that 250 m MODIS images are good candidates for large scale (think about all overexploited basins and aquifers in Central and Northern Mexico) agricultural water management surveys. The annual ET, biomass production and other parameters have been added to Table 12. Harvest indices are found from the international literature (e.g. Lobel et al., 2002) and adjusted to the local conditions for obtaining a harvestable yield that agrees with some published yield data. All harvest indices are rounded numbers to indicate that they need further fine-tuning from local agronomical measurements. The harvest index of chilies is an out layer because the pepper physically consists essentially out of moisture. The harvest index applied in this study is an apparent index that directly relates dry matter production to fresh yield. This can differ from

other harvest indices that reflect only the dry matter production of the harvested product; hence some caution is required with exchanging harvest index values.

The total evaporative depletion of 1.08 km<sup>3</sup> is smaller than the 1.95 km<sup>3</sup> reported by Parr Rosson et al. (2002) because the MODIS area relates to 101,006 ha only, and the other data refer to state scale. Alfalfa requires annual irrigation depths of 2400 to 2700 mm (Rodrigues and Ornona, 2004). Lauer (2004) report a value of 1800 to 2100 mm per year from surface irrigation on alfalfa, and estimates that a saving up to 1400 to 1600 mm can be achieved by the introduction of buried drip tape. Alfalfa measurements in Idaho indicated an annual ET<sub>act</sub> of 915 mm over a 18 year research period at Kimberly (Shewmaker et al. 2004). Hanson and Putnam (2000) mention that alfalfa can ET up to 1270 mm/yr. ET values measured in the deserts of Saudi Arabia exceed 2000 mm/yr (Al Ghobari, 2000). Our value of 1169 mm is thus reasonable.

The production of green forage in Chihuahua can be 127 ton/ha/yr for pivot systems, 110 ton/ha/yr for power rolls and 81 ton/ha/yr for surface irrigation systems. The moisture content of green forage is 85%, and the dry matter production is thus somewhere in the range between 12.2. to 19.1 ton/ha. Our remotely sensed yields are with 17.8 ton/ha in the same range, and should therefore be considered as reasonable. Whereas alfalfa yields in New Mexico maximally 13 ton/ha, San Joaquin Valley (California) is reaching yields up to 48 ton/ha (Hanson and Putnam, 2000). This reveals that there is scope to harvest more alfalfa per unit of land and per unit of water.

The crop water productivity of wheat (0.94 kg/m<sup>3</sup>) is a little below the world average value of 1.09 kg/m<sup>3</sup> (Zwart and Bastiaanssen, 2004). The crop water productivity of cotton (0.34 kg/m<sup>3</sup>) is more than the global average value for lint cotton of 0.23 kg/m<sup>3</sup>. This brief analysis reveals that the physical crop water productivity is at par with most other irrigation systems. The total biophysical water productivity can therefore not become significantly more, only 10 to 30% nominally. The marginal increases can be investigated further by inspecting the crop water productivity populations of each crop type.

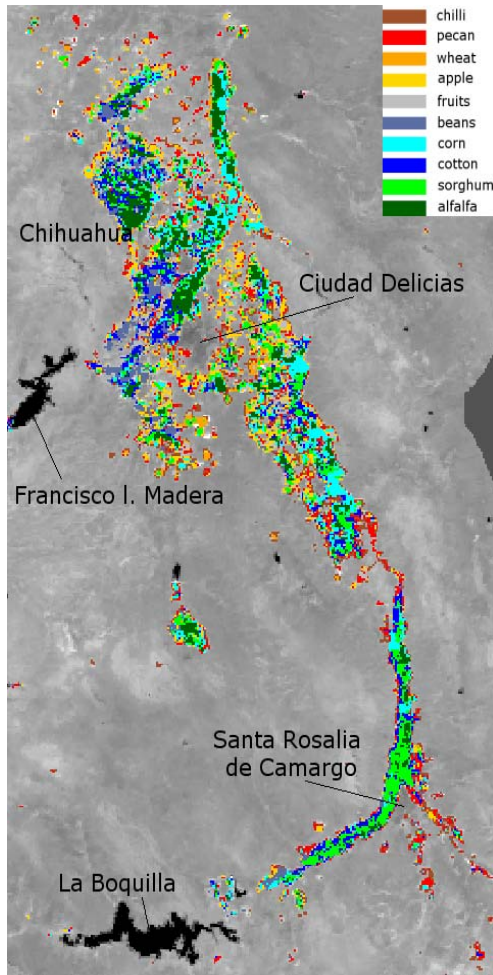


**Figure 32: Crop classification in the Delicias Irrigation District in the Rio Conchos (Chihuahua) based on 250 m MODIS images. The Presa de la Boquilla near Ciudad Camargo and the Las Virgenes reservoir near Ciudad Delicias are indicated**

#### 4.2.2 Crop water analysis Landsat

Landsat images provide essential details of the irrigation processes that take place at plot scale. MODIS can never see plot scale processes. Figure 33 displays the area North of Santa Rosalia de Camargo, and displays the changes in cropping conditions between March and October.

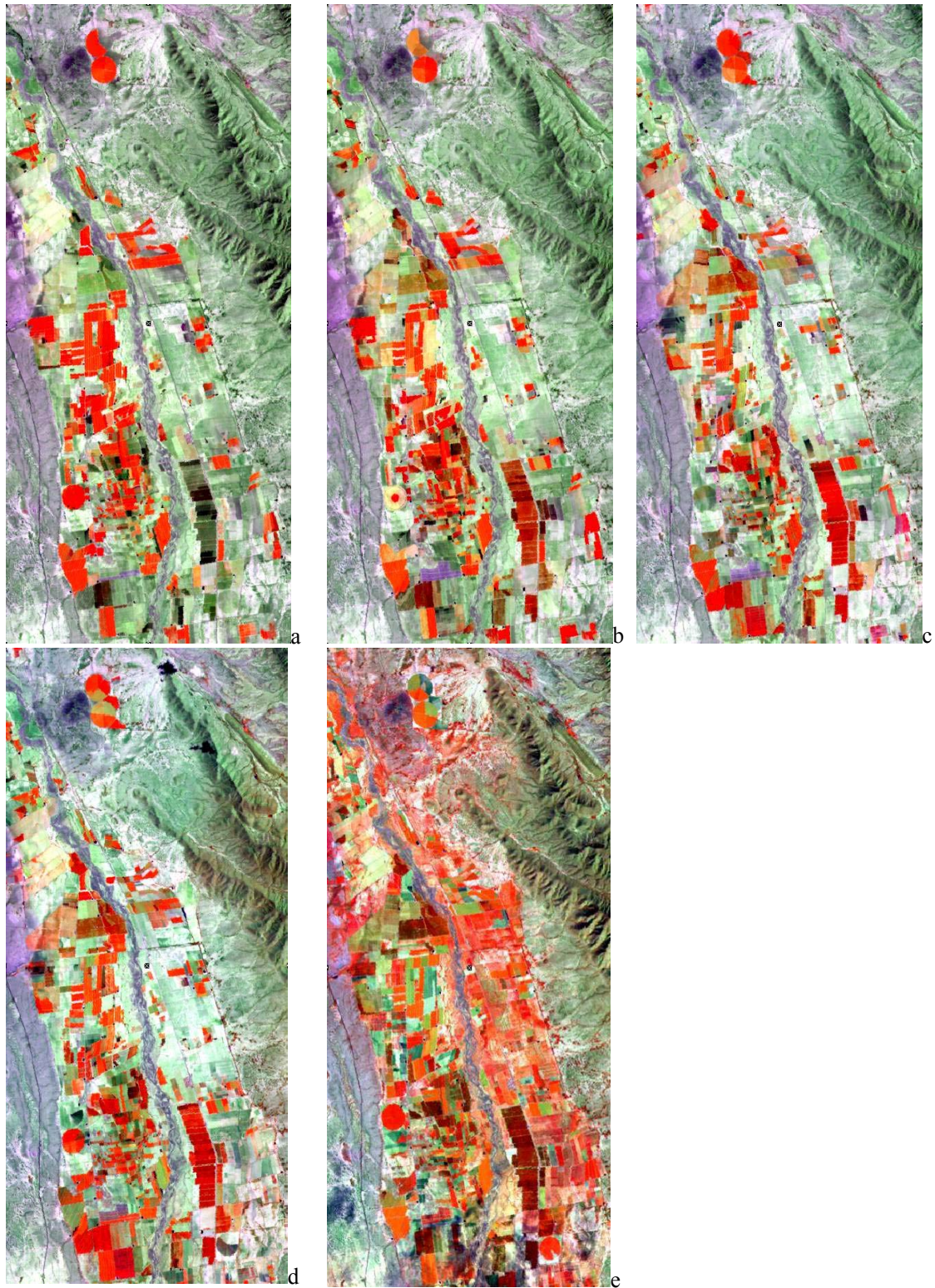
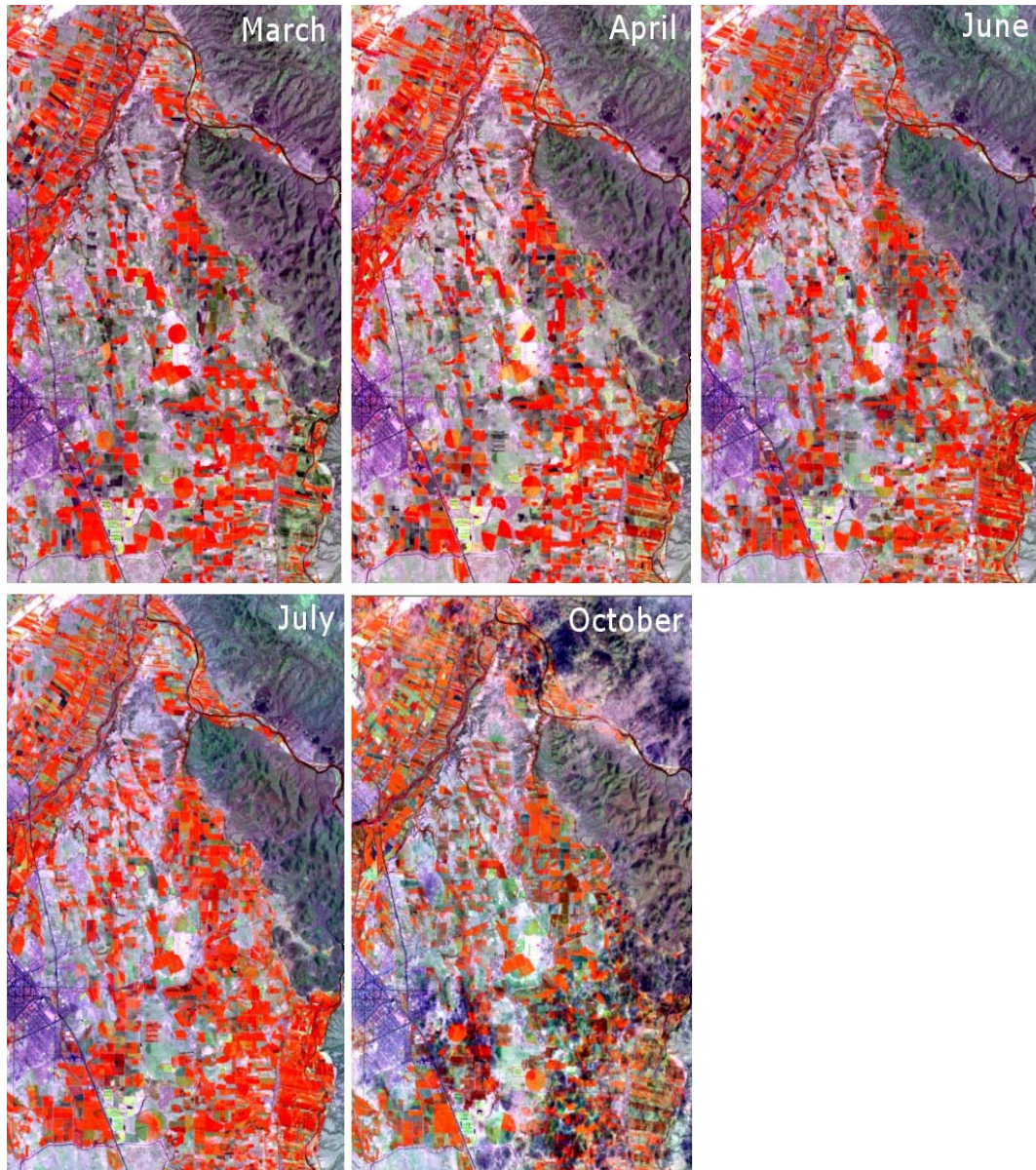


Figure 33: False color composite of the progression of crops from March 25 (a), April 26 (b), June 13 (c), July 15 (d) to October 3 (e). More red is associated with more crop vigor



**Figure 34: False color composite of the progression of crops from March 25 (a), April 26 (b), June 13 (c), July 15 (d) to October 3 (e). Ciudad Delicias is located on the image**

The cropping intensity in the wet Summer is larger than during the dry Winter. The intensive red color represent alfalfa fields and most of these fields are red in all seasons. The light red pixels are typically orchards with a lower LAI. Apple and pecan trees have a low LAI if the tree distance is large enough to see the bare underground with some weeds. An unsupervised crop classification was performed to obtain a plot scale crop map with the NDVI values of the 5 separated Landsat images. After excluding all non-cropped pixels, the agriculture system was mathematically divided into 10 clusters.

The SEBAL model has been applied to all 5 Landsat images. The resulting ET map of July 15 is displayed in Figure 35. Alfalfa, corn and sorghum fields have the highest ET (>6 mm/d). The ET strip along the eastern boundary of the valley is wetter, likely due to local seepage processes from the higher elevation desert areas.

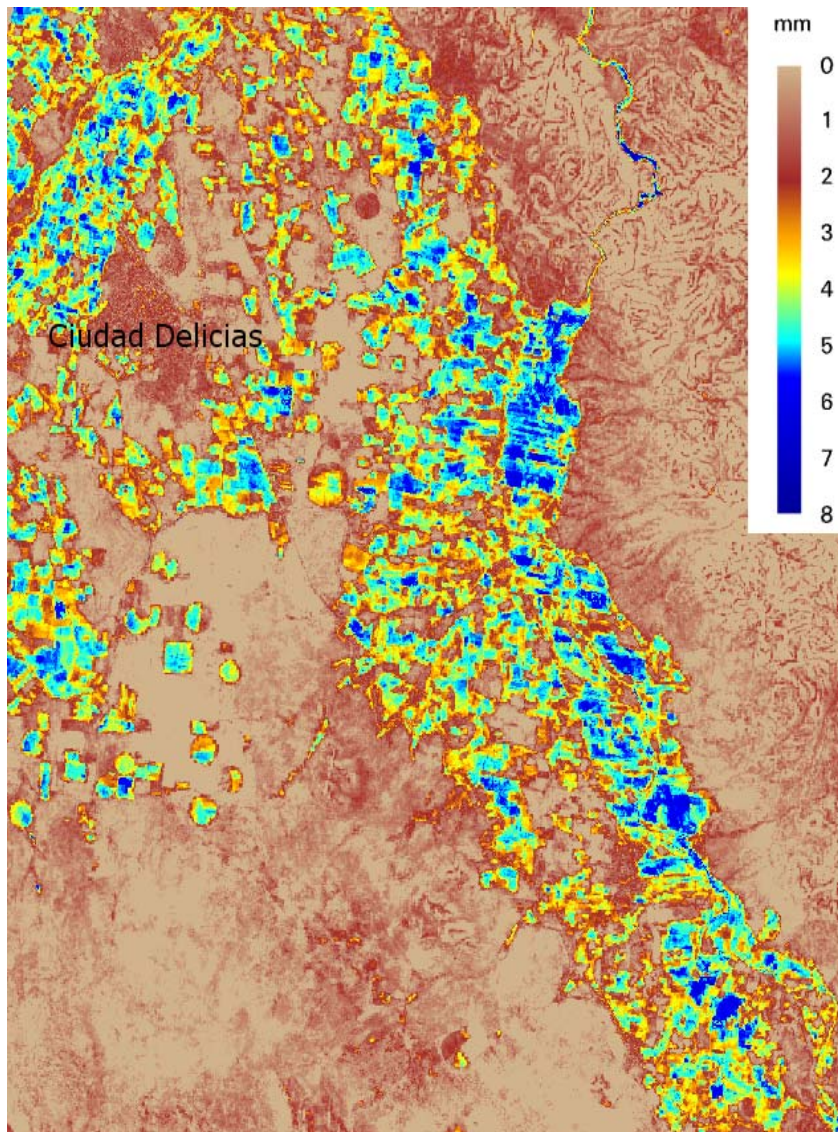


Figure 35: 24-h Actual evapotranspiration on July 15 (2003) based on SEBAL and Landsat images

The ET and biomass results obtained on individual Landsat days are integrated with the 15 day (bi-monthly) MODIS-based ET data. Each of the 5 Landsat images is considered representative for a certain MODIS period. The March image is for example considered to be representative for the MODIS period between January 1 to April 15 etc. The accumulated ET results of each of the 5 Landsat periods are derived from:

$$ET_{30m} = \{ET_{30m}(x,y)\}_i / \text{mean}\{ET_{30m}(x,y)\}_i \times \text{mean}\{ET_{1000m}\}_i$$

Where  $(x,y)$  represents a unique pixel ET value and  $i$  relates to the 5 land cover classes. The 1000 m pixels are from MODIS. This procedure implies that the MODIS-based accumulated ET values for the agricultural land cover class is used, and broken down by means of all the 30 m Landsat pixels that fall in the land cover class agriculture. The annual accumulated ET is obtained by adding together the results of the 5 Landsat results (see Figure 36). The area is smaller than for the MODIS ET map due to the partial coverage problem of Landsat path/row 31/40.

The average annual ET for all agricultural pixels is 857 mm and this includes also the fallow period. The fallow period has to be included because the duration of the cropping season varies between all plots, and the integration period is thus unknown.

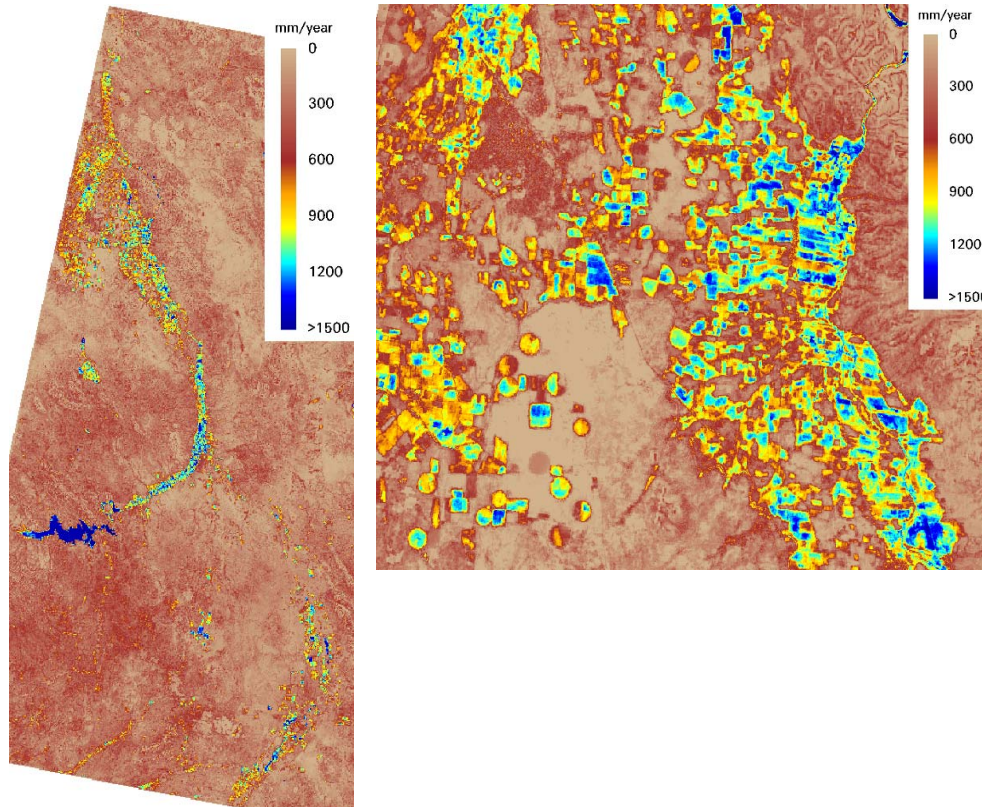


**Figure 36: Annual accumulated ETact for all agricultural fields in the Delicias Irrigation District. The ET has been computed independent from the crop identification. Part A shows the maximum coverage possible for Landsat path 31 and part B is an inset of the vicinity of Ciudad Delicias**

The ET frequency distribution follows a nice theoretical bell shape. The ET histogram has a wide range (Mean=857 mm; SD=446 mm; CV=52%) and this shows that real water savings are feasible, simply because half of the population of the farmers is already consuming much less water than their fellow colleagues. The 25% percentile of ET is 499 mm and the 75% percentile has a value of 1270 mm. Areas with lower than average ET are saving water already. Farmers on the transition between 857 to 1270 mm could save water by ET reduction (and not by improving irrigation efficiency).

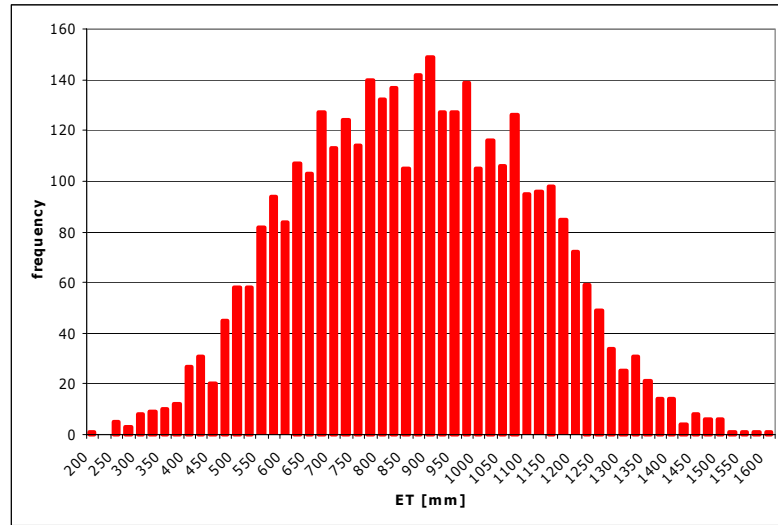


Figure 37: Frequency distribution of annual  $ET_{act}$  of irrigated crops in the Delicias Irrigation District (2003) based on SEBAL and Landsat/MODIS images

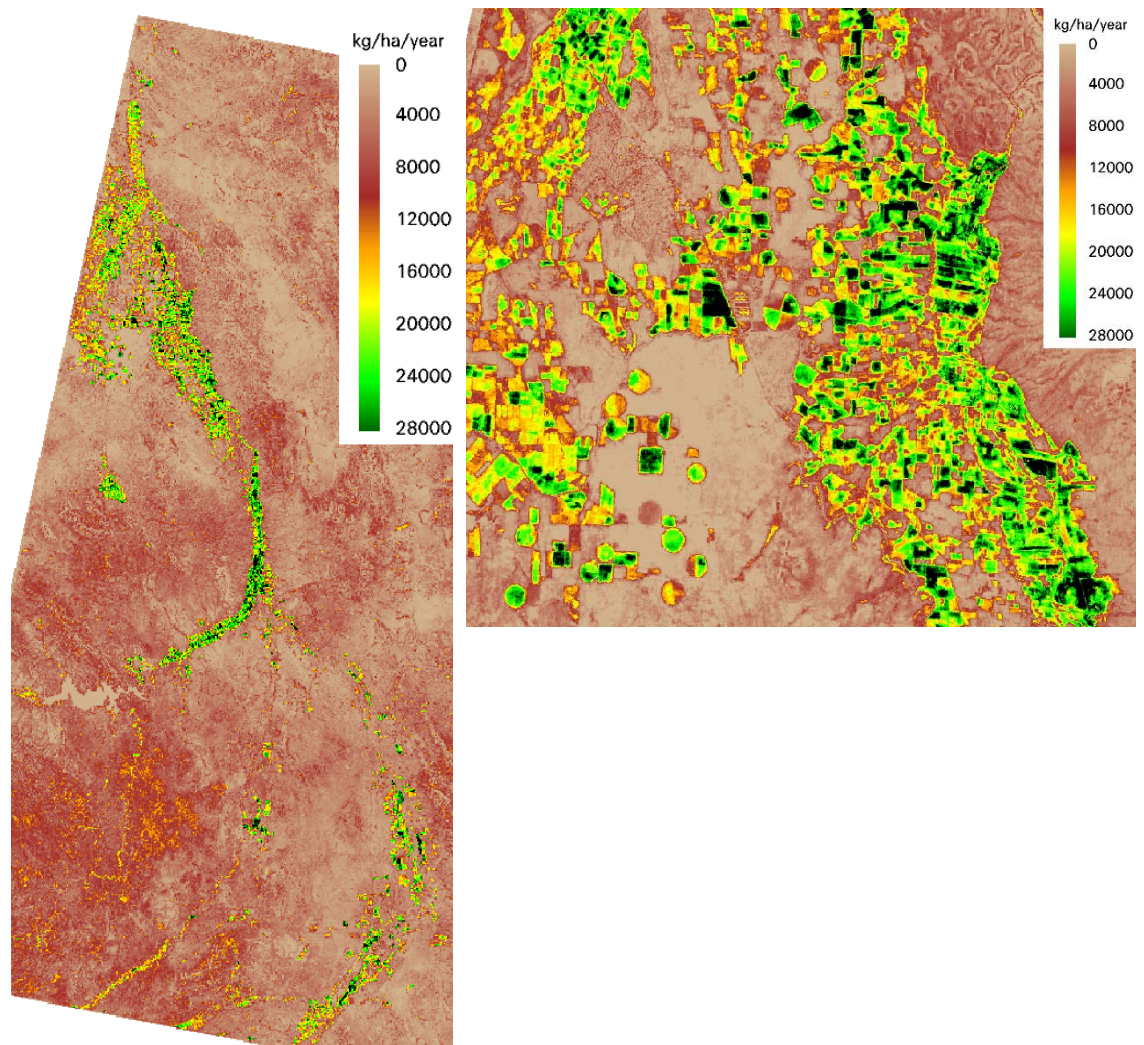
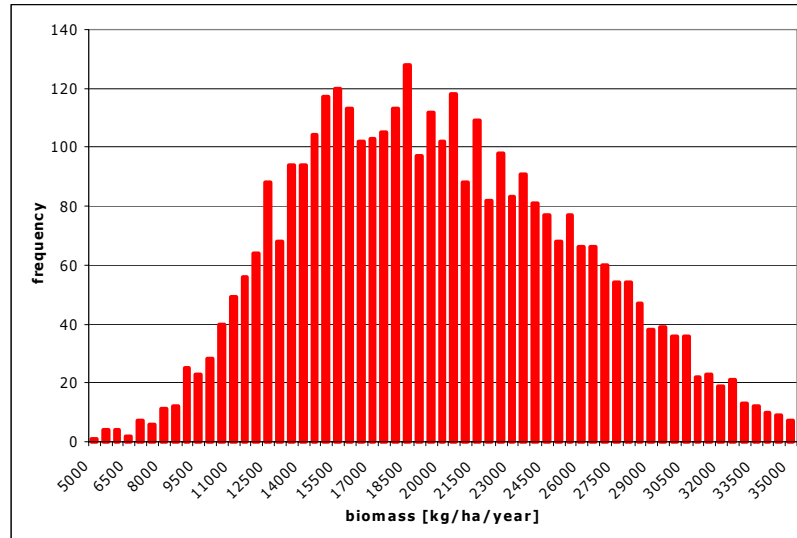


Figure 38: Accumulated biomass production of irrigated crops in the Delicias Irrigation District

The histogram of biomass production is skewed. If a crop gets insufficient water and nutrients, it will not mature and therefore the left hand side of the histogram is steeper than the right hand side. The mean biomass production of all crops together is 19,560 kg/ha/yr. The 25% percentile has a value of 11608 kg/ha and the 75% percentile is as high as 29020 kg/ha/yr.



**Figure 39: Frequency distribution of biomass production of irrigated crops in the Delicias Irrigation District based on SEBAL and Landsat/MODIS images**

**Table 13: Crop water productivity analysis on the basis of Landsat images. The area is smaller than for the MODIS area presented in Table 12. Net benefits are taken from Lauer et al. (2004). Annual values are considered independent of the length of the cropping season**

Crop type	Acreage (ha)	Acreage (%)	ET <sub>act</sub> (mm)	Biomass Production (kg/ha)	Harvest index (-)	Crop yield (kg/ha)	Net benefit (\$/kg)	Net benefit (\$/ha)	Crop water productivity (kg/m <sup>3</sup> )	Crop water productivity (\$/m <sup>3</sup> )
Chili	6236	7.6	714	16,258	2.0	33,056	0.276	9,115	4.46	1.28
Pecan	9115	11.1	710	15,722	0.1	1,572	7.486	11,769	0.22	1.66
Apple	6527	7.9	898	20,319	2.0	40,637			4.53	
Other fruits	7331	8.9	709	15,208						
Beans (soybeans)	6737	8.2	915	21,101	0.3	6,330			0.69	
Corn <sup>3</sup>	10185	12.4	847	34,024	1.5	51,036	0.102	5,206	6.03	0.61
Cotton	8052	9.8	997	22,708	0.15 (lint)	3,406	1.07	3,644	0.34	0.37
Alfalfa	16053	19.5	1128	27,233	0.6 (dry forage)	16,340	0.501	8,183	1.45	0.73
Sorghum <sup>4</sup>	11818	14.4	634	25,288	0.35	15,931			2.51	
<b>TOTAL</b>	<b>82,054</b>									

The cultivation of high value and low water consuming crops should be encouraged. Pecan nuts with a crop water productivity of 1.66 \$/m<sup>3</sup> is a good example. Converting 1 ha of alfalfa (1128 mm) into pecans (710 mm) saves an amount of 4180 m<sup>3</sup>/ha/yr (which are huge quantities of water) and earns 3636 \$/ha/yr extra ! Other fruit trees such as almonds, peaches, cherries, walnuts, pistachio etc. could

<sup>3</sup> Corn is a C4 crop and has a 80% higher light use efficiency than the c3 crops

<sup>4</sup> Sorghum is a C4 crop and has a 80% higher light use efficiency than the c3 crops

be evaluated as an alternative crop. Furthermore, it should be mentioned that ET can be reduced by increasing tree spacing, so the same crop can be cultivated with less water consumption at reduced benefits, but financial benefits still in favour than shifting to other crops.

The highest physical water productivity of the crops discerned is corn (6.03 kg/m<sup>3</sup>). The farmers' interests are in prosperous net benefits per unit of land that they own or tenure. Their profits is the highest for intensive crops such as pecans (11,796 \$/ha) and chilies (9,115 \$/ha). Alfalfa is also financial attractive crop to cultivate (8,183 \$/ha). Considering the over-arching water shortage problems in the Rio Bravo, it would be wiser to study the economic water productivity. Also here Pecans (1.66 \$/m<sup>3</sup>) and chilies (1.28 \$/m<sup>3</sup>) are favorite.

Grapes, pecans and chilies are relatively profitable, making them an attractive crop for those producers than can afford heavy initial investments. Although less profitable than pecans, alfalfa is still more viable than corn or sorghum. Subsidies can drive production decisions toward a more productive water use.

An independent crop water productivity study was described in Lauer et al. (2004). Their data agrees in large lines with our satellite scan of the agricultural water productivity (see Table 14).

**Table 14: Water productivity in the Rio Conchos Basin on the basis of conventional data collection procedures (after Lauer et al., 2004)**

<b>Crop</b>	<b>Gross water depth (mm)</b>	<b>Yield (kg/ha)</b>	<b>Net benefit (\$/ha)</b>	<b>Net benefit (\$/kg)</b>	<b>Water productivity (kg/m<sup>3</sup>)</b>	<b>Water productivity (\$/m<sup>3</sup>)</b>
Cotton	1731	3,500	3739	1.07	0.20	0.22
Peanuts	1747	3,500	3214	0.92	0.20	0.18
Chili	2958	25,000	6894	0.276	0.85	0.23
Onion	2767	35,000	5481	0.16	1.26	0.20
Corn	1313	48,000	4900	0.102	3.66	0.37
Alfalfa	2950	16,000 (dry forage)	8013	0.501	0.54	0.27
Pecans	2223	1,500	11230	7.49	0.07	0.51
Watermelon	1300	25,000	5013	0.20	1.92	0.39
Grapes	2034	18,000	23780	1.32	0.89	1.17

The total economical benefit is the weighted average of the net benefit of each crop class. Taking a mixture of chili, pecan, corn, cotton and alfalfa will yield an average economic productivity of 0.93 \$/m<sup>3</sup>, which is a quite good performance as compared to other irrigation systems in the world. A quick and rough calculation shows us that at a total evaporative depletion of 20.5 km<sup>3</sup>/yr in the Rio Bravo basin, a net profit of 19 billion \$/yr from irrigated land will be generated.



**Crop water productivity alfalfa**

The average crop water productivity is 1.45 kg/m<sup>3</sup> with the majority of the pixels between 1.35 to 1.60 kg/m<sup>3</sup>. This is a rather narrow range which indicates that within alfalfa, there are limited possibilities to harvest more forage from less water resources. Doorenbos and Kassam (1973) report a water productivity of 1.5 to 2.0 kg/m<sup>3</sup> in alfalfa to be feasible. Hanson and Putnam (2004) mention that in San Joaquin (California), alfalfa reaches even 3.0 kg/m<sup>3</sup>, while in Imperial Valley (California) values are not more than 0.93 kg/m<sup>3</sup>. Reasons can be ascribed to antecedent soil moisture, season length, climate variability, root development, experimental methods and crop maturity (Smeal et al., 1992).

**Irrigation District**

Possible water savings were investigated further by studying the biomass response to water. Intentionally, all crops are taken together for gathering an overall impression of the options to reduce ET while maintaining production. Figure 40 shows the relationship between biomass production and ET to be near-linear. There is a slight trend towards concavity noticeable, but this is not significant. This trend implies that crop yields in Delicias Irrigation District have a strong coupling to ET, and that ET reduction in agriculture will immediately be translated into a depression of food production and thus net profits. On-farm water savings thus go at a cost of income unless the Delicias farms and farmers will not be cooperative to conserve water. ET quota may prompt farmers to shift to higher value crops.

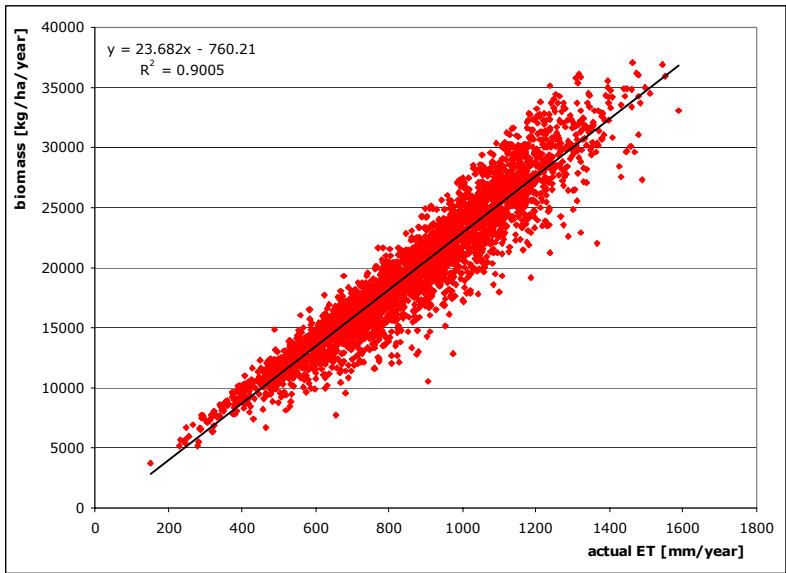


**Figure 40: Analytical relationship between biomass production and ET for all plots located on the Landsat path 31 image**

According to Table 14, the average applied water depth in Delicias Irrigation District is 2079 mm per year. The average depletion was found to be ET<sub>act</sub> is 857 mm. The net precipitation over this area is 236 mm. Application of the classical irrigation efficiency formula implies that the efficiency is 30.0 % only. After neglecting rainfall entirely from this process, the efficiency increases to 41%. Since the applied water

depth seems to be outrageous, we will assume that the average on-farm irrigation efficiency is 35%, which is not in contradiction with other reports on surface irrigation methods for Delicias

**Interim conclusions Rio Conchos**

- The cultivation of high value crops such as pecan nuts ( 1.66 \$/m<sup>3</sup>) needs to be boosted at the cost of growing traditional crops such as cotton (0.37 \$/m<sup>3</sup>) that consumes more water and provide less returns
- The population of ET values in the Delicias scheme shows a wide spatial variation (CV: 52%). The 25% percentile is 499 mm/yr and the 75% percentile is 1270 mm/yr. Some farmers deplete twice the amount of water that other farmers deplete. It is possible to save water in the irrigation sector by shifting to other crops
- Deficit irrigation and ET reduction will adversely affect crop yield. Real water savings should be gained from cropping pattern changes and more remote sensing research is required to detect the ET population of all the common crops
- The physical water productivity is comparable with values found in California (both lower and higher values are observed) and in the international literature. The overall impression is that water is productively used in the irrigation sector
- Plot scale crop yield and crop water productivity requires Landsat data
- A ceiling for ET should be created by means of a quota mechanism and ET reduction plans need to be designed and implemented to ensure that more

# 5. Results from hydrological modeling

## 5.1 SWAT vs. SEBAL

The first step in SWAT-based ET models is to ensure that the reference ET values between SWAT and SEBAL are similar. Since SEBAL is based on 12 cm short clipped grass and SWAT on the 50 cm long aerodynamically rough alfalfa, fine tuning stomatal ( $r_s$ ) and aerodynamic resistances ( $r_a$ ) was deemed necessary. The final resistances being used in the simulations are  $r_s = 80$  s/m and  $r_a = 170$  s/m. The aerodynamic resistance  $r_a$  is a function of wind speed. The canopy resistance is a function of the stomatal resistance and LAI (LAI= 2.9 for grass and LAI= 4.5 for alfalfa). The performance of the reference ET values is demonstrated in Figure 41. Except a few changes, the agreement is excellent. The spatial patterns of the two models are demonstrated in Figure 42. There is a clear  $ET_{ref}$  transition from the Gulf of Mexico to the inland area. High humidity and frequent cloud cover causes the reference ET in Tamaulipas to be a factor 2 smaller ( $ET_{ref}: \pm 1250$  mm/yr) than in the dry and sunny mountains of Coahuila ( $ET_{ref}: \pm 2500$  mm/yr).

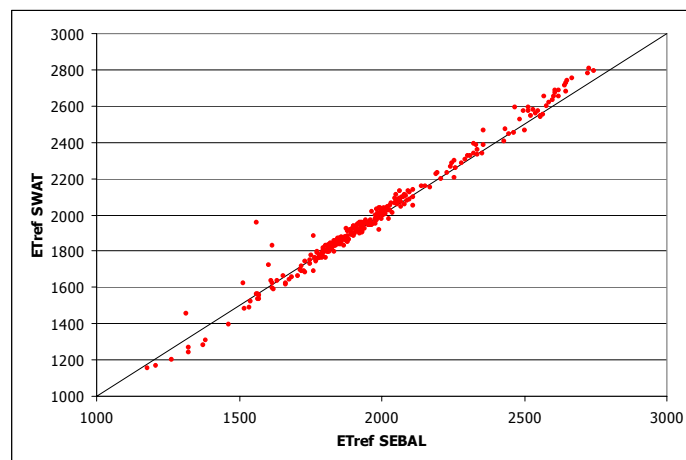


**Figure 41: Scatterplot of reference ET values of both models (2003)**

Traditionally, rainfall-runoff models are calibrated on the basis of stream flow measurements at a few hydro-meteorological gauging stations. Good matches on a few locations do not ensure that the spatially distributed hydrological processes are well enough understood. Exploring the areal  $ET_{act}$  patterns from SEBAL, is a leap forward in calibrating hydrological basin models. This is the first application to calibrate SWAT, with distributed remote sensing data, rather than fitting on flows on a few locations.

The SWAT model is calibrated in three steps:

- 1) The precipitation in the mountain area is slightly increased with a lapse rate until the new precipitation field exceeds the SEBAL  $ET_{act}$  values in mountain areas
- 2) The soil depths in the central part of the basin are adjusted for better reflecting moisture storage and moisture release mechanisms that have great impact on temporal ET behavior
- 3) In sub-basins fulfilling  $ET_{act}^{SEBAL} \gg ET_{act}^{SWAT}$ , capillary rise from the shallow aquifer to the unsaturated zone has been allowed to simulate lateral groundwater

movement (because SWAT is not a groundwater model) and root water uptake by pheatophytes

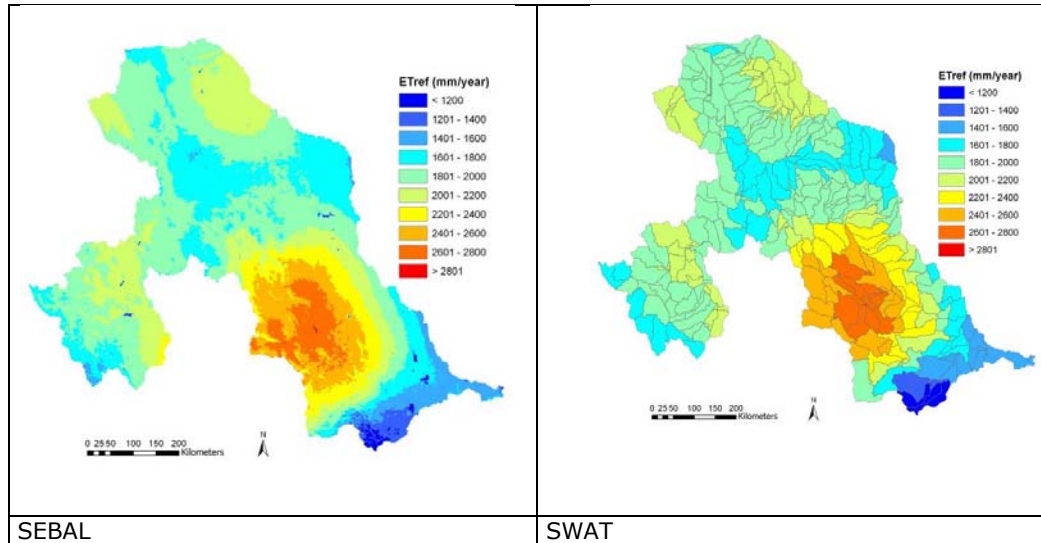


Figure 42: Spatial distribution of reference ET across the Rio Bravo Basin (2003) for both models

The soil and plant hydrology is responsible for causing differences between spatial patterns of reference ET and actual ET. Whereas the reference ET is the highest in the elevated areas of Coahuila, the actual ET is the highest in the lower flood plains where soil moisture is more easily available for plant ET. The good coincidence between the two  $ET_{act}$  outputs shows that SWAT is reproducing the SEBAL-based ET fields satisfactory. From here it can be concluded that the soil and plant parameters in the preliminary SWAT model are calibrated well. The hydrological data generated by SWAT are therefore thought to be good enough for water management analysis. Note that this is a preliminary version of the SWAT model for the Rio Bravo, and that further improvements in input data and model schematization can be accomplished by the use of local stream flow and groundwater data.

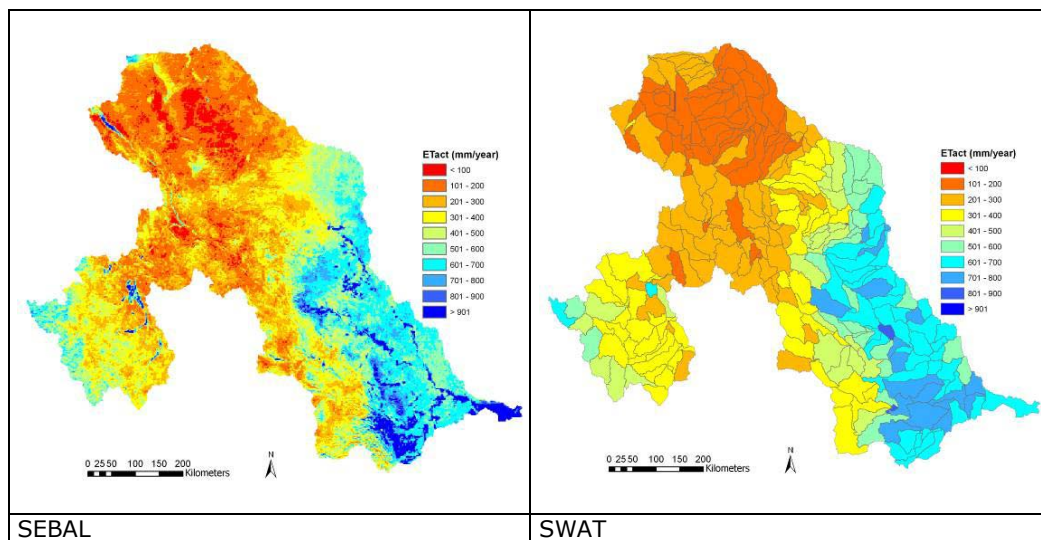
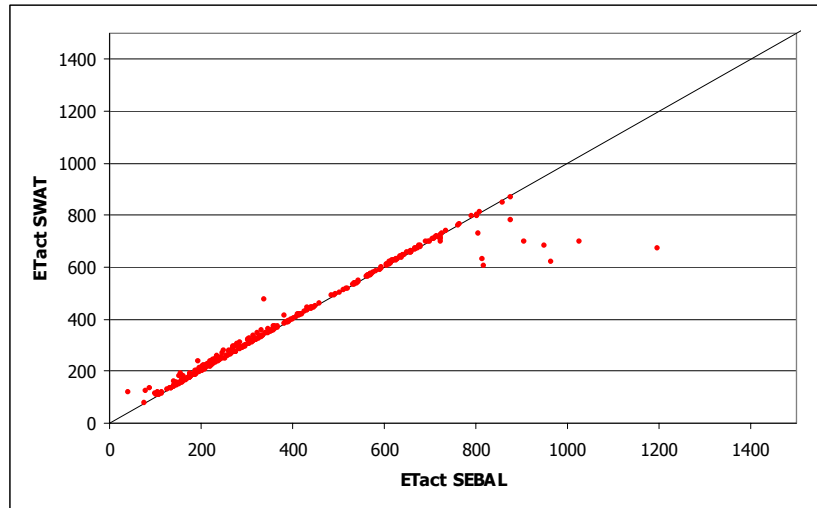


Figure 43: Spatial distribution of actual ET across the Rio Bravo Basin (2003) for both models



**Figure 44: Scatterplot of actual ET values of SEBAL and SWAT. Annual values averaged for sub-basins are shown**

For most of the 303 sub-basins, it was possible to obtain a good match between  $ET_{act}$  of the two models. SWAT had some difficulties in mimicking  $ET_{act}$  values exceeding 900 mm, and this must be related to insufficient water availability because  $ET_{ref}$  goes at these places up to 2800 mm/yr. Solutions for a better model fit have to be sought in reduced surface runoff and deep percolation.

## 5.2 The hydrology of Rio Bravo

The water balance of the Rio Bravo Basin domain modeled by SWAT is summarized in Table 15. The flows relate to the unsaturated zone where capillary rise and percolation are the governing exchange processes with the underground. The ET values by land cover type are not the same as in SEBAL, although the basin weighted average of 393 mm is near to the 397 mm of SEBAL (1.0 % error). The difference per land cover type is caused by the calibration of ET values at sub-basin scale and not per Hydrological Response Unit (which is a unique combination of land cover, soil type and drainage network).

Table 15 demonstrates that the storage in the unsaturated zone is positive (+23 mm on average) because rainfall is higher than in a normal year. The SEBAL soil moisture changes yielded a change of 34.4 mm. Wetter than normal conditions can also be interpreted from percolation (48 mm) exceeding capillary rise (13 m) and extractions for irrigation (7 mm). The net result is a 28 mm additional storage in the aquifer during 2003. Together the unsaturated and saturated zone ('total storage') store thus 51 mm. The peak of total storage occurs in the supplemental irrigation system where 87 mm percolates from the high 852 mm rainfall. It should be noted that 2003 cannot be considered as an average year and that more years are required for getting longer term water resources data.

Nevertheless, this data shows the magnitude of the water flows in the Rio Basin as one total system. A breakdown is presented in the subsequent table for sub-watersheds (see Table 16). The basin average runoff is for instance 6 mm only, while the gross precipitation is 450 mm. A runoff coefficient of 6/450 is 1.3% is extremely low and pinpoint that the basin is virtually closed. The 13 mm capillary rise reflects the disappearance of groundwater due to extraction of natural vegetation.

Table 15: Annual SWAT water balance per land cover class (2003)

<i>Land cover</i>	<i>Precipitation</i>	<i>Irrigation</i>	<i>ET</i>	<i>Surface runoff</i>	<i>Percolation</i>	<i>Capillary rise</i>	<i>Lateral outflow</i>	<i>Storage Change UNSAT</i>	<i>Total Change</i>
	(mm)	(mm)	(mm)	(mm)	(mm)	(mm)	(mm)	(mm)	(mm)
Urban	594	0	454	154	14	66	4	+38	-14
Irrigation delta	856	215	741	106	57	6	0	+173	+9
Irrigation Valley	261	449	667	36	40	81	1	+48	+7
Supplemental irrigation	852	166	754	98	87	0	3	+79	+166
Low open forest	468	0	464	1	84	137	5	+56	+3
Oak forest	552	0	542	6	29	59	2	+34	+4
Pine forest	576	0	536	5	142	153	7	+46	+35
Scrubland	348	0	367	3	46	90	1	+22	-22
Cultivated pastures	567	0	531	8	25	41	1	+44	+28
Natural pastures	398	0	372	4	39	29	2	+12	+22
<b>BASIN</b>	<b>450</b>	<b>7</b>	<b>393</b>	<b>6</b>	<b>48</b>	<b>13</b>	<b>1</b>	<b>+23</b>	<b>+51</b>

To make the description of the hydrological variability more prominent, the annual water balance of Table 16 has been broken down into sub-watersheds. The location of these sub-watersheds can be found in Figure 45. Water generation to downstream users is the sum of surface runoff, percolation and lateral outflow. Pine forests and low open forests generate the highest water depth available for others.

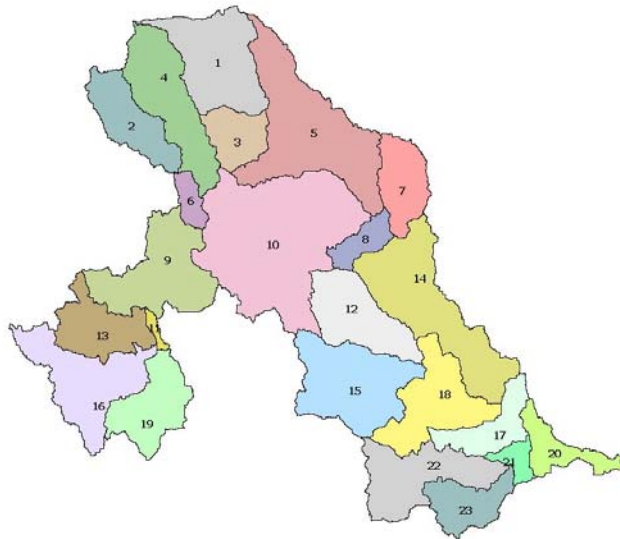


Figure 45: Location of 23 sub-watersheds in the Rio Bravo Basin

Table 16: Annual water balance terms of the 23 sub-watersheds

	Areal coverage (%)	Rainfall	Irrigation	Revap	ET	Percolation	Lateral outflow	Surface runoff	Balance
1	5.8	218	0	0	-170	-46	0	0	2
2	3.1	177	16	39	-217	-2	0	0	13
3	2.3	266	0	0	-171	-95	0	0	0
4	5.5	228	0	0	-175	-50	0	0	3
5	9.1	312	0	0	-265	-40	0	0	7
6	0.9	341	17	0	-265	-88	0	-4	1
7	2.9	444	0	199	-573	-37	0	-4	29
8	1.4	514	5	0	-437	-67	0	-2	13
9	5.9	319	7	0	-241	-80	0	-3	2
10	13.5	393	1	0	-264	-127	0	-1	2
11	0.3	313	116	28	-418	-4	0	-9	26
12	4.4	540	10	58	-555	-17	0	-2	33
13	3.5	414	12	6	-396	-18	0	-6	12
14	8.0	582	11	147	-640	-15	0	-6	79
15	6.4	480	6	0	-385	-92	0	-2	8
16	5.6	527	2	52	-504	-61	0	-2	14
17	2.6	736	7	91	-670	-61	0	-23	80
18	5.0	659	17	27	-587	-65	0	-11	39
19	3.8	402	13	0	-370	-29	0	-2	14
20	2.0	696	75	160	-678	-50	0	-48	154
21	0.8	795	21	115	-703	-130	0	-27	71
22	4.8	680	3	0	-504	-134	0	-18	27
23	2.6	851	4	101	-654	-179	-1	-51	71
<b>Basin</b>	<b>100</b>	<b>450</b>	<b>7</b>	<b>84</b>	<b>-393</b>	<b>-48</b>	<b>-1</b>	<b>-6</b>	<b>23</b>



---

# 6. Implications for water management

## 6.1 Irrigation efficiency

Irrigation efficiency is for long being considered to be the key process in irrigation management. Although the concept is still valid - it saves energy costs if irrigation water losses are kept minimal - it is from a water resources point of view not interesting if the efficiency is low, as long as return flow from a given scheme is recaptured back in the water process chain. The water quality usually deteriorates, but this is of secondary importance. Although being 1000 km apart, return flow from the Delicias scheme can be diverted for irrigation in Nuevo Leon. The net efficiency of different schemes that function as a cascade system must be higher, and efficiencies of 50% can go up to 85% or more (Abu Zheid and Seckler, 1992; Bastiaanssen et al., 2003). The classical irrigation efficiency is:

$$\text{Irr} = (\text{ET}_a - \text{P}_{\text{net}}) / \text{Q}$$

where  $\text{ET}_a$  is the actual evapotranspiration,  $\text{P}_{\text{net}}$  is the net precipitation, i.e. the gross precipitation with corrections for interception, surface runoff and deep percolation losses, and  $\text{Q}$  is the water withdrawn or diverted from a specific surface-water or groundwater source.

Irrigation Districts investigated in this study are mainly concentrated in 4 areas, and they have a completely different climatology and water management regime. Every of these 4 systems has been considered to be a sub-basin in SWAT terminology so that all output of the complete system can be gathered. The bulk behavior of each of the 4 systems was simulated using the following single effective crop:

Valle de Juarez	(39,233 ha)	Corn	May 15 to October 1
Rio Conchos	(149,118 ha)	Corn	May 15 to October 1
Valle del Monterrey	(331,140 ha)	Corn	June 15 to November 15
Delta Rio Bravo	(310,578 ha)	Sorghum/corn	February 15 to November 1

It is a limitation of SWAT to consider only one crop at the time. A single crop for a limited irrigation period will yield relatively low ET and irrigation values. As the Landsat compilation has demonstrated, in reality there will be continuous irrigation in certain fields. The ET frequency distribution – demonstrated before – had indicated that there is wide spread in ET values. The annual mean value of 857 mm from the combined Landsat-MODIS images is higher than the ET values for a single Summer crop in Table 17 (640 to 738 mm).

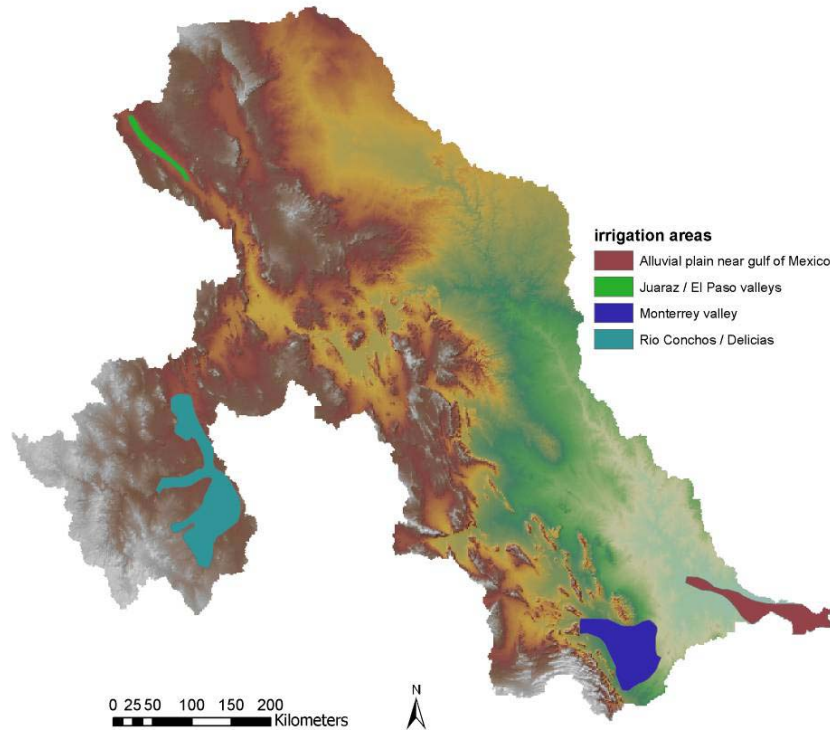


**Figure 46** Location of the major irrigation centers in the Rio Bravo Basin

The irrigation efficiencies between the 4 systems are widely diverging (see Table 17). Whereas Monterrey has a low efficiency (30%) because most water resources originate from rainfall, and applied water is 'dragged' downward together with the percolating rainwater flux, the schemes in Rio Conchos (Delicias) and Juarez are with 84 and 90 % respectively very efficient. One of the reasons behind this apparent high efficiency is their topographic location in narrow valleys, where left over water from irrigation is picked up again by the crops that are growing in the shallow water table area near the course of the river. The mathematical mean of the irrigation efficiency of the 4 large schemes separately is 64 %.

**Table 17: SWAT-based water flows related to classical irrigation efficiencies**

<b><i>Irrigation system</i></b>	<b><i>Irrigation (mm)</i></b>	<b><i>Net precipitation (mm)</i></b>	<b><i>ET<sub>act</sub> (mm)</i></b>	<b><i>Classical irrigation efficiency (%)</i></b>
Juarez	580	117	640	90
Conchos	535	236	684	84
Monterrey	271	593	674	30
Delta	497	474	738	53

Seckler et al (2003) called the neoclassical concept of effective irrigation efficiency – with recycling of water included - to be necessary for the evolution of interest in irrigation. They suggest a shift from the point of view of water-delivery systems to the broader perspective of irrigation management and policy within the context of water resources in the basin context. These theoretical concepts were addressed by Jensen (1977) and Keller and Keller (1995) in a mathematical way. The net efficiency can be formulated as:

$$\text{Irr}_{\text{net}} = (\text{ET}_a - P_{\text{net}}) / Q + E_r (1 - \text{Irr})$$

where  $E_r$  is the fraction of the traditional 'losses' that is potentially available for recovery, reuse or recycling somewhere in the hydrological system, i.e. reusable outflow. The term  $E_r$  is governed by the (i) availability of downstream irrigation systems in the basin, (ii) the conveyance losses under way between upstream and downstream schemes and (iii) physiographical setting of a given area. In the theoretical case of no losses to the underground, multiple downstream systems and closed basins,  $\text{Irr}_{\text{net}}$  can become 1.0 or 100%. In reality this will, however, never occur.

All the 4 irrigation systems were schematized to be one large effective scheme of 830,000 ha. Application of the same formula for classical irrigation efficiency for the total system, leads to the conclusion that the effective efficiency is 70 %. If we further assume the local on-farm efficiency to be 35 % (see Section 4.2), then the fraction of the traditional 'losses' that is potentially available for recovery, can be assessed to be  $E_r=0.54$ . The overview on how efficiency changes with scale is displayed in Figure 47. If one draws the efficiency change with scale, a logarithm relationship will arise.

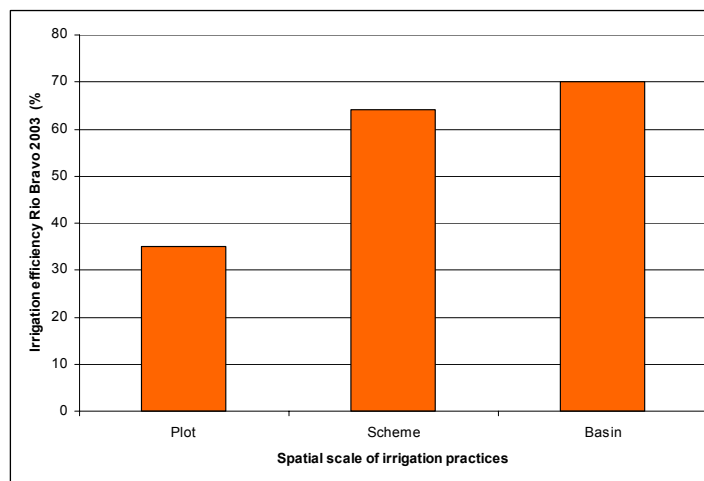


**Figure 47 Location of the major irrigation centers in the Rio Bravo Basin**

Hence, if the irrigation systems in Rio Bravo are considered as one continuous cascade system, the net efficiency is with 70% high and losses are for 54% recaptured. This finding has some paramount consequences for water management visions development:

- the efficiency for the irrigation sector as a total is already rather high and it will take unrealistic efforts to improve that further
- it does not make sense to improve local irrigation efficiencies, especially not in valley irrigation systems such as Rio Conchos and Juarez with system efficiency of 84 and 90% respectively

By narrowing the gap between  $Q$  and  $\text{ET}_{\text{act}}$  from say 35 % of conventional gravity systems to sprinkler efficiencies of 60 %, fewer diversions ( $Q$ ) will be required to maintain the same crop  $\text{ET}_{\text{act}}$ . Reduction in diversions ( $Q$ ) are, however, hard to achieve in real world circumstances without the appropriate institutional and legal frameworks. Unchanged diversions with higher efficiency systems will enhance the  $\text{ET}_{\text{act}}$  and essentially reduce the recycling coefficient from 54% to something lower. Hence, downstream irrigators could be adversely affected by more efficient upstream irrigation practices. These principles of upstream/downstream planning

and water allocation need to be considered by improving the total water productivity at the basin scale. This demands for a top down planning process, followed by a bottom-up implementation plan in the various Irrigation Districts.

## **6.2** Rio Bravo water utilization

The fast-growing Lower Rio Bravo region, comprising eight counties with a population of 919,505 in 1990, is projected to be home to 3 million people by 2050, hence a 228 percent increase. Municipal water use is expected to trail the tripling in population with a possible 171 percent increase in water needs. Groundwater and surface water resources supply almost equal shares of the state's water needs, but groundwater supplies have been receding year after year.

In 1997, 18 percent of the water in the Lower Valley was used by municipalities, an amount expected to increase to as much as 30 percent by 2050. Ciudad Juarez has already exhausted much of the area's readily accessible groundwater. Given the anticipated rapid-growth for these urban areas, future groundwater supplies come into question. El Paso already is converting some irrigation water to municipal use — about 43 percent of the city's annual supply comes from the Rio Grande.

Molden et al. (2003) argue that in the early stages of river basin development the emphasis was on constructing more storage, diversion and distribution facilities. Nowadays, the focus is increasing the productivity of water that could be established by turning less productive depletion into more productive depletion. In essence, the Rio Bravo basin water user groups are:

- ❑ Irrigation
- ❑ Municipal and Industrial Water Users
- ❑ Fish production
- ❑ Flood Control
- ❑ Pollution Disposal
- ❑ Hydropower
- ❑ Grazing and Logging
- ❑ Development
- ❑ Recreation

Water users in the Lower Rio Bravo Valley have found themselves in competition with natural river vegetation for the river's water. To make this competition more visible in numbers, data from several tables are re-organized and presented in Table 18.

Urban and industrial areas lose water through evaporation of parks, lawn trees, water ponds and turf. Although quantity wise this is a small component, this process yields to certain environmental enrichment in an urban setting, and is a result of artificial diversions and supplies. The benefits derived by depletion from trees and water bodies can be appreciable. Other non-organic water users will not deplete the resource, but instead return it back in the water flow path after usage: hydropower, effluent disposal and recreation.

A complicating factor is that water allocations by sector have to account for multiple uses of the same quantum of water. Because allocation is historically based upon diversion (and not on consumption), the same drop of water may serve forests, hydropower, domestic, fisheries and irrigated agriculture, where it is finally depleted as water vapor into the atmosphere. In overexploited basins, necessarily outflows to maintain and environmental balance to flush out salts and pollutants can not be met.

A first approximation of the water flows to *all* water use groups in Rio Bravo is outlined in Table 18. There is no specific class wetlands, because non of the land cover map units generated from the MODIS data can be interpreted as being wetlands. It is assumed that all river flow (=surface runoff in SWAT) goes through turbines. The diversions to irrigation are computed from the irrigation efficiencies in conjunction with depletion and rainfall, i.e. the application of classical irrigation efficiency in the inverse mode. The water diversion to urban areas is divided equally in municipal and industrial usage. This 50% share has also applied for the ET depletion of the parks and turf. The water allocation group 'fish' consumes water through the evaporation of water from reservoirs, ponds, creeks and streams. In future land cover classifications, a separation with reservoirs is necessary as reservoirs are related to hydropower, and fish production is a by-product. As mentioned before, wetlands need also to be more specifically appearing in the legend of the land cover map for better assessing water needs and return flows from wetlands.

**Table 18: Economical and ecological development of water use sectors in the 44 million ha Rio Bravo (2003)**

Water use sector	Benefit	Inflow rain (km <sup>3</sup> )	Inflow diversion (km <sup>3</sup> )	Depletion (km <sup>3</sup> )	Depletion (%)	Return flow (km <sup>3</sup> )	Return flow (% of total inflow)
Hydropower, Table 15	excellent	0.0	2.6	0.0	0.0	2.6	100
Irrigation, Table 9,17	excellent	6.5	4.7	10.5	6.0	0.7	15
Supplemental irrigation, Table 9,17	excellent	6.8	7.4	9.9	5.7	4.3	58
Municipal , Table 9	excellent	0.5	0.2	0.6	0.3	0.1	50
Industrial, Table 9	excellent	0.5	0.2	0.6	0.3	0.1	50
Forest, Table 9	Good	10.8	0.0	9.5	5.4	1.3	0
Fish species, Table 9,15	Good	0.0	2.6	0.8	0.5	1.6	61
Ecological (scrubland), Table 9	Little	151.0	0.0	123.9	70.8	27.1	0
Livestock (pastures) Table 9	Non	21.7	0.0	19.1	10.9	2.6	0
<b>TOTAL</b>		<b>197.8</b>	<b>17.7</b>	<b>174.9</b>		<b>40.4</b>	<b>18.7</b>

The water accounts show that the majority of the water resources to all water user groups originate from rainfall (197.8 km<sup>3</sup>/yr), which far exceeds the intake from diversions (17.7 km<sup>3</sup>/yr). This number is affected by the significant volumetric rainfall on the ecological scrublands. The irrigation sector withdraws 12.1 km<sup>3</sup>/yr, which is 68% of the total diversions. The 80% and 90% quotations that are often cited are thus overestimated, and probably emerge from a period that the population was smaller. The overall return flow of all water user sectors that withdraw water from streams, rivers and aquifers is 9.4 km<sup>3</sup>/yr, being 53% of the diversions (17.7 km<sup>3</sup>/yr).



---

# 7. Training and dissemination

## 7.1 Website application

To foster the accessibility of the project outputs, a user friendly GIS based website has been developed. The website is developed using Scalable Vector Graphics and the download of a small plug-in is required. The plug-in is a freely available adobe image viewer. The website is accessible via [www.waterwatch.nl/riobravo](http://www.waterwatch.nl/riobravo) and the site is activated since the end of March 2006.

Discussion on the future of the Rio Bravo will be stimulated by opening a public platform where at least a common dataset is posted. The objective of this website is to get access to the data for all stakeholders in the basin – and also for interested users outside the study area - for better comprehending the problems and water resources conditions determined in this Remote Sensing and Hydrological Modeling study. Standardized hydrological and ecological production data sets have the advantage of (i) covering large areas, (ii) possibilities for comparison between sub-basins and (iii) being unbiased because the data is not brought in by one particular water user group. The website does not show suggestions for improvement, but instead basic data that planners could use. This project report (in pdf format) is downloadable via the website.

The Rio Bravo website application contains a main menu that features the following options:

- MODIS/TRMM images Rio Bravo basin
- SWAT water balance Rio Bravo basin
- MODIS images Rio Conchos
- Landsat images Delicias irrigation scheme
- MODIS images Central Mexico (Aguascalientes) and Central Northern Valleys

The MODIS/TRMM images display the annual ET and rainfall values, together with a land use map and a Digital Elevation Model. A GIS interface with query and zoom functionalities allows the user to assess the pixel values with an associated legend. The spatial resolution of the maps is 1 km. By ticking the thematic boxes and zooming into certain areas of interest, it becomes feasible to study local rainfall and ET phenomena and how the aerial patterns change with land use class. To smear the rainfall patterns, original TRMM resolution of 25 km have been re-interpreted to a 1 km grid.

By clicking on the sub-basins, the annual water balance of each sub-basin will pop up in small window. This allows the user to get immediate access to quantitative water flows. It enables users to query the water balance on a sub-basin level and study for instance the level of overexploitation.

The power of expressing dynamical processes by means of remote sensing techniques is demonstrated with the example of Rio Conchos. Monthly values of ET, biomass production and soil moisture are demonstrated by means of an animation. For the sake of memory and time required to load these images, monthly values are not presented for the Rio Bravo basin.

The opportunity of field scale monitoring of water resources management is visualized with the Landsat applications around Ciudad Delicias. The site

demonstrates within field variations of soil moisture and crop consumptive use, as well as the water productivity expressed as a biomass production per unit ET.

The website also contains acknowledgements to the Comisión Nacional del Agua (CNA) and the World Bank. The Bank Netherlands Water Partnership is recognized for their financial support.

## **7.2** Workshop

The preliminary results of this study are presented in a workshop held between February 20 to 24 (2006) inside the premises of the Comisión Nacional del Agua in Mexico City. In the good hands of Ms. Griselda Medina Laguna and Mr. Clemente Trejo Domínguez, participants from all CNA departments and from several other Mexican water institutes were invited. There were more potential participants than could be located in the venue. A final list of 34 participants could be registered, and the attendees are presented in Table 19. The table shows that the participants come from 20 different institutes and departments. The design with representations from the various regions is excellent.

The overarching objective of the workshop was to introduce and expand the discussions regarding ET management as the overall strategy on improved water management with specific emphasis on the Rio Bravo. The practical aim of the workshop focussed on transfer of remote sensing images, model results and other data to the Mexican counterparts. Another aim was to provide more background on the assumption of the SEBAL and SWAT models, and how these advanced tools can be applied in an operational context. The workshop was scheduled with presentations and discussions in the morning. Afternoons were used for practical hands-on training on SEBAL and SWAT. A general discussion was organized at the end to discuss how these tools could be used in their near-future work of CNA.

All material as developed under the project was handed over to the participants:

- SEBAL images
- Viewer for images
- SWAT model
- Presentations
- Data sets

The workshop was received very well by the participants as well as the trainers who were impressed by the enthusiasm and the high level of competence of the participants. The workshop was closed with a ceremony shared by Eng. Ruben. Chavez and Dr. Torre Wolf.

**Table 19: List of participants attending the one-week training course on options for ET management**

<i>Name</i>	<i>Institute</i>
Ing. Claudia Leyva Suárez	Instituto de Geomática, Universidad Nacional Autónoma de México
Dr. Felipe Omar Tapia Silva	Centro de Investigación en Geografía y Geomática "Ing. Jorge Tamayo, A.C.
C. Irael Velasco Velasco	Instituto Mexicano de Tecnología del Agua, Secretaría del Medio Ambiente y Recursos Naturales
M. en I. Vicente Quezada Beltrán	Gerencia de Asuntos Fronterizos, Subdirección General de Infraestructura Hidráulica Urbana, Comisión Nacional del Agua
M. en C. Orlando García Rojas	Gerencia de Aguas Subterráneas, Subdirección General Técnica, Comisión Nacional del Agua
Ing. Víctor Castañón Arcos	Gerencia de Aguas Subterráneas, Subdirección General Técnica, Comisión Nacional del Agua
M. en C. Eliseo Vázquez Sánchez	Gerencia de Aguas Subterráneas, Subdirección General Técnica, Comisión Nacional del Agua
Ing. Anselmo Ordaz Ayala	Gerencia de Aguas Subterráneas, Subdirección General Técnica, Comisión Nacional del Agua
Biol. Luz del Carmen Velázquez Simental	Gerencia de Aguas Subterráneas, Subdirección General Técnica, Comisión Nacional del Agua
M. en C. Angélica Molna Maldonado	Gerencia de Aguas Subterráneas, Subdirección General Técnica, Comisión Nacional del Agua
Ing. Rodrigo Guadalupe Paredes	Gerencia de Aguas Subterráneas, Subdirección General Técnica, Comisión Nacional del Agua
Ing. José R. Chávez Hernández	Gerencia de Aguas Subterráneas, Subdirección General Técnica, Comisión Nacional del Agua
Ing. Laureano Mendoza Camacho	Gerencia de Aguas Subterráneas, Subdirección General Técnica, Comisión Nacional del Agua
Dr. José Y. Domínguez Esquivel	Gerencia de Aguas Subterráneas, Subdirección General Técnica, Comisión Nacional del Agua
Ing. Guillermo Bautista Barcenaz	Gerencia de Aguas Subterráneas, Subdirección General Técnica, Comisión Nacional del Agua
Ing. Isaac Felipe Morales Bravo	Gerencia de Aguas Subterráneas, Subdirección General Técnica, Comisión Nacional del Agua
Ing. Rodolfo Olivares Alva	Gerencia de Distritos y Unidades de Riego, Subdirección General de Infraestructura Hidroagrícola, Comisión Nacional del Agua
Ing. Máximo Mora Pérez	Gerencia Regional Golfo Centro, Comisión Nacional del Agua
Ing. Fabian Lárraga Acuña	Gerencia Regional Golfo Norte, Comisión Nacional del Agua
Ing. María avelina Carrilo López	Gerencia Regional Cuencas Centrales del Norte, Comisión Nacional del Agua
Ing. José Alberto Pérez Ortíz	Gerencia Regional Rio Bravo, Comisión Nacional del Agua
Ing. Amalio Cardona Rodríguez	Gerencia Regional Rio Bravo, Comisión Nacional del Agua
Ing. Sergio Marvín Galván Mancilla	Gerencia Regional Rio Bravo, Comisión Nacional del Agua
M. I. José Carlos Douriet Cárdenas	Gerencia Regional Pacífico Norte, Comisión Nacional del Agua
Ing. Jacinto Guzmán Muñiz	Gerencia Regional Lerma Santiago Pacífico Comisión, Comisión Nacional del Agua
Ing. Miguel C. Alfaro A.	Gerencia Regional Lerma Santiago Pacífico Comisión, Comisión Nacional del Agua
M.I. Iván Ruvalcaba Palacios	Gerencia Regional Balsas, Comisión Nacional del Agua
Ing. Samuel Villanueva Sánchez	Gerencia Regional Frontera Sur, Comisión Nacional del Agua
Ing. Arturo Rodríguez Villalobos	Gerencia Estatal Aguascalientes, Comisión Nacional del Agua
Ing. Carlos Enriquez becerra	Gerencia Estatal Aguascalientes, Comisión Nacional del Agua
Ing. José Luis Juárez Rubio	Gerencia Estatal San Luis Potosí, Comisión Nacional del Agua
Ing. Emigdio Negrete Castañeda	Gerencia Estatal Guanajuato, Comisión Nacional del Agua
Ing. Ernesto Pintado Hidalgo	Gerencia Estatal en Hidalgo, Comisión Nacional del Agua
Ing. José Arturo López Ibarra	Gerencia Regional Noroeste, Comisión Nacional del Agua

**Program Rio Bravo: options for ET management**

Venue: CNA, Mexico City

**Sunday February 19:** arrival of lecturers from Holland

Mrs. Annemarie Klaasse (WaterWatch)

Dr. Peter Droogers (FutureWater)

**Monday February 20**

Introduction to remote sensing and SEBAL

**Tuesday February 21**

Applications of Remote Sensing and SEBAL in the Rio Bravo basin

**Wednesday February 22**

Use of simulation models in ET management

**Thursday February 23**

Application of SWAT model in the Rio Bravo basin

**Friday February 24**

Discussions regarding integration SEBAL and SWAT in Rio Bravo

*SEBAL Remote Sensing model component*

Satellite remote sensing provides up-to-date information for large geographical areas such as the Rio Bravo basin. Satellite imagery analysis is relatively cheap and rapid (especially when compared with field work) and provides independent areas, even in inaccessible areas. Furthermore it facilitates cross-border analysis.

Satellite imagery varies in spatial, spectral and temporal resolution. Choosing the right satellite is essential in every remote sensing analysis. In general increased spatial resolution implies reduced temporal resolution. A combination of different satellites is sometimes necessary, for example daily MODIS imagery (coarse resolution) in combination with high-resolution Landsat imagery (8-days overpass).

Satellite imagery is especially suitable for land cover / land use mapping. Most classifications are based on spectral and/or temporal characteristics of the surface. The Normalized Difference Vegetation Index (NDVI) is an index based on the reflectance in red and near-infrared, and closely related to the amount of vegetation on the land surface. NDVI results are independent of illumination and very suitable for land cover / land use mapping.

The SEBAL model uses both the optical (visible and near-infrared) and thermal bands of satellite imagery. Furthermore it requires meteorological and elevation data. Evapotranspiration is calculated as a residual of the energy balance, based on the principle that evapotranspiration consumes energy.

Outputs of SEBAL include the actual evapotranspiration and biomass production, enabling calculation of the biomass water productivity. In contrary to the land productivity (yield) that provides biomass production per unit of land, the biomass water productivity provides biomass production per unit of water. Especially in basins such as the Rio Bravo basin, where water and not land is the limiting factor,

the biomass water productivity is a powerful tool to detect the areas with less productive water use.

#### *SWAT hydrological simulation model component*

It was demonstrated that the SWAT model can be used to fill two specific needs: (i) understanding the spatially distributed water balance of the entire Rio Bravo, and (ii) future scenarios.

Regarding the first point, it is clear that SEBAL provides actual evapotranspiration rates at an unsurpassed level of accuracy and spatial resolution of all land use classes. It was repeated frequently that water lost by ET is in fact the only real loss from the basin (except a relatively small amount of outflow to the sea). It was also emphasized that ET losses are much higher in natural vegetation than in the agricultural areas, since agriculture encompasses only a small fraction of the entire area. In order to understand the observed ET the entire water balance should be considered. The SWAT model was used for this and other factors such as percolation, runoff, erosion/sedimentation and groundwater contribution could be assessed from these analysis.

Future scenarios can be analyzed easily once the SWAT model has been fully calibrated and validated. The current version of the SWAT-Rio Bravo is preliminary, and based on public domain data. By inclusion of local data, the performance of SWAT can be improved further. The future scenarios might relate to uncontrolled or difficult to control impacts such as climate change and population growth. On the other hand can adaptation and mitigation activities explored. During the workshop participants explored some of these measures that might be included in policies.

#### *Future activities*

During the entire week the focus was on how to proceed from what has been done so far. On the last day a special session was organized in which future activities were discussed. The most important issues emerging from the discussions are:

- SEBAL should be used to detect real water use and can be used as a tool to regulate the amount of evaporative depletion. This would be a major leap forward to the current practice of only looking at the quantity of water diverted
- SWAT is very useful to understand process and to undertake scenario analysis
- The simulated percolation rates are in agreement with the general knowledge of water managers in the region
- The results indicate a considerable groundwater flow from the center of the basin to the east and are worth further investigations
- A more pro-active approach, in contrast to the current practice of re-active, is required. Water management plans should be already in place to respond quicker to for example dry periods, or excessive rainfall. The SWAT model can be used to develop these water management plans
- CNA is very much interested to have the capacity in house to apply SEBAL by themselves. Expertise to apply SEBAL and property right issues will be discussed over the next months
- The SWAT model as built now is only an initial version. Additional data, validation and calibration have to be undertaken before the model can be really applied at a reasonable level of confidence.



---

## 8. Future outlook

The twin SEBAL-SWAT modeling approach assists in the planning, monitoring and evaluation of water resources decision making. This general philosophy is elaborated in this chapter. The Comisión Nacional del Agua (CNA) has the formidable challenge to define targets in the allocation of water, and define consumption of water in agriculture vs. water in environment, groundwater abstraction quota and diversions from surface water resources. The water balance is the fundament to distinguish between water diversion, water consumption and return flows, and the distributed water balance is currently not fully understood. A system of water rights has to be put in place for a fair and controllable distribution of scarce resources. This pilot project demonstrates the power of remote sensing to diagnose vast areas in a uniform and consistent manner and clarify the precipitation – ET – land cover relationship for every sub-basin and aquifer type and administrative region.

By assimilating the remote sensing data into hydrological models, the opportunity arises to get also fairly good estimates of the other terms of the water balance. Assessment of return flows and regional scale lateral flow are key outputs from SWAT. The calibrated SWAT model allows simulating new actions that could adapt the water management in line with the basin objectives.

The broader implications for all of Northern and Central Mexico – and in particular for all the basins with irrigated areas - are that the hydrological flow path can be surveyed and described in a standardized way. It is for CNA a strong advantage to have a uniform computational methodology that can study implications of water allocation decision making for all their water short basins.

### ***Technical steps***

The blueprint of logical order of steps to be taken for achieving a successful implementation of IWRM tools is:

- (i) Understanding energy balances

The energy balance describes how shortwave solar radiation and longwave radiation are dissipated into ET fluxes. The ET fluxes are fundamental for describing the water balance and they also reflect the water stress conditions, thus where shortage of water is felt and which rural areas suffer the most.

- (ii) Description of land cover classes

Spatial land cover maps provide strategic information about the presence and location of agro-ecosystems. It tells you the acreages of environmentally rich heritages, irrigated land, forests, wetlands, scrubland etc. By combining land cover information with energy balances, it becomes feasible to determine how much water is needed for the environment and how much is available for other consumptive uses. It will also provide information on above-average water consumption in certain land cover classes.

- (iii) Unraveling water balances

Spatially distributed data on precipitation (from TRMM) and ET (from MODIS) in weekly or monthly time steps is a good fundament to describe the extent and duration of water yield periods (i.e. when  $P > ET$ ) and net depletion periods ( $P < ET$ ).

This is key information for stream and river flow, hence for the renewable water resources that provides water to the domestic and industrial use sectors. The SWAT model provides percolation, storage change, interactions between surface and groundwater systems etc. A good handle on the water balance for all combinations of land cover and soil types (i.e. Hydrological Response Units), makes it feasible to quantitatively express sustainability and how often a certain hydrological situation and - thus unsustainability practices - occur.

(iv) Target sustainability levels

Water resources planning in the basin context requires a top-down approach that ensures that upstream activities will not be harmful to downstream water resources developments. To foster the concepts of local sustainability, it is encouraged to achieve local sustainability levels. This implies that after having committed certain surface and groundwater resources for environmental purposes (native vegetation consumes significant amounts of groundwater), the left over to maintain zero overdraft can be allocated to the various water use sectors. A good sustainability plan must have a total allowable ET depletion per land cover class and per sub-basin. A plan without properly defined targets is like a ship on the ocean without destination. The plan could include implementation of a system of water allocations and water rights based on ET. Then the RS ET information could be incorporated into a water rights administration system, in order to monitor and control water consumption to amounts agreed in the plan.

(v) Evaluate management options

If the distributed water balances are known and maximum allowed depletion quotas are fixed, various management options (and investment) need to be evaluated using scenarios based on hydrologic, economic, environmental and social metrics. Each management option should meet the target sustainability levels defined. The economic and social benefits derived from the use of the water (income and jobs) for each scenario could be assessed. This needs to be done for irrigated crops, rainfed crops, scrubland, forests and other marginal land uses. The comprehensive consumption of water should be related to the economic value and the social benefits in terms of employment, income generation, empowerment of local societies, poverty eradication etc. It must be constantly recognized that the part of the diversion and abstraction that is not consumed (i.e. the majority of the resources), is nominally available for downstream users, and thus not necessarily bad.

(vi) Water rights

Under conditions of scarcity, water usage must be tempered and controlled. The legal umbrella for that are water rights. Water rights are highly suitable to provide beneficiaries with a volumetrically defined amount of water that is not harmful to the environment and that will provide maximum economical and social benefits for the sub-basin. The water rights must be in line with the overall water resources utilization plan. A tight enforcement and administration of water rights is essential to implement a quota-based division of scarce resources. Mechanisms will be included in the management of water resources to allow for transfer of water from low value to high value uses: water market.

(vii) Monitoring sustainability and compliances

The water use patterns can eventually be adjusted conforming the needs and availability to increase the social and economic benefits derived from sustainable utilization. The planning process needs to be dynamic, continuous and iterative.

A continuous monitoring and evaluation process needs to be defined that monitors the compliances. Allen et al. (2005) provides an excellent example how groundwater users on the Snake River Plain in Idaho are controlled by SEBAL-based ET computations to verify that they are not using more water than their entitlements. The effectiveness of the plan/management needs to be evaluated (is  $ET < P$  ?) and annually adjusted if needed, until everything is working great and sustainability has been reached. Remote sensing-based ET data is not just used to calibrate the SWAT model but to monitor implementation of the plan.

SEBAL allows reviewing effectiveness of actions taken by continuous monitoring of precipitation and ET. If ET systematically exceeds precipitation, then overexploitation in a given sub-basin or basin is a fact.

**Periodically, water allocation and evaluation processes need to be repeated:**

- Continue to collect data including remote sensing data
- (ET, P, water productivity, irrigated area)
- Adjust and refine the SWAT models when more data becomes available
- Adjust and refine the set of scenarios
- Adjust and refine economic response analysis
- Re-evaluate management and investment scenarios
- Adjust, refine and agree upon a revised plan
- Continue implementation of revised plan
- Continue monitoring and evaluation

**Organizational steps**

The roadmap to achieve an IWRM plan is by building confidence in the tools and creating modeling capacity in CNA staff, along with awareness creation of high level water policy makers.

The confidence can be built through the execution of validation studies where predictions of SEBAL and SWAT are compared against field measurements. For the groundwater study in Sonora, ITSON (Ciudad Obregon) and UNISON (Hermosillo) were involved in validating the ET fluxes from SEBAL over irrigated wheat in Valle del Yaqui area using advanced *in situ* equipment. Although the same research groups also conducted ET flux measurements over scrubland vegetation, the period of image analysis and field measurements did not match. As part of the validation process, CNA purchased two scintillometers that can operationally measure ET fluxes along a path of maximum 5 km length. This is highly suitable for the validation of SEBAL-based ET fluxes with a pixel size of 1 km.

Verification and validation of the SWAT model results should be done by the Surface Water division of CNA in close collaboration with the local CNA office in Monterrey.

The validation and verification work executed by Mexican academia should go along with the building of more demonstration studies to excite engineers and show policy makers the new opportunities that exist to make better decisions by the availability of having distributed maps. Further to Rio Bravo and the Central Northern aquifers and Central aquifers<sup>5</sup>, SEBAL has been applied to Sonora and Chihuahua states. This rich datasets should be presented in a way that is

<sup>5</sup> A separated report has been compiled to demonstrate the major findings in this separated region

understandable for the water policy makers. This implies that the ET maps need to be converted into maps of groundwater use by natural vegetation, groundwater use by irrigated crops, water productivity etc. In conjunction with other GIS layers of administrative boundaries and crop types, it would be possible to generate geographical maps of job employment in the irrigation sector, aquifer overexploitation etc. The possibilities to visualize the problem areas are very attractive for all stakeholders involved in the water allocation process. The availability of post-processing tools to better organize data and produce easily understandable maps is an essential expedient.

SEBAL is propriety software for which it has been agreed upon in an earlier stage that CNA can get licenses. WaterWatch can train the CNA staff in utilizing SEBAL and also on how to get other standard products out from SEBAL such as (i) weekly ET reports by land cover type for each administrative region or basin, (ii) water shortage in terms of ET deficit, (iii) comparisons of ET and volumetric water rights, (iv) Net Groundwater Use etc. MODIS images for SEBAL can be obtained daily and weekly for entire Mexico (see SATMEX report Bastiaanssen, 2003). The MODIS data is free of charge available, and CNA could eventually install an own ground link receiving facility in order that the images are instantly available when the satellite flies over. Both Terra and Aqua satellites are equipped with a MODIS instrument. Terra passes over every mid-morning and Aqua passes over every early-afternoon.

Simultaneously, SWAT modeling needs to be refined for the Rio Bravo, and preliminary SWAT models can be set up for all other major irrigated river basins in Central and Northern Mexico (Yaqui, Santiago, Lerma, Panuco, Soto la Marina, San Fernando). Having a standard hydrological modeling package applied and fine tuned to every basin would be a great asset for CNA. It is generally understood and recognized in the hydrological community that the limitation of distributed hydrological modeling at large river basins is the calibration of the water balance. This Rio Bravo project is innovative – and among the very first ones in the world – where a complex model has been perfectly calibrated using distributed remote sensing data. There is probably no alternative now – and in the next 10 years – to get a faster and more effective procedure to set up complex hydrological models.

Having SWAT for all major irrigated basins in Mexico available – in association with weekly SEBAL data analysis, will provide an instrument that allows working out IWRM plans for all the basin areas in a routine and standardized manner. Alternative water allocation scenarios can be defined and the impact on total economical and social development can be appraised. SEBAL produces critical input data for SWAT, as well as to other GIS layers. SWAT provides the hydrological data, and for optimization of the resources it is recommend using special water optimization models such as Water Evaluation and Planning System WEAP (<http://www.weap21.org/>).

The impact of water management can be visualized by the MODIS images and concurrent SEBAL analysis of ET, ET-deficit, soil moisture and biomass production. These maps can nowadays be viewed easily through a dedicated web application – like the one created for this project - and by general viewing tools such as Google Earth. An example of Google Earth for the Nile Basin is available via [www.waterwatch.nl](http://www.waterwatch.nl).

---

## 9. Conclusions

This study is a new approach to basin water management, and it includes some innovative elements that were not applied in water resources assessment studies before, such as:

- Considering ET as the major water depletion term in river basins and quantify it independent from hydrological data by means of an energy balance model and turbulent flow equation that govern the heat exchanges between land and atmosphere
- ET and rainfall determined from satellites yielding a spatially distributed data set for vast areas, also for mountainous areas where classical data collection is cumbersome
- Swiftly calibrating a comprehensive distributed hydrological model that includes surface water, soil water and a simple schematization of groundwater systems
- Economic analysis based on depletion and not on diversion or abstraction
- Evaluating hydrological flows by land cover class, so that the impact of certain vegetation and human interventions on depletion, water productivity and surplus can be assessed
- Determination of ET rates that are not harmful for overdraft and re-establish a proper balance between P and ET

### Selected Water Facts

- Irrigated acreage increases in Rio Bravo with a pace of 3.5% per year
- Irrigation water depletion is 11.7% of all Rio Bravo depletions
- The volumetric water depletion is for 70.8 % non-beneficial, 12.5 % semi-beneficial and for only 16.7 % beneficial. Scarce water resources are thus essentially wasted by natural desert scrubland
- Underground (international) basin water transfer takes place ( $\pm 1.5 \text{ km}^3/\text{yr}$ )
- Irrigation efficiency improves when moving from field scale (35 %) to scheme level (64 %) and basin level (70 %)
- Average return flow from diversion to planned processes is 53%
- The spatial variation of ET in irrigated crops is significant ( $\text{CV}=52\%$ ), which implies that 25% water savings could be achieved
- The majority of irrigation water diversion (54 %) is reused downstream
- Net economic benefit of  $0.93 \text{ \$/m}^3$  in the Rio Bravo is high when compared to world statistics

Due to the availability of these new analytical tools, it becomes feasible to get a more consistent picture of the water resources conditions in the 44 million ha area. The salient findings are:

- The basin average stream flow and surface runoff in the SWAT model is 6 mm per year, and the rainfall surplus (P-ET) is with 57 mm almost 10 times higher. This implies that the Rio Bravo is almost closed and that renewable water resources are allocated already
- There is a considerable underground water movement from the higher elevated Chihuahua desert to the lower located flood plain of the Rio Bravo
- Whereas seepage water can have benefits for crops grown on the lower local alluvial aquifers, it implies an additional loss of water in case submontane scrubland and in tamaulipas thornscrubland deplete this water. Hence,

seepage can be both good and bad for river basin management, and the extent of this process needs to be better understood

- Water consumption (ET) of desert plant species need to be brought to the agenda. The question to be answered is whether ET of scrubland can be technically reduced (e.g. more intense grazing), and if yes, whether that is supported by the larger community
- Local adaptation to pressurized irrigation systems is not likely to increase the irrigation performance at scheme level in Rio Grande. It saves local energy costs though and elicits re-distribution of water flows with existing irrigation schemes
- The water productivities in Delicias Irrigation District are, for the most common crops, comparable with world standard values. The economic profits from irrigation could improve further if more pecans, grapes and other high value crops are cultivated that consume less water
- A preliminary SWAT model has been set up that showed a remarkable good performance in terms of matching SEBAL-based ET surface layers (1% error at basin scale)
- The crop identification with MODIS and Landsat images are merely meant as an example of the methodology followed. The accuracy of the crop maps is unknown
- Sustainability targets of IWMPs need to be based upon land cover and pre-fixed ET quota. The required data is now available and more data for pixels and sub-watersheds can be generated
- Utilize SWAT to explore (i) land cover changes, more rainfed crops, more high value irrigation crops, shrinkage of irrigated acreages, (ii) design ET quota on agricultural and ecological water users, (iii) establish local sustainability and (iv) more diversions to urban water users and study the impact on environmental and economical benefits.

**The recommendations for a continuation of this study are:**

- prepare a supervised crop classification after collecting ground truth data
- study the ET population for the major irrigated and rainfed crops
- analyze more hydrological years, especially extreme years to appraise the strategic mechanisms of soil and groundwater storage
- calibrate ET and biomass production for each land cover unit in SWAT, rather than on the basis of ET and Hydrological Response Units
- comprehensively verify and validate SEBAL and SWAT outputs
- capacity building of SEBAL in Comisión Nacional del Agua
- target near-future sustainability levels
- determine the ET quota for each land cover type
- provide subsidies on water wise solutions such as cultivation of crops with high bio-physical and economical crops
- endorse a tight enforcement and administrative water right system
- evaluate water allocation and optimum profits with packages such as for instance WEAP
- prepare preliminary SWAT models for other basins in semi-arid and arid river basins in Mexico

---

## References

- Abo-Ghobari, H.M., 2000. Estimation of reference evapotranspiration for southern region of Saudi Arabia, *Irrigation Science* (19): 81-86
- Abu Zheid, M. and D. Seckler (eds.), 1992. Roundtable on Egyptian Water Policy, Conference Proceedings, Water Research Centre, Ministry of Public Works and Water Resources, Cairo, Egypt and Winrock International, Arlington, Virginia
- Allen, R.G., L.S. Pereira, D. Raes and M. Smith, 1998. Crop evapotranspiration, guidelines for computing crop water requirements, *FAO Irrigation and Drainage Paper 56*, FAO, Rome, Italy: 300 pp.
- Allen, R.G., M. Tasumi, A. Morse and R. Trezza, 2005. A Landsat-based energy balance and evapotranspiration model in Western US water rights regulation and planning, *Irrigation and Drainage Systems* 19: 251-268
- Barker, R., Christopher A. Scott, Charlotte De Fraiture, Upali Amarasinghe. 2000. Global Water Shortages and the Challenge Facing Mexico. *International Journal of Water Resources Development*, Volume 16, Number 4 Pages: 525 – 542.
- Bastiaanssen, W.G.M., C.W.J. Roest, H. Pelgrum and M.A. Abdel Khalek, 1992. Monitoring of the irrigation performance on the basis of actual evapotranspiration: Comparison of satellite data and simulation model results, in (Eds.) J. Feyen, E. Mwendera and M. Badji), *Advances in Planning, Design and Management of Irrigation Systems as Related to Sustainable Land Use*, Center for Irrigation Engineering and ECOWARM, Leuven: 473-483
- Bastiaanssen, W.G.M., 2003. Towards satellite based water resources management in Mexico – SATMEX, Informe no. 164, Organizacion Meteorologica Mundial (WMO, Swiss) and Comisi3n Nacional del Agua (CNA, Mexico): 26 pp.
- Bastiaanssen, W.G.M., E.J.M. Noordman, H. Pelgrum, G. Davids and R.G. Allen, 2005. SEBAL for spatially distributed ET under actual management and growing conditions, *ASCE J. of Irrigation and Drainage Engineering* 131(1): 85-93
- Bastiaanssen, W.G.M., M. Menenti, R.A. Feddes and A.A.M. Holtslag, 1998. The Surface Energy Balance Algorithm for Land (SEBAL): Part 1 formulation, *J. of Hydr.* 212-213: 198-212
- Bastiaanssen, W.G.M., M.D. Ahmad and Y. Chemin, 2002. Satellite surveillance of evaporative depletion across the Indus Basin, *Water Resources Research*, vol. 38, no. 12: 1273-1282
- Bastiaanssen, W.G.M., M.D. Ahmad and Z. Tahir, 2003. Upscaling water productivity in irrigated agriculture using remote sensing and GIS technologies, in (eds.) J. Kijne, R. Barker and D. Molden, *Water productivity in agriculture: limits and opportunities for improvement*, CABI Publishing, no. 1, Wallingford, UK ISBN 0 85199 669 8: Chapter18: 289-300
- Brutsaert, W. and M. Sugita, 1992. Application of self preservation in the diurnal evolution of the surface energy balance budget to determine daily evaporation, *J. Geophys. Res.* 97(D17): 18377-18362
- Crago, R.D., 1996. Conservation and variability of the evaporative fraction during the daytime, *J. of Hydr.* 180: 173-194
- Droogers, P. and W.G.M. Bastiaanssen, 2002. Evaporation in irrigation performance and water accounting frameworks: an assessment from combined hydrological and remote sensing modeling, *ASCE Irrigation and Drainage Engineering* vol. 128(1): 11-18
- Droogers, P., and G.W. Kite, 2002. Remotely sensed data used for modeling at different hydrological scales. *Hydrological Processes* 16: 1543-1556.

El-Khaisi., M., A. Berrada and M. Stack, 1997. Evaluating of irrigation scheduling program and spring wheat yield response in southwestern Colorado, *Agr. Water Man.* 34: 137-148

FAO/GIEWS - Foodcrops and Shortages. 2003. [http://www.fao.org/documents/show\\_cdr.asp?url\\_file=/docrep/005/y8872e/y8872e04.htm](http://www.fao.org/documents/show_cdr.asp?url_file=/docrep/005/y8872e/y8872e04.htm)

Farah, H.O., 2001. Estimation of regional evaporation under different weather conditions from satellite and meteorological data, Ph.D. thesis, Department of Agrohydrology, Wageningen University, The Netherlands: 170 pp.

Garatuza-Payan, J. and C.J. Watts 2005. The use of remote sensing for estimating ET or irrigated wheat and cotton in Northwest Mexico, *Irrigation and Drainage Systems* 19: 301-320

Gil, K. and N. Wilkins. 2003. Rio Grande/Rio Bravo Basin: A Bibliography. TWRI Technical Report 214. <https://landinfo.tamu.edu/projects/riogrande/index.cfm>)

Handbook of Texas Online. 2005. <http://www.tsha.utexas.edu/handbook/online/articles/RR/rnr5.html>. Hanson, Blaine and Dan Putnam, 2000, Can Alfalfa be produced with less water? Proceedings 29<sup>th</sup> National Alfalfa Symposium, Las Vegas NV Dec. 11-12, 2000

Hooghoudt, S.B. 1940. Bijdrage tot de kennis van enige natuurkundige grootheden van de grond. *Versl. Landbouwkd. Onderz.* 46: 515-707.

Howell, T.A., J.L. Steiner, A.D. Schneider, S.R. Evett and J.A. Tolk, 1997. Seasonal and maximum daily evapotranspiration of irrigated winter wheat, sorghum and corn – southern high plains, *Transaction of the ASEA, American Society of Agricultural Engineers*, 40(3): 623-634

<http://water.usgs.gov/nasqan/proqdocs/factsheets/riogfact/enql.html>

[http://www.cwrw.utexas.edu/gis/qishydro04/time/Rio\\_Grande-Bravo\\_Basin.htm](http://www.cwrw.utexas.edu/gis/qishydro04/time/Rio_Grande-Bravo_Basin.htm)

<http://www.srh.noaa.gov/wgrfc/basinList.html>

Ines and Droogers, 2002. Inverse Modeling to Quantify Irrigation System Characteristics and Operational Management, *Irrigation and Drainage Systems* 16(3): 233-252

Jensen, M.E., 1977. Water conservation and irrigation systems: climate. In: *Technical Seminar Proceedings*, Columbia, Missouri: 208-250

Keller, A. and J. Keller, 1995. Effective efficiency: a water use concept for allocating freshwater resources, *Water Resources and Irrigation Division Discussion Paper 22*, Winrock International, Arlington, Virginia

Kelly, M.E.. 20XX. Water Management in the Binational Texas/Mexico Río Grande/Río Bravo Basin. *Human population and freshwater resources. Bulletin* 107. p. 115-148.

Kustas, W.P., M.S. Moran, K.S. Humes, D.I. Stannard, P.J. Pinter, L.E. Hipps, E. Swiatek and D.C. Goodrich, 1994. Surface energy balance at local and regional scales using optical remote sensing from aircraft platform and atmospheric data collected over semiarid rangelands, *Water Resources Research* 30: 1241-1259

Lauer, David 2004, *Agricultural Production Trends and the Future Of the Trans-boundary Rio Grande/Rio Bravo Basin. Conference Proceedings*, May 2004, San Antonio, Texas

Lazarova, Valentina and Akica Bahri, 2004, *Water reuse for irrigation (agriculture, landscapes, and turf grass)*.

Lobell, D.B., Gregory P. Asner, J. Ivan Ortiz-Monasterio and Tracy L. Benning, 2003. Remote sensing of regional crop production in the Yaqui Valley, Mexico: estimates and uncertainties *Agriculture, Ecosystems & Environment*, Volume 94, Issue 2, February 2003, Pages 205-220

Lobell, D.B., J. A. Hicke, G.P. Asner, C.B. Field, C.J. Tucker and S.O. Los, 2002. Satellite estimates of productivity and light use efficiency in United States agriculture: 1982-98, *Global Change Biology* 8: 722-735

Lunetta R. S.; Alvarez R.; Edmonds C. M.; Lyon J. G.; Elvidge C. D.; Bonifaz R.; Garcia C. 2002. NALC/Mexico land-cover mapping results: implications for assessing landscape condition. *International Journal of Remote Sensing*, Volume 23, Number 16, 30 August 2002, pp. 3129-3148(20).

Menenti, M., T.N.M. Visser, J.A. Morabito and A. Drovandi, 1989. Appraisal of irrigation performance with satellite data and georeferenced information, Proc. Congress Southampton, in: J.R. Rydzewsky and K. Ward (eds.), *Irrigation theory and practice*, Pentech. Press London: 785-801

Molden, D., H. Murray-Rust, R. Sakthivadivel and I. Makin, 2003. A water productivity framework for understanding and action, CAB International 2003, *Water Productivity in Agriculture: Limits and Opportunities for Improvement* (eds.) J.W. Kijne, R. Barker and D. Molden: 1-18

Neitsch, S.L., Arnold, J.G., Kiniri, J.R., Williams, J.R., 2001. Soil and Water Assessment Tool Theoretical Documentation Version 2000. Texas: Grassland, Soil and Water research Laboratory and Blackland Research Center.

Nicols, W.E. and R.H. Cuenca, 1993. Evaluation of the evaporative fraction for the parameterization of the surface energy balance, *Water Resources Research* 29(11): 3681-3690  
NOAA National Weather Service, West Gulf River Forecasts Center.

Parr Rosson, C., Aaron Hobbs and Flynn Adcock, 2002. A Preliminary Assessment of Crop Production and Estimated Irrigation Water Use for Chihuahua, Mexico. Department of Agricultural Economics, Center for North American Studies, Texas A&M University

Patino, Carlos, Daene C. McKinney and David R. Maidment, 2004. Water Management Information System for the Rio Grande/Bravo Basin, GIS-Hydro 2004, Proceedings ESRI User Conference, San Diego, August 2004

Patino-gomez, C. Application of the WAM model for the Rio Grande basin including the Mexican side. [http://civilu.ce.utexas.edu/stu/patinoc/WAM\\_RIO\\_GR.pdf](http://civilu.ce.utexas.edu/stu/patinoc/WAM_RIO_GR.pdf)

Quiñones, P.H., Helene Unland, Waldo Ojeda and Ernesto Sifuentes, 1999. Transfer of irrigation scheduling technology in Mexico *Agricultural Water Management*, Volume 40, Issues 2-3, May 1999, Pages 333-339.

Río Grande/Río Bravo Basin Coalition. <http://www.rioweb.org/index.html>

Scott, C.A., W.G.M. Bastiaanssen and M.D. ud-Din Ahmad, 2003. Mapping root zone soil moisture using remotely sensed optical imagery, *ASCE Irrigation and Drainage Engineering*, 129(5): 326-335

Seckler, D., D. Molden and R. Sakthivadivel, 2003. The concept of efficiency in water resources management and policy, CAB International 2003, *Water Productivity in Agriculture: Limits and Opportunities for Improvement* (eds.) J.W. Kijne, R. Barker and D. Molden: 37-51

Shewmaker, G.E., J.L. Wright and R.G. Allen, 2004. Alfalfa irrigation fact

Shuttleworth, W.J., R.J. Gurney, A.Y. Hsu and J.P. Ormsby, 1989. FIFE: the variation in energy partitioning at surface flux sites, *IAHS Publ.* 186: 67-74

Smedema, L.K. and D.W. Rycroft. 1983. Land drainage—planning and design of agricultural drainage systems, Cornell University Press, Ithica, N.Y.

Spruill, C.A., S.R. Workman, J.L. Taraba. 2000. Simulation of daily and monthly stream discharge from small watersheds using the SWAT model. Transactions of the ASAE American Society of Agricultural Engineers, VOL. 43(6): 1431-1439.

Srinivasan, R.,T. Ramanarayanan, H. Wang, R. Jayakrishnan. 1997. Hydrologic Modeling of the Rio Grande/Río Bravo Basin. Texas Agricultural Experiment Station Blackland Research Center Temple, Texas 76502. Research Report.

Stewart, J.B., C.J. Watts, J.C. Rodriguez, H.A.R. de Bruin and A.R. van den Berg. 1999. use of satellite data to estimate radiation and evapotranspiration for northwest Mexico, Agr. Water Man. 38: 181-193  
US Library of Congress. 2003. Country studies US: Mexico. <http://countrystudies.us/>

USGS. 1987. Major World Crop Areas and Climatic Profiles. World Agricultural Outlook Board, U.S. Department of Agriculture. Agricultural Handbook No. 664.

Wang, J., T.W. Sammis, C.A. Meijer, L.J. Simmons, D.R. Miller and Z. Samani, 2005. A modified SEBAL model for spatially estimating pecan consumptive water use for Las Cruces new Mexico, New Mexico State University, Las Cruces, New Mexico, conference paper 7.13

Zwart, S.J. and W.G.M. Bastiaanssen, 2004. Review of measured crop water productivity values for irrigated wheat, rice, cotton and maize, Agr. Water Management 69: 115-133

# Appendix A Description of SEBAL procedure

## A1 Overview

The Surface Energy Balance Algorithm for Land (SEBAL) is an image-processing model comprised of 25 computational steps that calculates the actual ( $ET_{act}$ ) and potential evapotranspiration rates ( $ET_{pot}$ ) as well as other energy exchanges between land and atmosphere. The key input data for SEBAL consists of spectral radiance in the visible, near-infrared and thermal infrared part of the spectrum (see Figure C-48 and Figure C-49). SEBAL computes a complete radiation and energy balance along with the resistances for momentum, heat and water vapour transport for every individual pixel. The resistances are a function of state conditions such as soil water potential (and thus soil moisture), wind speed and air temperature and change from day-to-day.

Satellite radiances will be converted first into land surface characteristics such as surface albedo, leaf area index, vegetation index and surface temperature. These land surface characteristics can be derived from different types of satellites. First, an instantaneous evapotranspiration is computed, that is subsequently scaled up to 24 hours and longer periods.

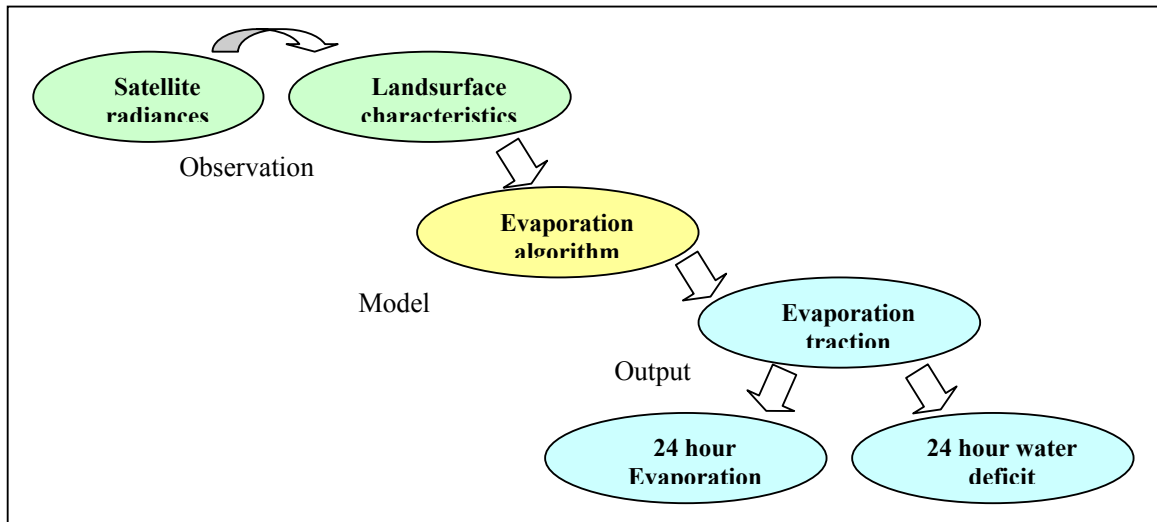


**Figure C-48, Flow chart of the principal steps in SEBAL to derive instantaneous 24-hour  $ET_{act}$  and  $ET_{pot}$  values**

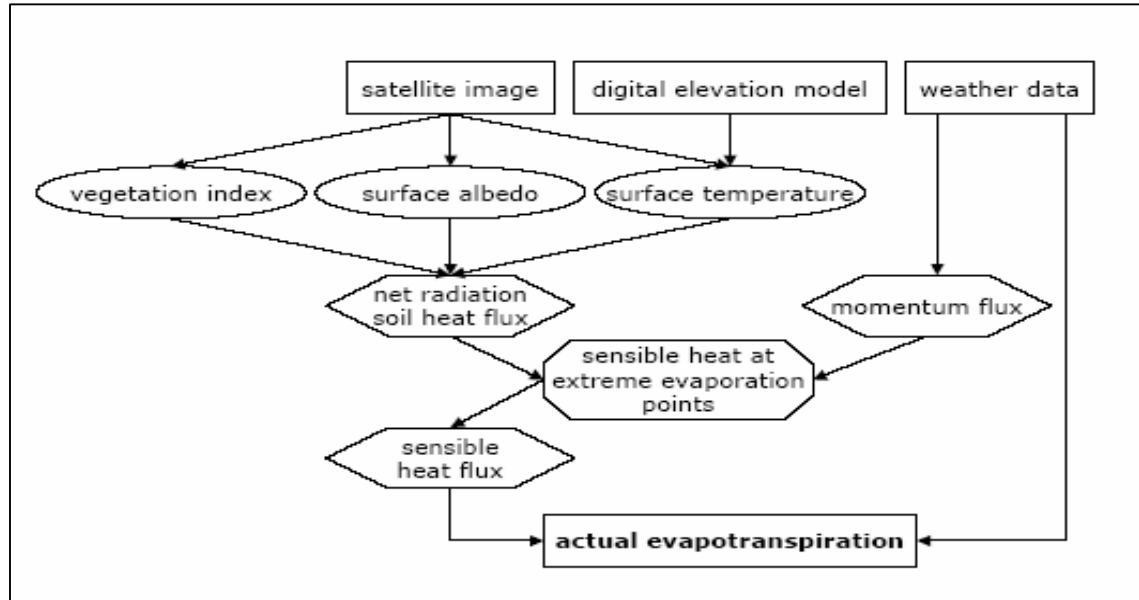


Figure C-49, Schematic view of energy balance and ET computations with SEBAL

## A2 Data requirements

In addition to satellite images, the SEBAL model requires the following routine weather data parameters:

- Wind speed
- Humidity
- Solar radiation
- Air Temperature

There is no data on land cover, soil type or hydrological conditions required to apply SEBAL.

## A3 SEBAL Evapotranspiration

The primary basis for the SEBAL model is the surface energy. The instantaneous  $ET_{act}$  flux is calculated for each cell of the remote sensing image as a 'residual' of the surface energy budget equation:

$$ET = R_n - G - H \quad (1)$$

where;  $ET$  is the latent heat flux ( $W/m^2$ ),  $R_n$  is the net radiation flux at the surface ( $W/m^2$ ),  $G$  is the soil heat flux ( $W/m^2$ ), and  $H$  is the sensible heat flux to the air ( $W/m^2$ ) (see Figure C-50).

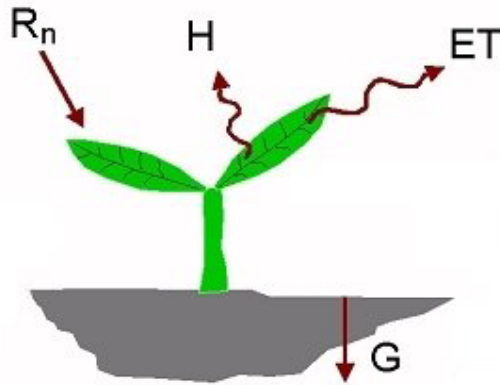


Figure C-50, Surface Energy Balance

$R_n$  represents the actual radiant energy available at the surface. It is computed by subtracting all outgoing radiant fluxes from all incoming radiant fluxes (Figure C-51). This is further specified in the surface radiation balance equation:

$$R_n = R_{S\downarrow} - \alpha R_{S\downarrow} + R_{L\downarrow} - R_{L\uparrow} - (1 - \epsilon_0) R_{L\downarrow} \quad (2)$$

where  $R_{S\downarrow}$  is the incoming short-wave radiation ( $W/m^2$ ),  $\alpha$  is the surface albedo (dimensionless),  $R_{L\downarrow}$  is the incoming long wave radiation ( $W/m^2$ ),  $R_{L\uparrow}$  is the outgoing long wave radiation ( $W/m^2$ ), and  $\epsilon_0$  is the surface thermal emissivity (dimensionless).

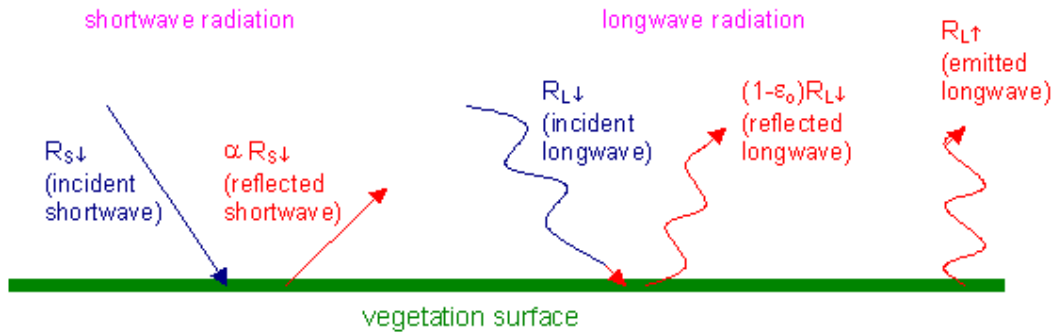


Figure C-51, Surface Radiation Balance

In Eq. (2), the amount of net short-wave radiation ( $R_{S\downarrow} - \alpha R_{S\downarrow}$ ) that remains available at the surface, is a function of the surface albedo ( $\alpha$ ). The broad band surface albedo  $\alpha$  is derived from the narrow band spectral reflectances  $a(\lambda)$  measured by each satellite band. The incoming short-wave radiation ( $R_{S\downarrow}$ ) is computed using the solar constant, the solar incidence angle, a relative earth-sun distance, and a computed broad band atmospheric transmissivity. This latter transmissivity can be estimated from sunshine duration or inferred from pyranometer measurements (if available). The incoming long wave radiation ( $R_{L\downarrow}$ ) is computed using a modified Stefan-Boltzmann equation with an apparent emissivity that is coupled to the shortwave atmospheric transmissivity and a measured air temperature. Outgoing long wave radiation ( $R_{L\uparrow}$ ) is computed using the Stefan-Boltzmann equation with a calculated surface emissivity and surface temperature. Surface temperatures are computed from the satellite measurements of thermal radiances.

In Eq. (1), the soil heat flux (G) and sensible heat flux (H) are subtracted from the net radiation flux at the surface (Rn) to compute the "residual" energy available for evapotranspiration ( $\lambda E$ ). Soil heat flux is empirically calculated as a G/Rn fraction using vegetation indices, surface temperature, and surface albedo. Sensible heat flux is computed using wind speed observations, estimated surface roughness, and surface to air temperature differences that are obtained through a sophisticated self-calibration between dry ( $\lambda E \approx 0$ ) and wet ( $H \approx 0$ ) pixels. SEBAL uses an iterative process to correct for atmospheric instability caused by buoyancy effects of surface heating.

The  $\lambda E$  time integration in SEBAL is split into two steps. The first step is to convert the instantaneous latent heat flux ( $\lambda E$ ) into daily  $\lambda E_{24}$  values by holding the evaporative fraction constant. The evaporative fraction EF is:

$$EF = \lambda E / (R_n - G) \quad (-) \quad (3)$$

Field measurements under various environmental circumstances have indicated that EF behaves temporally stable during the diurnal cycle. Since  $EF \sim EF_{24}$ , i.e. the 24 hour latent heat flux can be determined as:

$$\lambda E_{24} = EF R_{n24} \quad (W/m^2) \quad (4)$$

For simplicity, the 24 hour value of G is ignored in Eq. (4). The second step is the conversion from a daily latent heat flux into monthly values, which has been achieved by application of the Penman-Monteith equation:

$$\lambda E_{PM} = (s_a R_{n24} + \rho a c_p \Delta e / r_a) / (s_a + \gamma (1 + r_s / r_a)) \quad (W/m^2) \quad (5)$$

where  $s_a$  (mbar/K) is the slope of the saturated vapor pressure curve,  $\rho a c_p$  ( $J/m^3 K$ ) is the air heat capacity,  $\Delta e$  (mbar) is the vapor pressure deficit,  $\gamma$  (mbar/K) is the psychrometric constant and  $r_a$  (s/m) is the aerodynamic resistance. The parameters  $s_a$ ,  $\Delta e$  and  $r_a$  are controlled by meteorological conditions, and  $R_n$  and  $r_s$  by the hydrological conditions.

The SEBAL computations can only be executed for cloudless days. The result of  $\lambda E_{24}$  from Eq. (4) has been explored to convert the Penman-Monteith equation (5) and to quantify  $r_s$  inversely using  $\lambda E_{24} = \lambda E_{PM}$ . The spatial distribution of  $r_s$  so achieved, will consequently be used to compute  $\lambda E_{24}$  by means of Eq. (5) for all days without satellite image available (Bastiaanssen and Bandara, 2001). The total  $ET_{act}$  for a given period can be derived from the longer term average  $\lambda E$  flux by correcting for the latent heat of vaporization and the density of water.

## A4 SEBAL Biomass growth

The biomass production routine in SEBAL is based on solar radiation absorption by chlorophyll and the conversion of this energy into a dry matter production by means of a light use efficiency:

$$Bio = \int APAR(t) e(t) dt \quad (kg/ha) \quad (6)$$

The absorption of solar radiation (APAR) for photosynthesis depends on global radiation and light interception. The second component of Eq. (6) describes the light use efficiency  $e(t)$  that converts energy into dry matters.

Photosynthetic Active Radiation (PAR) (0.4 to 0.7  $\mu m$ ) is part of the short wave solar radiation (0.3 to 3.0  $\mu m$ ) that is absorbed by chlorophyll for photosynthesis in the plants. PAR is thus a fraction of the incoming solar radiation,  $R_{s\downarrow}$ . The PAR value

describes the total amount of radiation available for photosynthesis if leaves intercept all radiation. This is a rather theoretical value, because leaves transmit and reflect solar radiation. Only a fraction of PAR will be absorbed by the canopy (APAR) and used for carbon assimilation. APAR can be approximated as a fraction of the PAR using the Normalized Difference Vegetation Index (NDVI):

$$APAR = (-0.161 + 1.275 \text{ NDVI}) * PAR \quad (\text{W/m}^2) \quad (7)$$

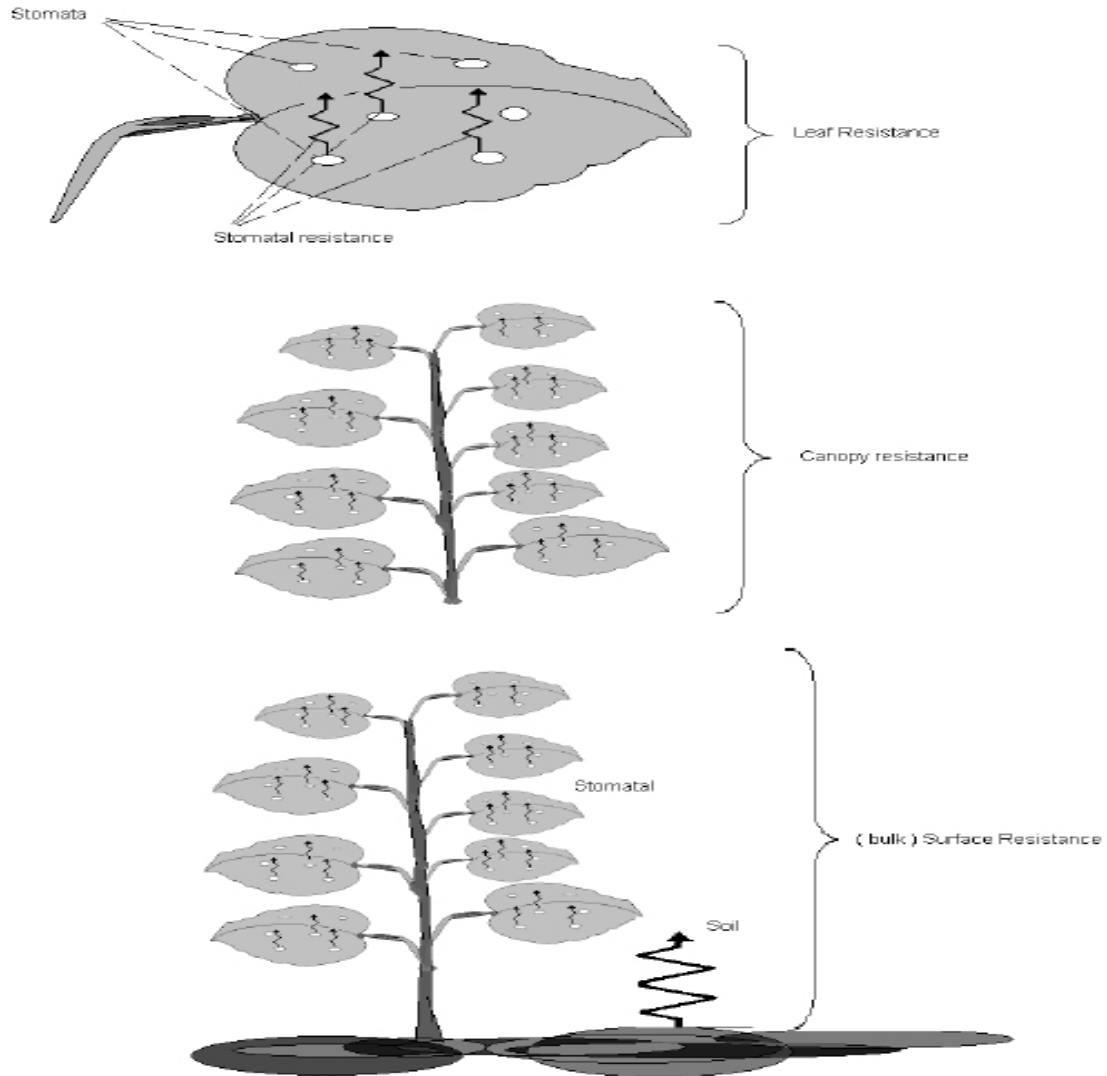


**Figure C-52, Various resistances that control the evapotranspiration rate**

The light use efficiency describes the climate impact and environmental stress on crop growth. Carbon dioxide is obtained from the atmosphere through the stomata's. The waste products of photosynthesis, oxygen and water vapor, are dispelled from the plant through the same stomata's into the air. The light use efficiency is coupled to the stomatal aperture that is expressed into the bulk surface resistance. The mathematical-biological description of the bulk surface resistance reads as:

$$r_s = \frac{r_{smin}}{LAI \cdot F_1(T_2) \cdot F_2(\Delta e) \cdot F_3(h_{rw})} \quad (\text{s/m}) \quad (8)$$

where  $r_{smin}$  (s/m) is the leaf or bulk stomatal resistance, LAI (dimensionless) is the Leaf Area Index,  $F_1(T_a)$  represents a function that describes the effect of air temperature on  $r_s$ , the function  $F_2(\square_e)$  represents the effect of the vapor pressure deficit on the stomatal aperture and the function  $F_3(h_{rw})$  is the effect of the soil water potential on  $r_s$ . By holding the soil water potential constant between two consecutive satellite overpasses, and making  $F_1$  and  $F_2$  variable,  $r_s$  can be re-computed for every individual day. In this case study in Sirsa, all  $F_1$ ,  $F_2$  and  $F_3$  values have been kept constant in between consecutive NOAA acquisition days.

When the stomata's close due to environmentally induced lower leaf water potentials with limiting expansion of the guard cells, light is no longer effectively converted into dry matter because carbon is absent in sufficient quantities. A resistance scalar is used to quantify the day-to-day value of the light use efficiency  $\square(t)$ . It is from experimental studies known that the light use efficiency has a prescribed maximum that depends on c3 and c4 crops. This maximum value is multiplied by the resistance scalar to obtain the actual value for light use efficiency:

$$\varepsilon(t) = \square_{max} * f(r_s) \quad (\text{gr/MJ}) \quad (9)$$

The SEBAL model formulation for crop growth is on large tracks similar to most numerical crop growth simulation models and global scale ecological production models. A significant difference, though, is that crop development due to soil type, prevailing water management conditions and farmer practices is not computed, but prescribed through satellite measured NDVI and temperature time profiles.